Doctoral Thesis for a doctoral degree at the faculty of medicine,

Julius-Maximilians-Universität Würzburg,

Department of Internal Medicine I, Section Cardiology

Director: Prof. Dr. med. Stefan Frantz

Age-related alterations of the immune system aggravate the myocardial aging process

*****

Altersabhängige Veränderungen des Immunsystems verstärken den Alterungsprozess des Myokards

Submitted by

Anne Maria van den Berg

from

Kleve

Würzburg, February 2019

CC BY SA

Submitted on:

18.02.2019

FIRST REVIEWER: Prof. Dr. med. Stefan Frantz

SECOND REVIEWER: Prof. Dr. med. Nicolas Schlegel

THIRD REVIEWER: Prof. Dr. med. Wolfgang Kastenmüller

DEAN: Prof. Dr. med. Matthias Frosch

Date of Public Defence:

16.12.2019

The doctoral candidate is an approbated physician.

Für meine Familie

1 TABLE OF CONTENTS

2 INTRODUCTION

2.1 CARDIOVASCULAR DISEASES - THE LEADING CAUSE OF DEATH WORLDWIDE

Cardiovascular diseases including heart attacks, strokes, heart failure and their complications are the leading cause of death worldwide. In 2016 they were responsible for 17.9 million deaths [1]. Notably, not only life expectancy is affected by cardiovascular diseases, but patients suffering from heart diseases also show a poorer quality of life [2,3].

On one hand, behavioral risk factors like unhealthy diet, physical inactivity, tobacco use and immoderate consumption of alcohol favor the genesis of raised blood pressure, raised blood glucose, dyslipidemia, and obesity which are major risk factors for the development of cardiovascular diseases [4]. On the other hand, aging is a crucial factor that increases the risk to suffer from cardiovascular diseases [5]. From 2011 to 2014 the prevalence of cardiovascular diseases in the U.S. was 41.4 % in the age group of 40-59 year old males (39.4% of females), 69.6% in the group of 60-79 year old males (68.6% of females), and 84.4% in the age group of males older than 80 years (86.5% of females) reflecting a distinct increase with age (Fig. 1) [6]. Even without correlating risk factors, intrinsic cardiac aging causes structural changes of the heart and functional decline in the elderly population [5,7] .

Given the world population growing continuously older, a rising number of people suffering from heart diseases and thus a need of new treatments, the role of aging in cardiac diseases is a field of future relevance and interest.

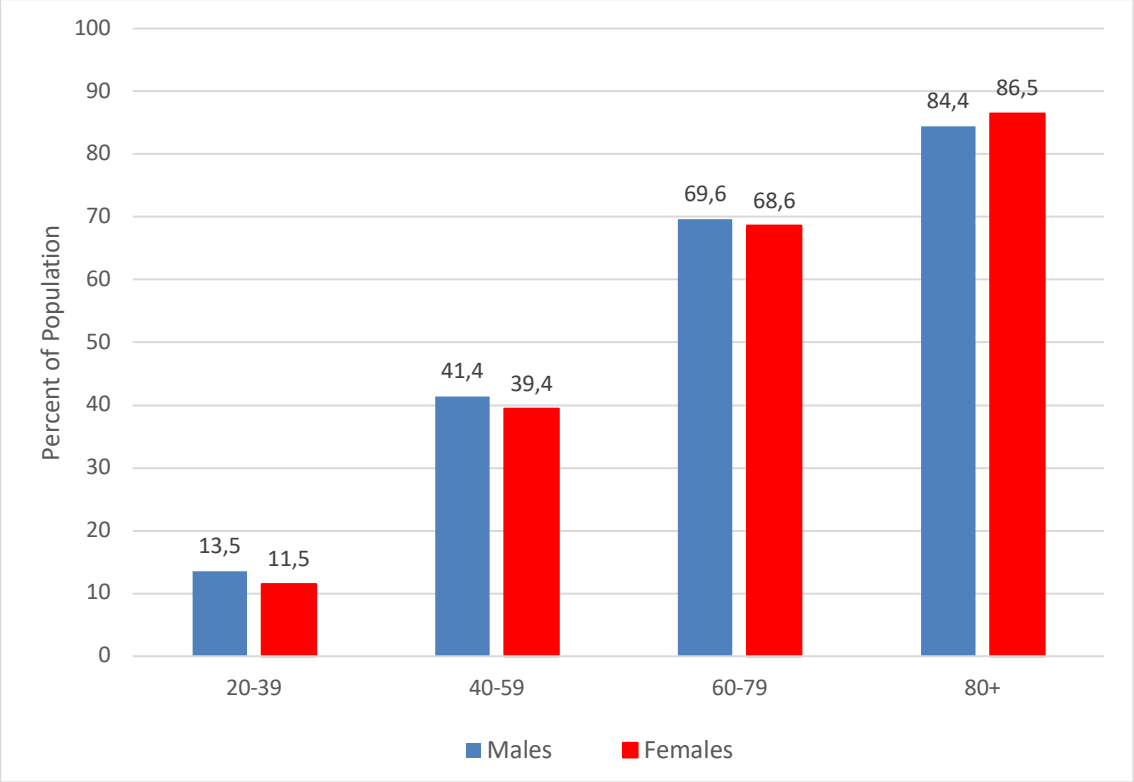

Fig. 1: Prevalence of cardiovascular disease in adults ≥ 20 years of age
Data including coronary heart disease, heart failure, stroke, hypertension. Presented data were collected for the NAHNES (National Health and Nutrition Examination Survey) between 2011 and 2014 [6].

2.2 COMPONENTS OF THE CARDIAC AGING PROCESS

Cardiac aging is a multifactorial process characterized by functional decline as well as structural, cellular, and molecular changes that proceeds even in the absence of concomitant cardiovascular diseases and systemic risk factors [8,9].

Left ventricular hypertrophy, increased cardiomyocyte size, a reduced number of cardiomyocytes, and an increasing total amount of collagen resulting in fibrosis are structural characteristics of an aging heart [8]. Structural transformations together with molecular alterations contribute to an increased ventricular stiffness and impaired ventricular relaxation, which is considered to be causative for diastolic functional deterioration [9-12]. In elderly, the prevalence of left ventricular diastolic dysfunction is considerably increased compared to young individuals. The early diastolic filling rate impairs as early as from an age of 20 years, leading to a decreased E:A ratio in

echocardiographic doppler, which can be interpreted as decreased diastolic function[13-16]. To maintain a sufficient ventricular filling, the atrial contraction, responsible for late diastolic filling, is intensified. In long term this causes atrial hypertrophy and enlargement. As a consequence, remodeling processes can promote the development of atrial fibrillation which is more prevalent in the aged population [7,8,17]. In contrast to reduced diastolic function, systolic function measured by ejection fraction (EF) remains preserved during aging and functional alterations are rarely observed at rest [8]. However, during exhaustive exercise aged hearts show a lower maximum EF and heart rate, indicating a reduced cardiovascular reserve [8,18]. Therefore, the heart becomes more vulnerable to stress and predisposed to heart failure [17,18].

Numerous approaches exist to elucidate the molecular processes behind structural changes and functional deterioration with aging, comprising altered calcium homeostasis, extracellular matrix remodeling, activation of neurohumoral signaling, a deficient β-adrenergic, sympathetic regulation, aging and loss of cardiac stem cells, and finally mitochondrial dysfunction linked to the effect of reactive oxygen species [5,19-25]. Additionally, myocardial aging is associated with cardiomyocyte damage, causing an increased release of intracellular molecules and heart specific antigens. Those can be recognized by immune cells, resulting in an immune response that might consequently lead to an inflammatory state [26]. Current evidence indicates, that inflammation might be the underlying mechanism for many molecular alterations associated with aging and that chronic inflammation increases the risk for cardiac diseases in elderly [26-30].

2.3 THE IMMUNE SYSTEM

Historically, the immune system's most established role was the protection of an individual against foreign pathogens, harmful substances and the damage they cause [31]. Continuative knowledge developed in the last decades. Besides this canonical role, accumulating evidence revealed that the immune system is also crucial for maintaining tissue homeostasis under baseline conditions. Immunological activities modulate physiological processes such as wound healing and tissue repair, prevention of malignancies or cardiac electrical conduction [31-33]. In recent years, the impact of the immune system on different organ systems became progressively evident and is focus of ongoing research. The complex immune network is basically divided into two parts, the innate and adaptive immunity, consisting of numerous cells, organs, molecules and messengers. Innate and adaptive immunity work hand in hand and ensure a balanced function by continuous interaction [31].

2.3.1 Innate immunity

The innate immune system is the first line of defense against intruders, immediately available and acting rapidly. It is composed of mechanical barriers like skin and mucosal epithelia, humoral factors like complement or antimicrobial molecules and cellular components including monocytes, macrophages, dendritic cells, natural killer cells and neutrophilic, eosinophilic and basophilic granulocytes [31]. The presence of pathogen specific molecules, referred to as pathogen-associated molecular patterns (PAMPs) is detected by germline-encoded receptors (pattern recognition receptors=PRRs) which are continuously expressed on innate immune cells and can induce their activation [31]. PRRs are moreover capable of identifying damage associated molecular patterns (DAMPs), self-molecules released during cell stress and tissue injury with immuno-stimulatory properties on neutrophil granulocytes (=neutrophils), dendritic cells or macrophages [34].

Macrophages, granulocytes and dendritic cells are phagocytes [31]. Macrophages populate the tissue since the early embryonic development and are recruited from circulating blood monocytes under inflammatory conditions [35]. In the context of immediate immune defense, macrophages eliminate invading pathogens by phagocytosis and digestion. Antigens are processed and presented on major histocompatibility complexes (MHC), which constitutes a requirement for T-cell activation [31]. Macrophages thereby form a link to the adaptive immune system. The activation of macrophages results in a release of cytokines and chemokines, creating an environment of inflammation and initiating an inflammatory response [31].

Pro-inflammatory mediators like TNF, IL6 and IL1β as well as products of tissue damage attract neutrophils [36]. Neutrophils are the first and most numerous cells that accumulate at the side of infection or injury and have a highly potent phagocytic activity. Their capability of eliminating pathogens is remarkably effective, however, the defense mechanisms are rather unspecific and can cause collateral damage of the surrounding healthy tissue [37,38].

Immature dendritic cells (DCs) represent the third class of phagocytes. DCs are the most potent antigen presenting cell and are competent to prime naïve T-cells. A more detailed picture about their functionality is given in chapter 2.3.2.3.

Besides its function as host defense system, the innate immune system plays a fundamental role in tissue homeostasis and repair. Activated innate immune cells contribute substantially to clearance of cell debris and affect the regulation of local metabolism. By producing growth factors and pro-angiogenic mediators they provide essential conditions to the development process and wound healing [37,39,40]. Furthermore, secreted cytokines initiate fibroblast proliferation and collagen synthesis, thereby regulating tissue remodeling [41].

2.3.2 Adaptive immunity

The adaptive immune response is closely connected to the innate immune system. In case of pathogen defense and inflammation, both form a cross-linked system and work hand in hand. Other than the innate immunity, the adaptive part reacts after a time delay [31]. However, after activation it provides an immunological highly specific immune response and is characterized by selective antigen recognition. The cellular components are B- and T-lymphocytes [42]. Following antigen contact, the adaptive immune system imprints an immunological memory with the potential to remember previous encountered pathogens, thereby providing a long-lasting protection against recurring disease. Upon re-exposure to a familiar antigen, an immune response can be executed faster and in an amplified manner [42,43]. Finally, the adaptive immunity is involved in the development of autoimmune processes. As it loses the competence to distinguish between self and foreign antigens, autoimmunity results [31].

2.3.2.1 B-Cells

B-cells produce specific antibodies, so called immunoglobulins, which are central players of the adaptive humoral immune response [43]. B-cells originate from hematopoietic stem cells in the bone marrow. During the developmental episode they generate a functional B-cell receptor with multiple antigen specificities [31,44]. Before emigration from the bone marrow, B-cells have to pass immunological checkpoints that sort out cell without sufficient surface Ig-signaling or, on the other hand, potentially autoreactive cells [45,46]. After maturing entirely in the spleen, B-cells circulate through the body as fully competent immune cells[47]. Antigenic contact at this stage will induce B-cell activation and differentiation. During a process called germinal center reaction, B-cells undergo clonal expansion, somatic hypermutation, affinity maturation, and isotype switch of the antibody, resulting in the formation of a highly specific memory B-cell compartment [31,46]. Successful B-cell activation and differentiation into plasma cells leads to the production of highly specific antibodies.

Antibodies contribute to the immune defense via neutralization, opsonization, and binding complement, which enhances phagocytosis or induces lysis of a microorganism [48]. Different immunoglobulin classes ensure versatile functions. While IgM and IgD are expressed on all naïve B-cells, switched IgA and IgG are the predominant antibody classes [31].

B-cells play a protective, indispensable role in immune defense, but they can also have harmful effects and induce damage in autoimmune disease or after myocardial infarction [46,49]. The production of autoantibodies, the presentation of self-antigens to T-cells and the release of proinflammatory cytokines induce and maintain self-reactive activity [50,51]. B-cells have to pass a number of checkpoints in the course of development, each providing different strategies to eliminate cells with deficient self-tolerance and an inappropriate affinity against self-molecules [52]. When regulating strategies fail due to alterations in gene expression, variations in signaling pathways or an imbalance between activating and inhibitory signals, B-cells become a player in autoimmune diseases [53].

2.3.2.2 T- cell development and maturation

T-cells are key players of the cellular adaptive immunity. They secrete mediators to regulate an immune response, help B-cells producing effective antibodies and provide signals for further cell activation. Cytotoxic T-cells can induce death of cells infected by viruses or other pathogens as well as damaged or dysfunctional cells [31].

T-cells originate from multipotent hematopoietic stem cells (HSC) residing in the bone marrow. HSC-derived lymphoid progenitors emigrate from the bone marrow and populate the thymus, the major site of T-cell differentiation and maturation [54]. The thymus is a multi-lobular organ subdivided in cortex and medulla. Each area provides a specialized environment of cells and signaling molecules required for T-cell development. T-cell progenitors, called thymocytes, have to undergo a number of maturation steps before leaving the thymus as immune competent T-cell [55].

The cortex is place of thymocyte proliferation by cell division. During stages of development T-cells first do not express one of characteristic T-cell co-receptors CD4 or CD8, later carry both CD4 and CD8 and finally, after successful recombination and somatic recombination, express an antigen specific T-cell receptor (TCR) [31,56]. If this process fails, T-cells die. The emerging, highly diverse TCR repertoire still contains inoperable and potentially autoreactive receptors. Therefore, thymocytes soon enter the process of positive selection to identify the most convenient lymphocytes and the process of negative selection to sort out potentially harmful, autoreactive T-cells. Meanwhile they lose either CD4 or CD8 and become single positive cells [57].

For the final differentiation step of negative selection, single positive thymocytes enter the thymic medulla. In case of immoderate, strong interaction of the TCR to self-peptides presented by medullary thymic epithelial cells, dendritic cells or macrophages, thymocytes die by apoptosis [57]. A fraction of cells bears a TCR of intermediate-high affinity to self-molecules. Those cells develop to naturally occurring, thymus derived, $Foxp3^+$, $CD4^+$ regulatory T-cells (tT_{regs}) [58].

During the process of T-cell maturation, the majority of T-cell progenitors dies. Those who survive leave the thymus as immune competent, mature T-cells, qualified to recognize specific antigens [59].

2.3.2.3 Antigen presenting cells and T-cell priming

After emigration from the thymus, T-cells populate secondary lymphoid organs and enter a continuous process of recirculation; T-cells migrate into lymphnodes via high endothelial venules, leave it via efferent lymph vessels, reentry the vascular system via thoracic duct and finally, recirculate to lymphoid tissue [31] . Circulating T-cells that did not encounter their antigen (Ag) yet, are called naïve T-cells [60]. The recirculation process is highly important and ensures that rare antigen-specific, naïve T-cells get contact to new antigens, triggering their activation and participation in the immune response [61]. This first activation, also referred to as T-cell 'priming', takes place in secondary

lymphoid organs. Naïve T cells are not able to enter the side of infection, whereas effector T cells are [62].

In secondary lymphoid organs peptides of antigens are presented to T-cells. They are bound to major histocompatibility complexes (MHC) on the surface of specialized antigen presenting cells (APC), particularly dendritic cells (DC). Beside DCs, macrophages, monocytes, and B-cells operate as APCs, but are less important for T-cell priming [31]. APCs phagocyte an antigen at side of infection, process it, and present peptides on MHC I and MHC II molecules [63]. Binding of a foreign or self-antigen as well as contact to necrotic cells results in APC activation [64]. Activated APCs modify their surface molecules, start synthesizing cytokines required for T-cell activation and differentiation and migrate to secondary lymphoid tissue. While migrating to the T-cell zone of lymphoid tissues, APCs mature and arrive fully developed [63].

Circulating, naïve T-cells move selectively through T-zones, where they can bind to APCs. In absence of a specifically matching presented antigen, T-cells return to the circulation. As soon as the matching peptide:MHC complex is recognized, a tight ligation is formed. Thereby, T-cells are immobilized by APCs, a process called T-cell 'trapping' [65]. $CD8^+$ T-cells recognize antigens in context with MCH I receptors, whereas $CD4^+$ T-cells need antigen presentation by MHC II receptors [31].

APCs (DCs) provide different kinds of signals required for naïve T-cell activation and differentiation [63]. Depending on environmental conditions in which APCs were activated, different cytokines are produced inducing the differentiation of various T-cell effector subsets [66]. Moreover, the strength of TCR interaction with the peptide:MHC complex might be relevant (Fig. 2)[67]. Differentiated effector T-cells feature all competences to independently perform an immune response against a target cell. No co-stimulation is needed [31].

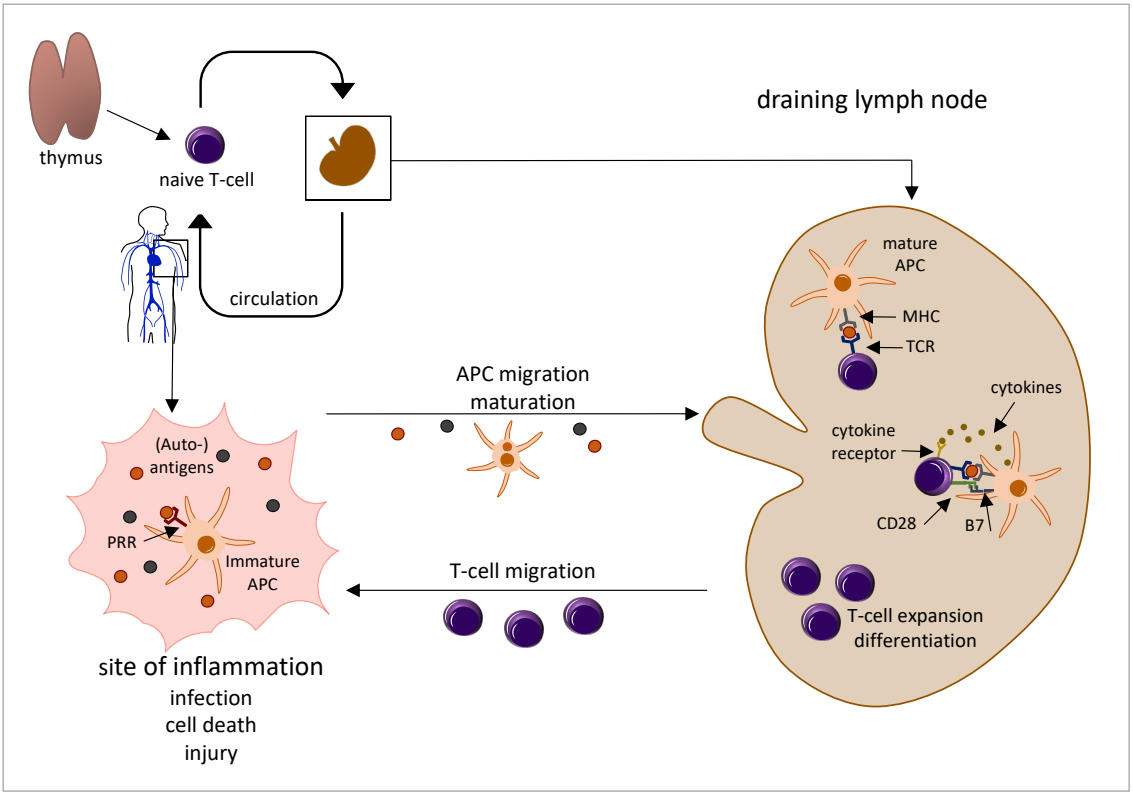

Fig. 2: T-cell priming
After emigration from the thymus, naïve T-cells recirculate between secondary lymphatic organs. Immature DC precursors are spread all over the body. APCs phagocyte the antigen at side of infection, degrade and process it intracellularly and present peptides on MHC I and MHC II molecules. Simultaneous interaction of PAMPs or DAMPS with the TLR induces APC activation, which results in the upregulation of B7 surface molecules, required for T-cell activation, and the simulation of cytokine synthesis. Finally, migration to secondary lymphoid tissue is initiated. APCs (DCs) provide different kinds of signals required for naïve T-cell activation and differentiation: 1. Engagement of TCR with the antigen peptide:MHC complex assisted by CD4 and CD8 coreceptors. 2. Co-stimulation by molecule B7 which is upregulated on activated APCs, interacts with the CD28 surface molecule on T-cells and induces interleukin-2 (IL2) synthesis as well as high affinity IL2 receptor expression. This is essential for T-cell survival. 3. Different cytokines released by activated APCs induce T-cell differentiation [31,63].

2.3.2.4 Conventional T-Cell subsets and function

After successful T-cell priming, different subsets are established. Figure 3 gives an overview of the major T-cell subsets and cytokines that induce their differentiation and function. $CD8^+$ as well as $CD4^+$ T_H1, T_H2, T_H17 and T_{FH}-cells are part of a collective called `conventional T-cells´ (T_{conv}), promoting immune response and providing activation of their target cell [68].

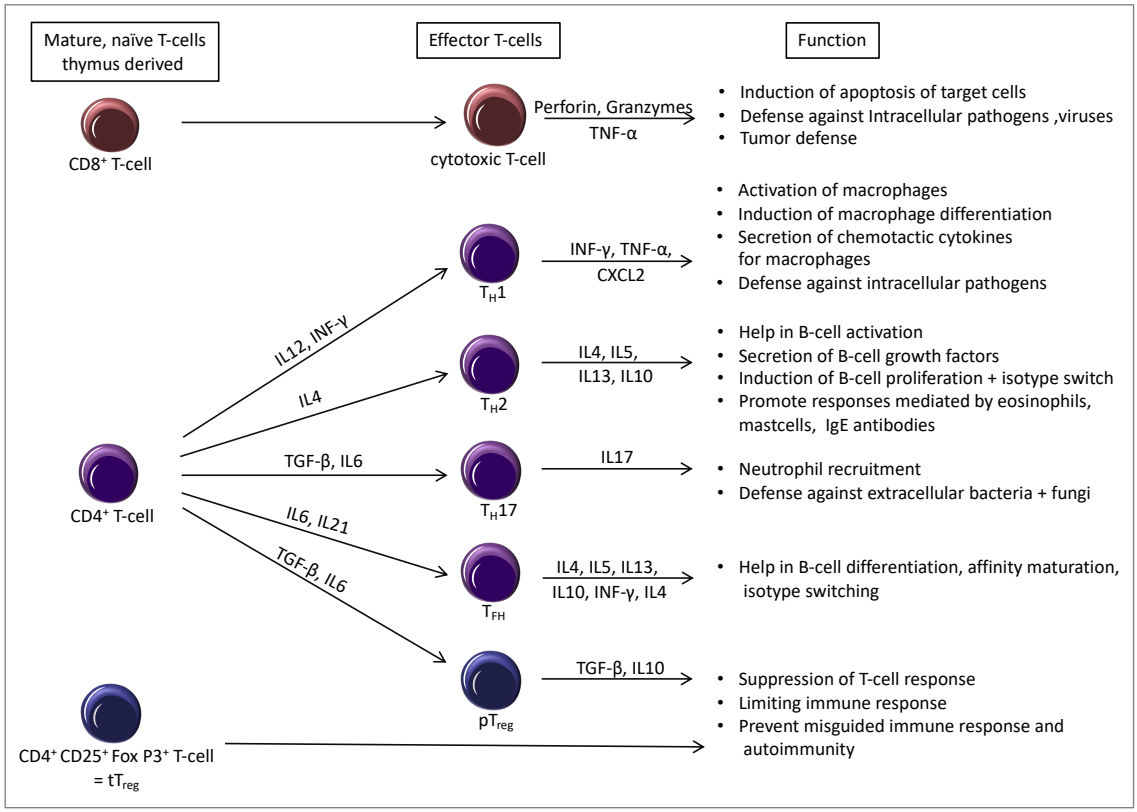

Fig. 3: T-cell subsets, cytokine impact and functions
$CD8^+$ T-cells differentiate into cytotoxic T-cells, specialized in destruction of target cells either being infected with intracellular pathogens (primarily viruses) or malignant cells. Peptide fragments are presented on MHC I molecules on the surface of infected cells. Identification of the foreign antigen leads to release of zytolysin, perforins and granzymes perforating the target cell and inducing cell death. IL12 and interferon-γ (INF-γ) are required for differentiation towards T_H1-cells. T_H1 cells itself produce the proinflammatory cytokines INF-γ and TNF and contribute to macrophage activation. T_H2-cells can be characterized by synthesis of IL4, IL5 and IL13. Their differentiation is triggered by IL4 and T_H2 cells are functionally involved in antibody class switch of B-cells towards IgE. TGF-ß and IL6 polarize differentiation towards T_H17-cells that secret IL17. IL17 mediates local cells to produce cytokines recruiting neutrophils, mainly for the protection against extracellular bacteria and fungi. A rather new identified subset is the population of T_{FH}-cells. They are produced in presence of IL21 and IL6. T_{FH} secrete cytokines characteristic for other subsets such as INF-γ or IL4, both providing support to maturing B-cells and for the generation of high-affinity antibodies [31,66,68].

2.3.2.5 Regulatory T-cells

Besides the conventional T-cell compartment, a further class of $CD4^+$ T-cells, called regulatory T- cells (T_{regs}), can be identified in the periphery. Unlike conventional T-cells they exhibit primarily immunoregulatory properties.

Regulatory T-cells display CD25 on their surface and express transcription factor forkhead box protein 3 (FoxP3). FoxP3 plays an important role for the development and suppressive function of T_{regs} [69,70]. T_{regs} are specialized in maintaining peripheral tolerance, suppression of an ongoing immune response, and prevention of auto-immunity [31,58]. In chronic inflammation and autoimmune disease, an inadequate activation of T_{regs} can be observed often [71,72]. Whereas immunoregulatory functions are usually beneficial, they can be unfavorable for example in limiting anti-tumor immunity [73].

Based on their development, two different types of regulatory T-cells are distinguished; first, thymus-derived, naturally occurring regulatory T-cells (tT_{regs}) and second, peripheral regulatory T-cells (pT_{regs}), induced in the periphery [74]. As described above, tT_{regs} are selected during maturation in thymus by TCR binding with intermediate-high affinity towards self-peptide:MHC complexes, consequently being potentially self-reactive [58]. They are considered to be important for tolerance to self-antigens [75]. Polarization toward pT_{regs} occurs when naïve T-cells are activated in the presence of TGF-ß and retinoid acid, but in the absence pro-inflammatory cytokines such as IL6 [76]. For a long time it was assumed that pT_{regs} limit primarily immune responses to foreign, non-self-antigens such as allergens, dietary antigens and bacteria. Recent studies showed that tT_{regs} were unable to suppress autoimmunity against self-antigens in the absence of pT_{regs}, indicating a close collaboration of both subsets [77,78].

Regulatory T-cells feature a repertoire of mechanism to control and suppress immune activity. They produce regulatory cytokines like IL10, TGF-ß or IL35, interact with DC and interfere with sufficient T-cell activation [72,79-81]. Moreover, T_{regs} compete with T_{convs} for available IL2 molecules, leading to reduced immunogenic effector T-cells or even cell death [58,82]. These regulatory sequences are only some examples, how T_{regs}

provide regulatory properties. Immunosuppression by T_{regs} is a field of scientific interest and further mechanisms are already identified or subject of current research.

2.3.2.6 Development and Maintenance of T-Cell memory

Immunological memory is essential for an immediate immune response to previously encountered pathogens and it is the underlying mechanism of vaccination [31]. As mentioned above, antigen contact as well as vaccination usually cause a dramatic increase of effector T-cells that become dispensable after termination of the immune response. Therefore, most activated T-cells die, with exception of a small amount migrating to lymphoid or nonlymphoid tissues. This minority represents the long-living population of memory T-Cells including the two subsets of central memory T-cells (T_{CM}) and effector memory T-cells (T_{EM}). Both, $CD4^+$ and $CD8^+$ T-cells can differentiate into memory T-cells [31,83].

The conditions and processes determining the destiny of a stimulated T-cell to become either an effector T-Cell and die or, a long-living memory T-cell belonging to the T_{CM} or T_{EM} subset have been long discussed. One important factor which determines T-cell differentiation is, for example, the signal strength for TCR activation [83].

T_{EM}-cells and T_{CM}-cells show a low activation threshold against antigens compared to naïve cells, but present phenotypically and functionally different. T_{EM}-cells lost lymph node homing receptors, but recognize proinflammatory cytokines, migrate to inflamed tissue, mature rapidly to effector T-cells when targeting an antigen, and provide immediate effector function [65,83,84]. Human T_{CM}-cells do express receptors for lymph node homing, show a slow turnover and reside in T-zones of lymphoid tissue [65,84]. Compared with naïve T-cells, the activation threshold is distinctly lower, the affinity of TCR is increased and less co-stimulation is needed to trigger differentiation. T_{CM}-cells show a high responsiveness to antigenic stimulation; nevertheless, their transformation into effector T-cells is slower than it is for T_{EM}-cells and the cytokine production is less. The function of T_{CM}-cells is rather providing reactive memory in terms of maintaining the size of the memory compartment and replacing lost T_{EM}-cells than direct, protective

memory. The size of the memory compartment remains almost stable during life. In the rare event of naïve T- cell numbers decreasing below a certain threshold, memory T cells can proliferate and fill this gap [65,83-85].

Recent studies identified a third population, tissue resident memory T-cells (T_{RM}), that colonizes tissues without recirculation. T_{RM} -cells were, so far, shown to reside in frontlines of infection and mediate protection in a number of different tissues such as the skin, gut and lungs [85].

2.4 THE IMPACT OF AGING ON THE IMMUNE SYSTEM - IMMUNOSENESCENCE

The aging process has a fundamental impact on living organisms and results in various alterations of function and homeostasis of different organ systems. The immune system is no exception. It has been long recognized and many times described that aging of the immune system goes along with major and determining changes leading to an imbalanced function. The mainly described and most decisive changes of the aged immune system are [86-90]:

a) Age dependent decline in immune competence against pathogens
b) Increased prevalence of cancer
c) Extenuated response against vaccination
d) Increased susceptibility to autoimmune disease
e) Chronic low-grade inflammation
f) Defective wound healing
g) Decreased CD4:CD8 ratio
h) Skewing of the T-cell repertoire
i) Clonal hematopoiesis

So far, the underlying mechanisms are not entirely decoded, but in recent years shifts in cell composition, signaling or DNA expression have been identified to be involved in age related alterations. A number of studies indicated an association between persistent CMV (cytomegalovirus) infections and aging of the immune system as well as age associated diseases [87]. In a recent clinical trial with more than 700 octogenarians, CMV seropositivity and resulting T-cell senescence were linked to increased cardiovascular mortality [91]. Heart failure patients with positive CMV serology exhibited lower ejection fraction and a more advanced T-cell senescence phenotype compared to CMV negative patients [92].

Still, many questions remain unanswered. Although the adaptive immunity has been reviewed more extensive regarding this topic, age-related changes apply to both, innate and adaptive immunity.

2.4.1 Age-associated alterations of the adaptive immune system

2.4.1.1 Conventional T-cells and aging

Commonly, a shrinking naïve T-cell compartment and a narrowed TCR repertoire, causing for example impaired ability to respond to new antigens, are linked with deteriorations of immune function. Thymus involution, unavoidable during aging, is often regarded as origin of T-cell changes [89]. Whereas this is applicable for mice in which the entire naïve T-cell compartment is thymus derived and contracts after thymic involution, a translation of this principle into human is not offhandedly possible [93,94].

In men, the size of the naïve T-cell compartment is largely preserved by homeostatic proliferation (by division) of peripheral T-cells [94]. It has been observed, that the absolute number of naïve $CD4^+$ T-cells only slightly decreases with aging, whereas the number of naïve $CD8^+$ T-cells shrinks in opposite to a growing $CD8^+$ memory compartment [95,96]. Moreover, a sufficient TCR repertoire, ensuring response to all kind of peptides, is highly preserved up to the eight decade of life, probably due to a sufficient initial clonal size and quantity of varying TCRs in young age together with steady homeostatic T-cell proliferation [97-99]. However, a skewing TCR-repertoire in elderly individuals can be observed in the $CD4^+$ T-cells, most likely due to peripheral selection rather than ceasing T-cell output (by thymus) [100].

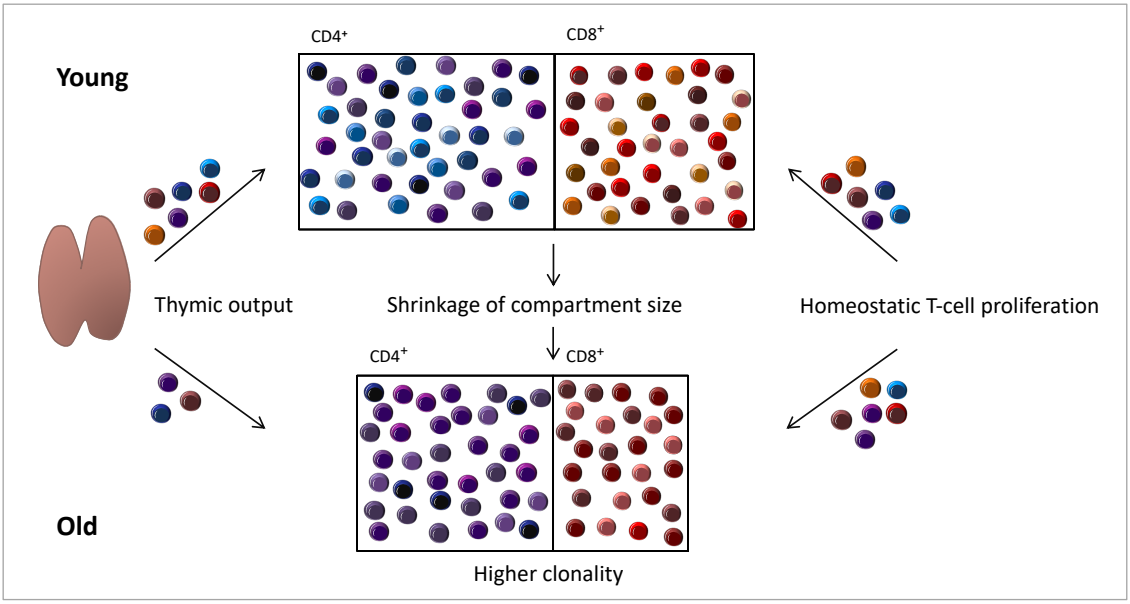

Fig. 4: The naïve T-cell compartments and homeostasis during aging
Although thymic output decreases with aging, the naïve T-cell compartment is maintained by homeostatic T-cell proliferation in adult humans. This kind of reproduction can entirely maintain the richness of the TCR repertoire. Nevertheless, richness decreases with aging and clonality increases, probably due to peripheral selection. The naïve $CD8^+$ T-cell compartment is affected more than the $CD4^+$ T-cell compartment. Furthermore, shrinkage of the $CD4^+$ and $CD8^+$ T-cell compartment can be observed in old adults [89,101].

Those alterations are not only causative for a debilitated immune response against exogenous antigens, but are also regarded as a possible reason for developing autoimmune processes [102]. Peripheral selection pressure could lead to accumulation of an autoreactive TCR repertoire [102]. In murine models increased homeostatic proliferation has been shown to cause selection of T-cells with higher affinity for self-peptides [103,104]. Additionally, variations of signal regulation for negative thymic selection, generally outsourcing T-cells with high affinity self-recognition, were found with aging [105]. Furthermore, uneven distribution of clonal sizes is a determinant of function. On one hand infrequent clones might go along with decreased response to immune challenges. On the other hand, expanded clones can cause increased responsiveness, in case of high affinity to self-peptides resulting in autoimmunity [97,106].

Moreover, intracellular processes influence T-cell effectivity. A reduced activity against foreign antigens can be explained by a decrease of T-cell sensitivity to respond to stimuli. In $CD4^+$ T-cells, changes in gene expression have been observed, causing alterations in signaling pathways. Subsequently, the threshold for signal transduction is

too high and under suboptimal activation conditions, priming of naïve T-cells will fail [86]. Interestingly, in several models reduced TCR signaling induces autoimmunity, possibly explained by adaptation of the signaling to reduced input, thereby being more susceptible to spontaneous activation [102].

Aside its impact on naïve T-cells, aging entails deterioration of T-cell memory. A reduced response to vaccination, recurrence of chronic infections such as VZV and lower activation levels during contact to previously encountered antigens has been observed [86,107]. Again, contraction of the existing memory T-cell repertoire and age associated changes in clonality of the memory compartment can be called in account [97]. As mentioned above, chronic infections such as CMV are discussed to be involved in this process [97]. A deviation of metabolic elements in aged memory T-cells can cause a reduced cytokine production and restricted expression of functional molecules like CD40L, which are important for B-cell activation. As a consequence, clonal B-cell expansion, immunoglobulin class-switch, recombination, and hypermutation are diminished [86]. Furthermore, the expression pattern of regulatory receptors on cell surfaces, mostly affecting $CD8^+$ memory T-cells, has been observed to be altered with aging [86]. While most of the "new" molecules exhibit inhibitory properties, some are stimulatory and can provide activation signals even in absence of antigen, causing a higher immune response or even autoimmune activity [102].

2.4.1.2 Regulatory T cells and aging

As T_{regs} are a key player in maintenance of immune homeostasis and suppression of autoreactivity, gain of T_{reg} function implicates reduced defense against infections and malignancies, whereas loss of function is associated with higher risk for autoimmunity and chronic inflammation [108]. Comparable with conventional T-cells, thymic output of natural regulatory T-cells is reduced during thymic involution while the overall compartment size is maintained by homeostatic proliferation and peripheral recruitment [97]. The entirety of $CD4^+$ and $CD8^+$ T_{regs} has, beyond that, shown to be increased in elderly mice and humans [109,110]. Regarding the T_{reg} differentiation, a decline

of naïve $CD4^+$ and $CD8^+$ T_{regs} was observed together with an increase of memory T_{reg}-cells [108].

In contrast to accumulating tT_{regs} in aging, the pT_{reg} compartment shrinks and the peripheral induction of T_{regs} was shown to be impaired in elderly. This is regarded as one reason for failing tolerance and inflammatory control [108,111]. Another study showed a misaligned balance between effector and regulatory $CD4^+$ T-cells with shift towards increased T_{reg} compartment in elderly [112].

If the regulatory function is maintained or reduced in old individuals is still unclear and diverging findings lead to an ongoing discussion. Some studies revealed identical suppressive functions of $CD4^+$ T_{regs} with aging. FoxP3 expression was stable or even increased indicting an augmented suppressive function [109,113,114]. In contrast, other groups showed reduced regulatory capacities of $CD4^+$ T_{regs} and reduced FoxP3 expression levels in $CD8^+$ T_{regs} [115,116] . Finally, more studies are necessary to examine age related functional alterations of regulatory T-cells and underlying mechanisms.

2.4.1.3 B-cells and aging

As expected, not only T-cells, but also B-cells are affected by aging. Regarding B-cells, a reduction of progenitor cells, diminished cell generation and bone marrow output has been observed [117,118]. While total numbers of circulation B-cell in the periphery appear to remain equal, subset sizes shift significantly with age and the B-cell repertoire is in increasingly skewed [119,120]. Furthermore, both T-cell independent and T-cell dependent antibody responses are limited in elderly, the latter causing less germinal center reaction [119]. This in turn is considered to be one reason for reduced B-cell receptor diversity, specificity and affinity. Furthermore, totals antibody titers are increased in elderly while they are less protective due to lower affinity [118,121]. However, alterations in the aged B-cell population are called to account for increased susceptibility to infections or cancer, an increased incidence of autoimmune disease and poor response to vaccinations in elderly, whereupon the latter might be consequence of age associated T-cell changes and less T-cell help [122].

2.4.2 Age associated changes of the innate immune system

Although investigations regarding age dependent changes of immune function focus primarily on the adaptive immune system, alterations in number, migration, function, and signaling of diverse innate immune cell lineages have been described [123-125].

Neutrophil numbers remain equal in elderly while their performance as fast acting phagocytes is impaired [126]. Cell migration was shown to be decelerated and chemotaxis occurs to be less precise, causing more collateral damage of healthy tissue and leading to delayed wound healing [127,128]. Moreover, phagocytosis is compromised and the efficiency of intracellular and extracellular killing of pathogens diminished [129,130]. Thereby, clearance of cell debris is less effective as well. Neutrophils undergo apoptosis after completing their task. As phagocytosis is not only impaired in neutrophils during aging, but also in macrophages, the clearance of neutrophils is deficient. Numbers of dead cells remain in the tissue, being a pro-inflammatory stimulus [128,131].

Macrophages exhibit further defects in effector function. Antigen presentation is reduced in aged macrophages, possibly due to lower MHC II expression, causing an altered communication between innate and adaptive immunity [132,133]. As a result of dysregulated TLR expression and modified intracellular signaling pathways, the production of co-stimulatory molecules, important for the efficiency of antigen presentation, and the production of pro-inflammatory cytokines as well as chemokines appear to be inappropriate with aging [134,135].

Similar findings of altered signal transduction and receptor characteristics have been reported for dendritic cells of aged individuals, generating an unbalanced activation state [125,136]. There is evidence that the basal cytokine production is increased in elderly while the response to stimuli by foreign antigens is decreased [137,138]. Furthermore, the efficiency to prime and recruit T-cells is reduced and maintaining peripheral tolerance becomes less sufficient [125,139,140].

Conclusively, several cellular alterations and signaling variances contribute to an unbalanced immune function in elderly.

2.5 CHRONIC LOW-GRADE INFLAMMATION IN ELDERLY – INFLAMM-AGING

Aging is characterized by a progressive, chronic, low-grade inflammatory state, a condition also referred to as 'inflamm-aging' [30]. Several studies describe a rising amount of pro-inflammatory cytokines particularly IL6 and TNF during aging. However, some anti-inflammatory cytokines were revealed increased as well, pointing to a generally more activated inflammatory system [141-144].

First, persistent chronic infections such as CMV were considered the causal stimulus for this ongoing inflammation, but then endogenous processes became more apparent to be the decisive trigger for inflammatory responses [144,145]. Aging is attended by various cellular alterations increasing the probability for cell damage or death such as the accumulation of metabolism end-products, misfolded proteins and dysfunctional organelles, decreased autophagy, dysfunctional telomeres, DNA-damage, and the exposure to reactive oxygen species [144,146]. Consequences of cell damage are, among others, a release of self-molecules and organelles, the emergence of misplaced molecules in unaccustomed compartments, and the accumulation of cell debris [144,147]. Usually, cell debris is promptly eliminated by professional phagocytes in order to maintain tissue homeostasis preventing thereby the production of antigenic molecules causing inflammatory response [148,149]. A reduced capability for adequate clearance in combination with augmented accumulation of cell debris and misplaced self-molecules might cause an intensified recognition of these particles by the immune system [150]. As explained in chapter 2.3.1, pattern recognition receptors (PRR) are continuously expressed on innate immune cells and are capable of identification and reaction towards self-molecules (DAMPs). The detection of stressed respectively dying cells, organelles or misplaced self-molecules by PRRs provokes an autoimmune, inflammatory response against these self-structures [144]. Moreover, senescent cells secrete pro-inflammatory cytokines and signaling molecules that do not only affect the immediate environment but are able to spread and cause systemic inflammatory effects [144,146].

Finally, the inflammatory response is primarily initiated by chronic stimulation of innate immune cells (like macrophages), subsequently inducing the secretion of pro-inflammatory cytokines by cells of the innate and adaptive immune system [151]. This

systemic inflammatory status on one hand interferes with the immune system, on the other hand causes tissue degradation and has been numerous times described to be a critical risk factor for chronic diseases like neurodegenerative diseases, atherosclerosis or diabetes type II [28,147,151].

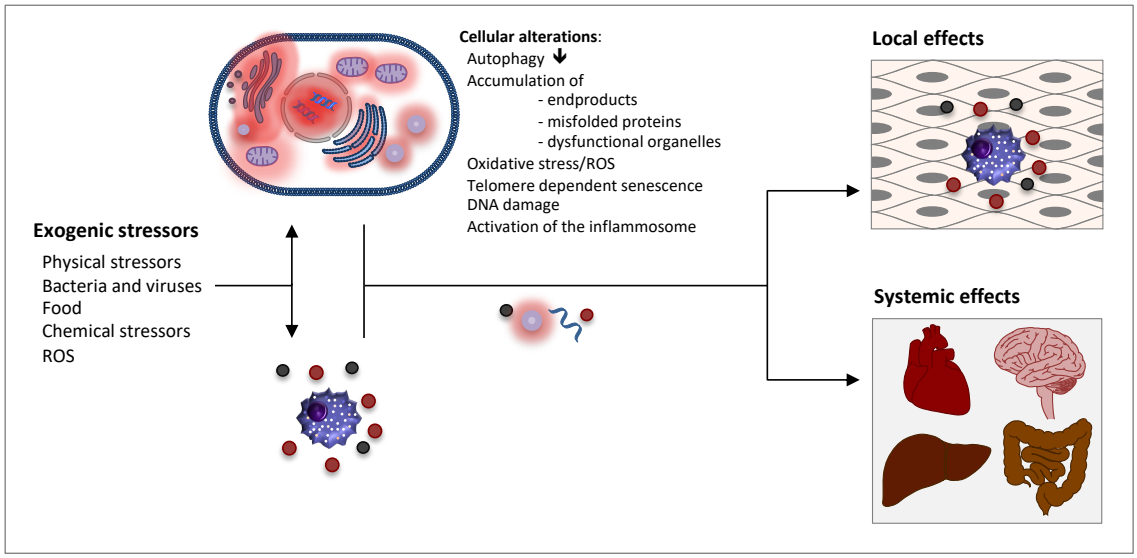

Fig. 5: Inflamm-aging
With aging, the number of stressors and harmful factors increases. Macrophages are continuously stimulated by exogenic stressors and molecular garbage which results in the release pro-inflammatory cytokines or further mediators. Additionally, extracellular garbage, generated by progressive cell death, accumulates and finally exceeds the clearing competences of macrophages. This leads to a local inflammatory response that can expand to a global pro-inflammatory state. Senescent cells secret factors that affect neighboring cells and can finally cause a disruption of tissue homeostasis. Furthermore, cellular garbage, organelles released during cell death, and signaling molecules circulate in body fluids. They spread all over the body and reach distant tissues or organs where misplaced molecules can cause and promote further pro-inflammatory activity [30,144,146].

2.6 CARDIAC LEUKOCYTE POPULATIONS AND THEIR ROLE IN HOMEOSTASIS, PATHOGENESIS AND REPAIR OF HEART DISEASES

The cardiac tissue is composed of manifold cell populations including - besides cardiomyocytes - fibroblasts, endothelial cells, and leukocyte populations residing in the myocardium [152]. Their presence has been described in recent years and their role in myocardial homeostasis and repair is subject of ongoing research [152-155].

Cardiac macrophages represent the majority of cardiac leukocytes and are a heterogenous population with different ontogenetic and phenotypic characteristics [153,155,156]. With aging, the composition of the macrophage population changes even in the absence of disease and inflammation [157]. During the neonatal period, cardiac macrophages promote tissue development and are essential for the regenerative capacity of neonatal hearts after injury [158,159]. After ischemic injury, they are critical for healing and reconstitution of tissue integrity by playing a crucial role in scar formation, left ventricular remodeling and angiogenesis [156,160-162].

Dendritic cell populations have been found in the myocardium with niches near cardiac valves [163]. Under steady state conditions DCs sample antigens and present cardiac antigens such as α-myosin heavy chain to T-cells in heart draining lymph nodes [164]. Cardiac injuries like myocardial infarction cause an increased DC infiltration of the heart. DCs get activated and attain a mature state resulting in the induction of autoreactive T-cells [164].

Neutrophils are rare in the healthy, steady state myocardium, but they are rapidly recruited after ischemic injury or pressure overload [156]. By clearing cell debris and secreting chemokines to attract further leukocytes, neutrophils might contribute to inevitable conditions for healing [165]. However, since neutrophils release inflammatory mediators and cytotoxic substances like proteolytic enzymes and reactive oxygen species, they maintain a sterile injury resulting in damage of surrounding cells [165,166]. Therefore, they are regarded as harmful in the context of myocardial healing.

Besides the innate immune system, adaptive immune cells participate in myocardial physiology. While the knowledge about cardiac B- and T-cells and their role in cardiac homeostasis is limited, diverse effects on inflammatory conditions and

modulating impact after injury have been reported [156]. Viral and parasitic infections of the heart can cause a loss of self-tolerance of lymphocytes against cardiac antigens resulting in an induction of autoimmune myocarditis [167]. T-cells specific for cardiac myosin were shown to be mediators of this autoimmune disease [168,169].

However, it was shown that non - infectious injuries are modulated by T-cells, too. Sterile cardiac injuries like ischemia and myocardial infarction initiate lymphocyte activation directed against cardiac antigens [170,171]. $CD4^+$ T-cells became evident to have a protective function during cardiomyocyte damage, promote tissue repair and improve wound healing after myocardial infarction [172,173]. Furthermore, T_{regs} were shown to play a particular role in sufficient scar formation and have a beneficial effect on remodeling by modulating macrophage, monocyte and fibroblast function [174-176]. On the contrary, in ischemia- reperfusion models pro-inflammatory $CD4^+$ T-cells can be deleterious and contribute to myocardial injury [170,177].

Moreover, different hemodynamic conditions such as pressure overload, causing only minimal tissue damage and low-grade inflammation, are sufficient to trigger T-cell response [173,178]. In this context T-cells were shown to be involved in chronic cardiac remodeling and contribute to development and progression of heart failure [178-180].

Taken together, the heart is an immunological active site and leukocytes contribute to cardiac homeostasis under physiological conditions. Although recent evidence identified lymphocytes, particularly T-cells, to be involved in pathogenesis of inflammatory processes and repair of myocardial tissue damage, their function in the steady state remains largely unknown. Furthermore, immunological processes are affected by aging, a state of increased inflammatory tone. Contemporaneous, aging is a mayor risk factor for heart disease. Based on these considerations, it was objective of this study to investigate the correlation between immunosenescence and the myocardial aging process.

3 MATERIALS AND METHODS

3.1 MATERIALS

3.1.1 Fine chemicals and reagents

The chemicals and reagents listed here were used in different experiments. The substances were aquired from eBioscience (Waltham, USA), B.Braun (Melsungen, Germany), cp-pharma (Burgdorf, Germany), Carl Roth GmbH (Karlsruhe, Germany), Life Technologies (Carlsbad, USA), Merck (Darmstadt, Germany) , Roche Diagnostics (Basel, Schweiz), Ratiopharm (Ulm, Germany), Sigma-Aldrich (Steinheim, Germany) and Vector Laboratories (Burlingame, USA).

Aqua as injecatabilia
Aqua destillata
BSA (Bovine serum albumin)
Benzyl alcohol
Benzyl benzoate
Calcium chloride
DAPI (4´6-diamino-2-phenylindole)
Disodiumhydrogenphosphate
Dry milk, fat free
Ethanol
FCS (Fetal Calf Serum)
Formaldehyde
Glycerol
Hematoxylin
Heparin-Natrium 25000
n-Hexan
Hydrogen peroxide
Horseradish peroxidase streptavidin (HRP)
Ionomycin
Isopropyl alcohol
Isoflurane
Isopentane
Liquid nitrogen
Methanol
Monensin
Mowiol
Normal Goat Serum
Picric acid
Phorbol-12-myristate-13-acetate
Rotihistol A+B
Sirius red (Direct Red 80)
Sodium azide
Sodium chlorid (NaCl 0,9%)
Sodiumdihydrogenphosphat
Sodiumpyruvat
Tetramethylbenzidine
Tris (Tris(hydroxymethl)aminomethane
Triton X
Tween 20
Xylene

3.1.2 Antibodies

Fluorophore labeled antibodies (against mouse antigens) for flow cytometry
All antibodies were produced by BioLegend (San Diego, USA) or ThermoFisher Scientific (Waltham, USA). The fluorophore-conjugated antibodies indicated below were used in different combinations, depending on the experimental setup.

Antibody	Color	Clone
anti-CD3ε	Efluor 450	145-2c11
anti-CD4	Alexa®647	RM4-5
anti-CD8	PE-Cy7	53-6.7
anti-CD11b	PE	M1/70
anti-CD25	PE	PC61
anti-CD44	APC Fire	IM7
anti-CD45	BV421	30-F11
anti-CD45	FITC	30-F11
anti-CD45	Efluor 450	30-F11
anti-CD45/B220	Alexa®647	RA3-6B2
anti-CD62L	Alexa® 488	MEL-14
anti-CD206	Alexa®647	C068C2
anti-Foxp3	APC	MF-14
anti-Ki67	PE	16a8
anti-Ly6g	APC/Cy7	1a8
anti-Ly6c	PE-Cy7	Hk1.4

Antibody for Light Sheet Microscopy

anti-CD45	Alexa®647	30-F11

Antibodies for intracellular cytokine staining

anti-TNF	Pacific Blue	mp6-xt22
anti-IFN-γ	PE	xmg1.2
anti-IL-10	PE	jes5-16e3
anti-IL-13	e450	ebio13a

Fluorophore labeled antibodies (against mouse antigens) for immunofluorescence

Primary Antibodies	Color	Clone	Supplier
anti-CD68		MCA1957	BioRad Serotec (Hercules, USA)
anti-B220		RA3-6B2	Biolegend (San Diego, USA)
anti-CD3ε		145-2c11	Biolegend (San Diego, USA)
anti-CD4		GK1.5	Biolegend (SanDiego, USA)
anti-CD8a		53-6.7	Biolegend (SanDiego, USA)
Phalloidin	Atto-488		SigmaAldrich (Steinheim, Germany)
WGA	Alexa® 647		ThermoFisher Scientific (Waltham, USA)

Secondary Antibodies for immunofluorescence
Secondary antibodies were produced by ThermoFisher Scientific (Waltham, USA).

Anti-mouse IgM	Alexa® 555	polyclonal
Anti-mouse IgG	Alexa® 488	polyclonal

3.1.3 Buffers and solutions

Buffers and solutions were prepared in desalted water.

PBS	NaCl (pH 7.4)	137.0 mM
	Na_2HPO_4	10.0 mM
	KCl	2.6 mM
	$KH_2 PO_4$	10.0 mM
FACS buffer	NaCl (pH 7.4)	137.0 mM
	Na_2HPO_4	10.0 mM
	KCl	2.6 mM
	$KH_2 PO_4$	1.8 mM
	BSA	0.1%
	NaN_3	0.1%
BSS/(BSA)	KCl	5.33 mM
	$KH_2 PO_4$	0.44 mM
	NaCl	138.0 mM
	$NaHCO_3$	4.0 mM
	Na_2HPO_4	0.3 mM
	(BSA)	(5%)
Mayer´s Hematoxylin		
	Acetic acid	2%
	Glycerol	30%
	Hematoxylin	1%
	Aluminium sulfate	5%
Picro-sirius red	Picric acid	1.5%
	Sirius red	0.1%

3.1.4 Ready for use kits and solutions

Kit/Solution	Supplier
Carbo-Free Blocking Solution®	Vector Laboratories (Burlingame, USA)
Carbonate coating Buffer	Biolegend (San Diego, USA)
CountBright™ Absolute Counting Beads	Invitrogen (Carlsbad, USA)
DNase1 Amplification Grade, AMP-D1	Sigma-Aldrich (Steinheim, Germany)
FoxP3 Transcr. Factor Staining Buffer Set	eBioscience (Waltham, USA)
iScript cDNA Synthesis Kit	Bio-Rad (Munich, Germany)
RNeasy Micro Kit	Qiagen (Venlo, The Netherlands)
RNeasy Mini Kit	Qiagen (Venlo, The Netherlands)
RNAlater Solution	ThermoFisher (Waltham, USA)
TaqMan Master Mix	Life Technologies (Darmstadt, Germany)

3.1.5 TaqMan probes

All probes for Real Time PCR analyses were purchased from Life Technologies (Darmstadt, Germany):

house-keeping genes (Probe number)

Gusb	(Mm01197698_m1)	Gapdh	(Mm033002249_g1)
Actb	(Mm00607939_s1)		

tissue stress/ myocardial damage genes (probe number)

Hspd1	(Mm00849835_g1)	Hspa4	(Mm00434038_m1)
Hspa1a	(Mm01159846_s1)	Hif1a	(Mm01198376_m1)
Gata4	(Mm00484689_m1)	Hmox1	(Mm00468922_m1)
Tlr2	(Mm00442346_m1)	Tlr4	(Mm00445273_m1)
Myd88	(Mm00440338_m1)	Casp1	(Mm00438023_m1)
Nfkb	(Mm00476361_m1)	Rela p65	(Mm00501346_m1)

Myh6	(Mm00440359_m1)	Myh7	(Mm01319006_g1)
Anp	(Mm00435329_m1)	Adrb1	(Mm00431707_s1)

pro-inflammatory genes (probe number)

Il1b	(Mm00434228_m1)	Il6	(Mm00446190_m1)
Tnf	(Mm99999068_m1)	IFN-γ	(Mm01168134_m1)
Il17a	(Mm00439618_m1)	Nos2	(Mm00440488_m1)
Ccl2	(Mm00441242_m1)	Ccl5	(Mm01302427_m1)
Nox1	(Mm00549170_m1)	Cxcl13	(Mm04214185_s1)
Cd80	(Mm00711660_m1)		

anti-inflammatory genes (probe number)

Il10	(Mm00439614_m1)	Mrc1	(Mm00485148_m1)
Foxp3	(Mm00475162_m1)	Pparg	(Mm01184322_m1)
Pdl1	(Mm00452054_m1)		

angiogenesis/ extracellular matrix remodeling genes (probe number)

Vegfa	(Mm00437304_m1)	Vwf	(Mm00550376_m1)
Col3a1	(Mm01254476_m1)	Col1a1	(Mm00801666_g1)
Mmp2	(Mm00439498_m1)	Mmp9	(Mm00442991_m1)
Agtra1	(Mm00616371_m1)	Tgfb1	(Mm01178820_m1)
Tgfb3	(Mm00436960_m1)	Timp1	(Mm00441818_m1)
Timp2	(Mm00441825_m1)	Spp1	(Mm00436767_m1)
Vim	(Mm01333430_m1)		

3.1.6 Enzymes and Sera

Collagenase Type 2	Worthington Biochemical (Lakewood, USA)
DNase I	Sigma-Aldrich (St. Louis, USA)

3.1.7 Animals

Mouse strain		**Supplier**
C57BL6/J mice	(stock No. 000664)	Jackson laboratory
CD4KO mice	(stock No. 002663)	Jackson laboratory
MHC-II-deficient mice	(stock No. 003584)	Jackson laboratory
OT-II mice	(stock No. 004194)	Jackson laboratory
µMT mice	(stock No. 002288)	Jackson laboratory

Mice in the age of 2 months to 15 months were examined in this study. All selected mouse strains are on the same genetic background (B6/J) and suitable wild type mice (C57BL6/J) were chosen as control animals. The mice were permanently housed under specific pathogen free conditions (SPF) with a controlled 12-hours light-dark cycle. A standard diet was used for feeding.

All experiments which included animals were performed according to the provisions of the Animal Welfare Act and were approved by the Regierung von Unterfranken in Tierversuchsantrag (TVA) 65/13.

3.1.8 Consumables

Consumable	**Supplier**
Cell Strainer (70 + 100µm mesh)	BD Bioscience (Franklin Lakes, USA)
Centrifuge Tubes	Greiner (Frickenhausen, Germany)
Cover Slips 24 x 50mm	Fisher Scientific (Pittsburgh, USA)
Cryo tube (1.8ml)	Nunc (Roskilde, Denmark)
Entellan	Merck (Darmstadt, Germany)
Elisa plates	R&D (Minneapolis, USA)
FACS tubes	BD Bioscience (Franklin Lakes, USA)
ImmEdge™ Hydrophobic Barrier Pen	Vector Laboratories (Burlingame, USA)
Microseal film for PCR plates	Bio-Rad (Munich, Germany)
Feather® Microtome blades S35	pfmmedical (London, England)
Needles (25 gauge and 19 gauge)	B.Braun Melsungen AG (Melsungen, Germany)
Object slide, Super Frost Ultra plus	R. Langenbrinck (Emmendingen, Germany)
PCR Tubes (0.2ml)	Eppendorf (Hamburg, Germany)
Pipette tips (10µl, 200µl, 1000µl)	Starlab (Hamburg, Germany)
Reaction tubes (1.5ml and 2ml)	Eppendorf (Hamburg, Germany)
Scalpel	Hartenstein (Würzburg, Germany)
Sterilium	Bode Chemie (Hamburg, Germany)
Suture Silk Black 6/0	FSSB GmbH (Jestetten, Germany)
Terralin®	Schülke (Norderstedt, Germany)
Tissue Ruptor Disposable Probes	Qiagen (Venlo, The Netherlands)
TissueTek®	Sakura Finetek (Torrance, USA)
96-well plates (U-bottom, V-bottom)	Greiner (Frickenhausen, Germany)
96-well PCR plates	Bio-Rad (Munich, Germany)

3.1.9 Instruments

The following instruments were used for preparation, measurements and analyzes:

Instrument	**Supplier**
Visual Ultrasonic Vevo 1100 + 30MhZ Transducer	Fujifilm Visualsonic Inc. (Toronto, Canada)
Automatic pipette: Pipetboy acu	Bio-Rad (Hercules, USA)
Axioskop 2 plus	Carl Zeiss Microscopy (Jena, Germany)
AxioCamHRc (high resolution camera)	Carl Zeiss Microscopy (Jena, Germany)
Axio Imager Z1m	Carl Zeiss Microscopy (Jena, Germany)
Biofuge pico	Heraeus Instruments (Hanau, Germany)
Centrifuge 5810 R	Eppendorf (Hamburg, Germany)
Elisa Reader Dynex MRX Revelation TC 96	Magellan Bioscience (Tampa, USA)
Flow Cytometer LSR II	BD Biosciences (Erembodegem, Belgium)
Flow Cytometer FACS Canto II	BD Biosciences (Erembodegem, Belgium)
iCycler	Bio-Rad (Munich, Germany)
Incubator: BB6220	Heraeus Instruments (Hanau, Germany)
Isoflurane Vaporizer	Harvard Apparatus (Holliston, USA)
Light-Sheet microscope	Designed by the Heinze group [181] (Würzburg, Germany)
Magnetic stirrer	Labinco (Breda, The Netherlands)
Microtome Leica CM 1850 Cryostat	Leica Microsystems (Wetzlar, Germany)
MPVS-ultra foundation system	AD Instruments (Oxford, England)
Nano Drop 2000c	Thermo Scientific (Waltham, USA)

Pipettes	Eppendorf (Hamburg, Germany)
Refrigerators	Liebherr (Bulle, Switzerland)
SPR-839 Catheter	Miliar Instruments (Houston, USA)
Surgical instruments	B.Braun Melsungen AG (Melsungen, Germany)
Thermocycler	Eppendorf (Hamburg, Germany)
Tissue Ruptor	Quiagen (Venlo, The Netherlands)
Vortexer IKA® MS3 basic	IKA®-Werke (Staufen, Germany)
2100 Bioanalyzer	Agilent (Santa Clara, USA)

3.1.10 Electronic data processing, Software

The following software was used for data acquisition, analysis and presentation:

Software	**Supplier**
Axiovision 4.8	Carl Zeiss Microscopy (Thornwood, USA)
BD FACS Diva™	BD Bioscience (Franklin Lakes, USA)
EndNote X7	Clarivate Analytics (Philadelphia, USA)
FlowJo 7.6	Tree Star (Ashland, USA)
GraphPad Prism 7.0	GraphPad software (San Diego, USA)
Image J	NIH Softwares (Bethesda, USA)
Imaris	Bitplane (Zuerich, Switzerland)
Keynote	Apple Inc. (Cupertino, USA)
LabChart	AD Instruments (Oxford, England)
Microsoft Office 2011	Microsoft Corporation (Redmond, USA)
Powerpoint Figure Pattern	Motifolio Illustration Toolkit (Maryland,USA)
Nice software package	Toshiba Medical Systems (Ötawara, Japan)
Zen lite	Carl Zeiss Microscopy (Jena, Germany)

3.2 METHODS

3.2.1 Echocardiography

Echocardiography is an established method to investigate function and anatomy of the heart. To facilitate an adequate examination, mice were kept under light isoflurane anesthesia (1,5%) to avoid cardio-depression. Mice were prepared in a supine position and a short axis echocardiography was performed using the Visual Ultrasonic Vevo1100 system coupled to a 30 MhZ ultrasound transducer, as previously described by our group [174]. Two-dimensional cardiac images were recorded sonographically on mid-papillary and apical levels of the left ventricle. Using transversal M-Mode, luminal end-diastolic (EDD) and end-systolic diameters (ESD) were measured by the same researcher. EDD and ESD were applied for determination of left-ventricular fractional shortening (FS) to estimate left-ventricular contractile function.

Left-ventricular fractional shortening was calculated as follows[182]:

$$FS\ (\%) = 100 \times [(EDD - ESD) / EDD]$$

Mice with a basal heart rate >500 bpm were included in the analysis. Echocardiography measurements were performed by experienced examiners.

3.2.2 Hemodynamic measurements

Mice were kept under anesthesia using 2% isoflurane atmosphere. To guarantee deep anesthesia, mice were intubated and ventilated with 100% oxygen supplemented with 0.8% isoflurane. The pressure-volume catheter was calibrated previously as described in manufacturer´s instructions to ensure an accurate measurement. The MPVS (Micro-Tip® Pressure Volume System) – ultra foundation system was used.

A heating plate was prepared, and mice were immobilized on the plate to guarantee a steady body temperature and to prohibit a decreased heart rate due to lower body temperature. The animal´s head was fixed in a position providing a stretched neck. An incision was made at the middle-neck and the right carotid artery was uncovered and

ligated without damaging the vagus nerve. After preparing the carotid artery with sutures, a longitudinal incision was made, and the pressure volume catheter was carefully inserted into the vessel. Next, it was moved forward into the left ventricle. The correct position was achieved as soon as a pressure-volume signal showed up. Measurements were performed as described before [183]. To analyze the recorded data, LabChart software was used. After hemodynamic studies were completed, mice were euthanized, and organs were extracted as described below.

3.2.3 Perfusion and organ preparation

To collect the mice organs for further investigation, the animals were euthanized in an approved procedure and 40UI heparin were injected intraperitonally to prevent blood coagulation. The mice´s bodyweight was determined. A perfusion was performed with PBS (phosphate buffered saline) organs from blood. In the next step, the heart, gastrocnemius muscle, mediastinal, inguinal and popliteal lymphnodes were collected and processed variable.

To follow different approaches, hearts were weighted and divided it into basis for histology, “middle section” used for flow cytometry and apex for RNA analysis. The basis was embedded in TissueTek® (Sakura Finetek), immediately frozen with liquid nitrogen, and, after transferring into a cryo-conservation tube, stored at -20°C. Apical tissue for RNA analysis was submerged in RNA later RNA stabilization Reagent (Ambion) at 4°C for 24 h. After incubation, the tissue was transferred to a cryo- conservation tube, immediately frozen with liquid nitrogen and stored at -80°C. Cardiac tissue and gastrocnemius muscle collected for flow cytometry analysis were processed subsequent to organ extraction and prepared as described below in 3.2.4.

Mediastinal, inguinal and popliteal lymphnodes were collected in BSS/BSA and prepared for flow cytometry staining in parallel to myocardial and skeletal muscle.

3.2.4 Flow cytometry

Flow cytometry is a method to study cellular populations which provides the potential to characterize, analyze and quantify cells by immune-phenotyping [184].

Cardiac tissue collected for flow cytometry analysis was cut into small pieces and digested with collagenase type II (100 IU/ml) at 37°C for 30 min. Afterwards remaining pieces were grinded through a cell strainer of 100 µm pore size to obtain a single cell solution of cardiomyocytes. The reaction was stopped by adding ice cold PBS solution up to a volume of 15 ml. A centrifugation step was performed and the supernatant fluid was discarded. Next, a cardiomyocyte suspension was generated with a small volume and transferred it into a 96-plate well plate for staining. Again, a centrifugation step was done and the supernatant discarded.

To prevent unspecific Fc-receptor binding during the staining process, 25 µl of a solution containing monoclonal antibody against Fc-receptor CD16/32 diluted in FACS buffer was added to the cardiomyocyte suspension, mixed well and incubated at 4°C for 15 min. Now a mixture containing all fluorescence labeled antibodies needed for the specific approach was prepared. Again, 25 µl of the antibody mixture were added and the suspension incubated at 4°C for 15 min.

With this protocol surface characteristics are stained. If staining of intracellular components was not necessary for an approach, supernatant was discarded and after resuspension in FACS buffer, cells were prepared for measurement.

To perform staining of intercellular components such as FOXP3, cells were not resuspended in FACS buffer, but in 100 µl of fixation-permeabilization buffer in order to fixate them. The suspension was incubated for 30 min at room temperature. After washing with permeabilization buffer, cells were suspended in 50 µl of a mixture containing all intended fluorescent labeled antibodies for intracellular staining diluted 1:50 in permeabilization buffer and incubated for another 30 min at 4°C. Finally, cells are dissolved in FACS Buffer and measured under these conditions. Gastrocnemius muscle was used as control in some approaches and prepared identically.

To determine the amount of spill over across different channels during measurement, single cell compensation was applied using oneComp eBeads

(ThermoFisher Scientific). Cell suspensions and compensation beads were processed identically.

Lymphnodes were prepared similarly. To generate single cell suspensions, they were grinded through a 40 µm pore size cell strainer and stained after the same protocol as cardiomyocytes.

In order to analyze intracellular cytokines, bulk lymph node derived cells were stimulated with ionomycin (1 µg/ml, Sigma), phorbol-12-myristate-13-acetate (50ng/ml, Sigma) and monensin (1:1000, BD Bioscience) over an incubation time of 5 hours. Afterwards staining was completed as described above.

3.2.4.1 Calculation of absolute cell numbers

For some experiments it was important to quantify absolute cell numbers instead of only examining the fraction of one cell type among the cell suspension. Therefore, counting beads were used (CountBright™ Absolute Counting Beads, Invitrogen) as recommended in the producer´s manual. A defined volume (50 µl) of the bead suspension was added to each sample. The CountBright™ suspension contains a specific number of beads per volume. During measurement, bead events and cell events are counted. By comparing the ratio of bead evens to cell events, absolute cell numbers can be calculated for the sample:

$$\text{Concentration of sample (cells/µl)} = \frac{\boldsymbol{A}}{\boldsymbol{B}} \times \frac{\boldsymbol{C}}{\boldsymbol{D}}$$

A = number of cell events

B = number of bead events

C = assigned bead count of the lot (beads/50 µl)

D = volume of the sample (µl)

3.2.5 Molecular biology

3.2.5.1 RNA isolation

RNA isolation is the first step in a process leading to analysis of RNA expression in myocardial cells. In our lab the RNeasy Mini Kit (Quiagen) was used to purify RNA from murine cells. To get a good RNA yield, 20-30 µg of tissue were disrupted and homogenizing with a rotor-stator homogenizer in 600 µl of RLT lysis buffer. Subsequently, the lysate was centrifuged for 3 min at 10000 rpm at room temperature and only the supernatant was used in the following steps. 70% Ethanol was added in a ratio 1:1 to improve binding conditions and the sample was transferred to a RNeasy spin column, containing an RNA binding membrane. While the sample was centrifuged for 15 sec at 10000 rpm, RNA was expected to bind to the membrane. Flow-through was discarded. To wash the membrane, 700 µl of RW1 buffer were added to the spin column and centrifuged for another 15 sec at 10000 rpm. Again, the flow-through was discarded. Two further washing steps were performed by adding 500 µl Buffer RPE respectively, followed by two more centrifugation steps. Finally, the spin column was carefully transferred into a new collection tube and 30-50 µl of RNAse-free water were added to solve RNA from the binding membrane during a final centrifugation step for 1 min at 10000 rpm. Isolated RNA was stored at -80°C when not processed immediately.

3.2.5.2 RNA quantification

Next, a quantification of RNA content and determination of contaminants in each sample was performed. In order to analyze the samples, a Nanodrop Spectophotometer (ThermoFisher Scientific) was used. RNA concentration is calculated by analyzing the amount of light absorbance in the sample. Therefore, it is exposed to ultraviolet light. Each substance absorbs the ultraviolet light at a specific wavelength, RNA at a wavelength of 260 nm. Contaminants have their maximum of absorbance in different wavelengths, for instance proteins at 280 nm or organic contaminants at 230 nm. To

identify impurity, the 260/230 ratio and 260/280 ratio were calculated. A 260/280 ratio of 2.0 and a 260/230 ratio of 2,0 – 2,2 are considered to show pure RNA [185].

3.2.5.3 DNA digestion (genomic DNA degradation)

For a precise RNA measurement, it is important to prevent DNA contamination. The DNAse1 amplification grade kit (Sigma-Aldrich) was used for digestion and elimination of DNA in samples.

For this purpose, the following contents were added to a tube cooled on ice:

1 µg RNA sample

1 µl 10x DNase 1 Reaction Buffer

1 µl DNase 1, Amp Grade, 1U/µl

Nuclease free water up to a total volume of 10 µl

The tubes were spun down to create a homogeneous mixture and incubated for 15 min at room temperature. To inactivate the DNAse1, 1µl of 25mM EDTA solution was admixed and after centrifugation the samples were incubated at 70°C for 10 min. To stop the reaction, mixtures were cooled down to 4°C. .

3.2.5.4 Reverse transcription of RNA (cDNA generation)

To analyze gene expression with real time polymerase chain reaction (RT-PCR), mRNA needs to be transcribed into double-strand complementary DNA (cDNA) before. The generation of cDNA was realized using the iScript cDNA synthesis kit (Bio-Rad). Following contents were added to a tube and centrifuged to obtain an equable mixture:

1 µg RNA

4 µl iScript reaction mix

1µl reverse transcriptase

4 µl nuclease-free water

To synthesize cDNA, the mixture was incubated at the Thermocycler (Eppendorf) with the program stated below, after completion the cDNA was stored at -20°C:

5 min	25°C
30 min	42°C
5 min	85°C
(optional) hold at 4°C	

3.2.5.5 Real-time polymerase chain reaction (RT-PCR)

RT-PCR is a method to quantify the amount of RNA within a sample. Here, the expression levels of genes of interest were monitored by quantitative PCR based on Taqman chemistry [186].

For RT-PCR, a TaqMan probe-based system (Life Technologies) was used, working with a green fluorescent dye reporting DNA amplification. The TaqMan system consists of sequence specific reporter probes labeled with a fluorescent dye on their 5´end and a quencher on their 3´end, suppressing the reporter signal when in close proximity. Primers and probes bind to the target sequence of the template during the annealing step and by heating the samples DNA polymerase starts elongation of the primers. Attaining the probes 5´end, DNA polymerases will eliminate it through its intrinsic 5´to 3´exonuclease activity resulting in a spatial separation of reporter and quencher. Consequently, suppression of the reporter is abrogated, and the fluorescent signal can be monitored and reported after each cycle. Thus, increasing amounts of amplicons lead to a proportional increase of fluorescence intensity.

For this approach working solutions for each target gene were prepared according to the manufacturer´s protocol:

12,5 µl	TaqMan Gene expression Master Mix (BioRad)
1,25 µl	ABI Sondenmix
6,25 µl	nuclease free water

96-well PCR plates were loaded with 5µl cDNA of each sample diluted 1:10 in nuclease free water per well, 20 µl of working solution were added and centrifuged to ensure a

good mixture of all contents. For the custom-made PCR array, plates containing primers for the genes of interest were provided by the producer and processed identically.
RT-PCR was performed using the iCycler™ Real Time PCR detection system (Bio-Rad) with a defined program:

Cycle 1	(1x)		
	Step 1:	50°C	2 min
Cycle 2	(1x)		
	Step 1:	95°C	10 min
Cycle 3	(40x)		
	Step 1:	95°C	15 sec
	Step 2:	60°C	1 min
Cycle 4	(1x)		
	Step 1:	15°C	HOLD

All samples were run in triplicates in order to prevent incorrect measurement. The reported signal was used to calculate the original DNA copy number.

To avoid incorrect calculation, the differentiation between unspecific fluorescence and significant increase of the signal which represents relevant amplification is crucial. Therefore, a threshold level for the detection of reporter fluorescence is set slightly above the background signal. The cycle at which the signal exceeds the threshold level is denominated threshold cycle (Ct). Quantification of the initial amount of DNA was performed using the ΔCt-method. The Ct value of a house keeping gene like Glycerinaldehyd-3-phosphate-Dehydrogenase (GAPDH) acts as reference gene for normalization of the target genes Ct value. Relative expression changes were presented as $2^{-\Delta Ct}$.

3.2.6 Histology

3.2.6.1 Hematoxylin and Eosin staining (HE staining)

Hematoxylin and Eosin staining was performed to get a first impression of the cardiac structure, cardiomyocyte size and an idea about present cells.

Cardiac tissue frozen in TissueTek® (Sakura Finetek) was sliced into 15µm slices and applied to an object slide. After drying overnight, the tissue was prepared for staining. Slides were submerged into PBS solution for 3 minutes to wash away Tissue Tec. Frozen cryosections were thawed for 1 hour in advance. Then, slides were stained in hemalaun solution for 10 minutes and subsequently washed in a bath of circulating, running tap water for another 10 minutes. After washing in Aqua destillata, slides were incubated in eosin for 7 min and consecutively washed again. To dehydrate the sections, an ascending alcohol series consisting of ethanol 50%, 75% and 90% was used and the tissue was incubated for 2 min respectively. Finally, slides were transferred into xylol/ethanol (1:1), xylol and rotihistol I+II solutions for 5 min each, before being mounted with Entellan and stored at room temperature.

3.2.6.2 Picrosirius red staining (PSR staining)

Picrosirius red is a dye binding to collagen fibers. Cardiac sections of young, adult and aged mice were stained to get an impression of cardiac fibrosis.

First, the cardiac tissue frozen in TissueTek® (Sakura Finetek) was sliced into 15 µm slices, applied to an object slide and dried overnight. Frozen cryosections were thawed for 4 h before staining. For the staining, slides were incubated in PSR solution for 20 min and subsequently washed in aqua destillata by dipping it 2 to 3 times into 3 fresh water baths. Next, the cardiac tissue was dehydrated using ascending alcohol series with ethanol 50%, 75% and 99% for 2 minutes respectively. Finally, slides were transferred into xylol/ethanol (1:1), xylol and rotihistol I+II for 5 min each, before being mounted with Entellan and stored at room temperature.

3.2.6.3 Immunofluorescence staining of cardiac sections

Immunofluorescence microscopy is a method to visualize cells and cell components using fluorochrome- labeled antibodies binding to specific cell characteristics or receptors. Fluorophores are excited with light of specific wave length causing them to emit light in a defined quality which is recorded by a detector. With an appropriate combination of fluorochromes and filters, the simultaneous visualization of different targets and cell components is possible.

Here, a number of immunofluorescence stainings was performed to investigate the lymphocyte and macrophage distribution in the heart under steady state conditions. Cardiac tissue frozen in TissueTek® (Sakura Finetek) was sliced into 5 µm slices, applied to an object slide and dried over night at room temperature. The tissue was washed in PBS two times for 5 min in order to remove TissueTek® (Sakura Finetek) before being incubated in formaldehyde (4%) for 10 min for fixation. After washing another three times for 5 min in PBS (from here: washing step), a blocking step preventing unspecific binding was performed by covering the tissue with goat serum (3%) diluted in PBS for 30 min. For the staining, the tissue was then incubated for 1 hour at room temperature with the primary antibody binding to cell characteristics specific for one subpopulation. Antibodies were chosen depending on the approach and diluted in goat serum (3%). CD 68 (1:100) was used to detect macrophages, B220 (1:100) for B-cells, and CD3ε (1:50) for T-cells. Afterwards a washing step followed. To visualize the cells, a fluorescence labeled secondary antibody binding to the primary one was applied to the slides next. Besides Anti-mouse IgM (Alexa 555) and Anti-mouse IgG (Alexa 488), phalloidin-Atto 488 (1:200) was used to stain fibrillar actin in order to illustrate cardiomyocyte background. After 25 min, a drop of DAPI solution was added for nuclear staining, surplus solution was washed away. In the end, sections were mounted with Mowiol and stored in the dark at -4°C.

3.2.6.4 Wheat Germ Agglutinin staining

WGA (wheat germ agglutinin) staining was performed to assess cardiomyocyte size. WGA is a lectin binding to cardiomyocytes surface, in our approach labeled with a fluorophore to make it visible in fluorescence microscopy.

A fixation step was performed as described in "immunofluorescence staining" above. To prevent false positive binding the tissue was covered with Carbo-Free Blocking Solution® (Vector Laboratories) diluted 1:10 for 30 min. To remove blocking solution, a washing step was performed. Next, the sections were covered for 30 min with WGA conjugate diluted 1:5000 in blocking buffer and fluorophore-labeled phalloidin to visualize fibrillar actin. To stain the nuclei, a drop of DAPI solution was added 5 min before the end of incubation time. Before mounting the sections with Mowiol, tissue was washed for the last time. The slides were stored in the dark at 4°C.

3.2.6.5 Light Sheet Fluorescence Microscopy

One aim of our study was to learn about the lymphocyte distribution in a physiological, healthy heart at different ages. Therefore, we performed light sheet fluorescence microscopy as a method offering the possibility to examine a whole, unsliced organ histologically.

To prepare the hearts, mice were anesthetized and euthanized and 40IU heparin were injected intaperitoneally to prevent blood coagulation. Hearts were excised entirely preserving the aortic arch. Subsequently, organs were perfused retrograde via aorta, first with PBS to clean them from blood and second with formaldehyde 4% for 2 h for fixation of the tissue. Next, the hearts were washed in PBS for 15 min twice. For further preparation, hearts were bleached for 30 min using 15% hydrogen peroxide in methanol followed by a washing step in PBS. Then the tissue was blocked with 2% FCS (in PBS) and in 0.1% Triton-X (in PBS) for 24 h in 4°C. Hearts were again washed with PBS. Next, samples were incubated with anti-CD45-Alexa®647 (1:100 in PBS with 0.1% Triton X) for 72 h in order to stain leukocytes before washing in PBS again. The tissue

was then dehydrated in an ascending alcohol series consisting of ethanol 30%, 50%, 75% and 90% at room temperature for 2 h respectively. In the end, it was left in 100% ethanol overnight. Afterwards a solution of Benzyl alcohol and Benzyl benzoate (1:2, BABB) was prepared. Hearts were put into a Falcon with n-Hexan for 2 h. n-Hexan was then stepwise replaced by BABB. Hearts were incubated in BABB for at least 24 h. The result is an optically transparent organ which is stuck to a glass rod and positioned on a movable stage.

3.2.6.6 Measurement of cardiomyocyte size

To measure cardiomyocyte size, tissue slices where stained with HE and pictures of the tissue were recorded using the Axioskop microscope and a high-resolution camera. Afterwards, measurements were conducted using Image J. The circumference of 15-20 cardiomyocytes per slice was measured and the cross-section area calculated. Five slices per animal were analyzed. The average cross-section area was calculated for each animal. All measurements were performed by the same person.

3.2.6.7 Image acquisition

Bright field microscopy to examine tissue stained with HE, PSR or WGA staining was performed using an Axioskop 2plus (Zeiss). Immunofluorescence images were acquired using an Axio Imager Z1m (Zeiss) epifluorescence microscope with appropriate filter sets.

3.2.7 Detection of autoantibodies

Two different experimental setups were performed investigating the existence of heart specific autoantibodies. First, autoantibodies were visualized in a histological approach using fluorescent dyes. Second, indirect Enzyme-linked Immunosorbent Assay (ELISA) was practiced to detect myosin-specific autoantibodies.

3.2.7.1 Immunofluorescence detection of heart-specific autoantibodies

For the detection of heart-specific autoantibodies via immunofluorescence histology, hearts from B-cell deficient mice were used. The resulting absence of antibodies was required to prevent falsification of the results by binding through donors' antibodies.

Cardiac sections were prepared for staining as described in 3.2.6.3, fixated with formalin 4% for 10 min at room temperature and then blocked with Carbo-Free Blocking Solution® (Vector Laboratories) for 30 min. Plasma obtained from tested animal groups was diluted 1:20 in blocking buffer and subsequently added to the sections for 1 h at RT. After a washing step, the heart slices were incubated with anti-mouse IgM-Alexa®555 (1:200) and anti-mouse IgG-Alexa®488 (1:200) for 1 hour at room temperature to detect the different autoantibodies reacting against cardiac antigens present in the plasma of young versus aged mice. For visualization of the cardiomyocyte surface, WGA-Alexa®647 (1:500) was utilized. All images were acquired using the Axio Imager Z1m (Zeiss) with the same exposure time to provide comparable conditions.

3.2.7.2 Enzyme-linked Immunosorbent Assay (ELISA)

Next, we performed indirect ELISA to assess the myosin-specific antibody titers in the plasma of young versus aged mice.

ELISA plates (R&D) were coated with 4 µg myosin per well, diluted in 100 µl PBS containing Carbonate coating Buffer pH 9,5 (Biolegend), overnight at 4°C. After

incubation, plates were washed using PBS with 0,05% Tween®20 (Sigma-Aldrich), from here washing solution, and subsequently blocked with PBS containing 1% non-fat dry milk for 1 h at room temperature. The blocking solution was discarded, and mouse plasma diluted in PBS with 1% non-fat dry milk was added into the wells in serial dilutions of 1:200, 1:400, 1:800, 1:1600, 1:3200, 1:6400, 1:12800 and 1:25600 for an incubation time of 1 hour. Afterwards, plates were washed 6 times to ensure elimination of serum before adding a biotinylated goat-anti-mouse IgG antibody conjugated with horseradish peroxidase streptavidin (HRP) in a dilution of 1:6000 for 1 h at RT. To remove unbound IgG antibodies, the plate was washed 5 times. Next, we added Tetramethylbenzidine, an HRP substrate to develop a colorimetric reaction as read out for myosin- specific antibodies. After 20 min the reaction was stopped with sulfuric acid, turning the color from blue to yellow.

For the quantification of antigen-antibody complexes, representing the amount of anti-myosin antibodies in murine serum, extinction was measured at 450nm in a 96-well plate ELISA reader (Dynex MRX Revelation TC 96 (Magellan Bioscience)).

3.2.8 Statistics

Statistical analyses were performed using Graph Pad Prism (7.0.). The graphs present results in mean ± SEM (standard error of mean) obtained from *n* animals (*n* is indicated in each figure legend).

For the comparison of two groups, an unpaired t-test was performed. For multiple comparisons, one-way ANOVA followed by Dunnett´s post hoc test was conducted when one independent variable in different groups had to be compared. Two-way ANOVA followed by Turkey post hoc test was used when two independent variables had to be analyzed in different groups.

Values were considered significantly different at $P<0.05$.

3.2.9 Permissions

Some graphs or pictures containing results were published in the journal ‘Proceedings of the National Academy of Sciences” before. The journal provides permission for authors to include published data as part of their dissertation. Further figures were created by the author. For some figures, patterns provided by Motifolio Illustration Toolkit (Maryland, USA) were used.

4 RESULTS

4.1 THE HEALTHY MYOCARDIUM HARBORS ALL MAJOR LEUKOCYTE POPULATIONS UNDER STEADY-STATE CONDITIONS

To investigate the presence of different leukocyte populations in the myocardium under physiological conditions, primarily flow cytometry analyses were performed. Cell suspensions from murine hearts were prepared as described above and compared with suspensions from murine skeletal muscle (M. gastrocnemius) which were processed identically. 2-3 months old mice were examined. A considerable population of leukocytes representing all major subsets was detected in the heart. In order to determine absolute cell numbers, a bead-based flow cytometry strategy was used and the acquisition of approximately 10^3 leukocytes per milligram cardiac tissue appeared to be possible. Comparing cardiac to skeletal muscle, 12-fold more leukocytes per mg tissue were found to be located in the heart than in periphery (Fig. 6A).

For a more detailed differentiation of the leukocyte population, a gating strategy for flow cytometry analysis was established, facilitating to distinguish between cardiac leukocyte subsets among all single cells. Overall, monocytes/macrophages (defined as $CD45^+$, $CD11b^+$, $Ly6G^-$), granulocytes (defined as $CD45^+$, $CD11b^+$, $Ly6G^+$), B-cells (defined as $CD45^+$, $CD11b^-$, $Ly6G^-$, $B220^+$) and T-cells (defined as $CD45^+$, $CD11b^-$, $Ly6G^-$, $CD3\varepsilon^+$) were identified and monocytes/macrophages represented the main fraction of cardiac leukocytes followed by B-cells, T-cells and granulocytes (Fig. 6B).

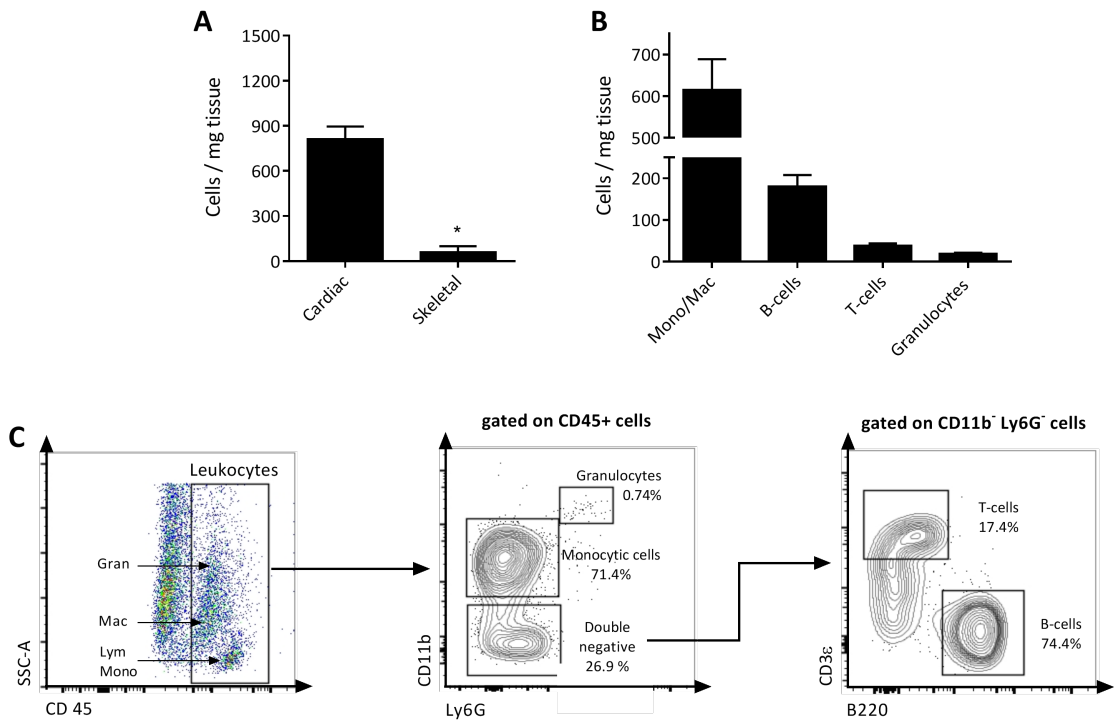

Fig. 6: Leukocyte populations within the healthy, steady-state myocardium of 2-3 months old mice analyzed with flow cytometry

A: Cardiac muscle contains an abundant leukocyte population compared to skeletal muscle, the same digestion and staining protocol was applied to both tissue samples (n=6-8). **B**: Subset analysis revealed macrophages as the most frequent leukocyte subset (614 ± 74 cells/mg of tissue), followed by B-cells (180 ± 28 cells/mg tissue), T-cells (38 ± 6 cells/mg of tissue), and granulocytes (19 ± 2 cells/mg of tissue) (n=6-8). **C**: Gating strategy applied to examine cardiac resident leukocyte populations. $CD45^+$ cells were subdivided using CD11b and Ly6G expression. The population of $CD11b^-$ and $Ly6G^-$ cells was further split up into $CD3\varepsilon^+$ cells and $B220^+$ cells. Leukocyte subsets were defined as macrophages = $CD45^+$, $CD11b^+$, $Ly6G^-$, granulocytes = $CD45^+$, $CD11b^+$, $Ly6G^+$, T-cells = $CD45^+$, $CD11b^-$, $Ly6G^-$, $CD3\varepsilon^+$ and B-cells = $CD45^+$, $CD11b^-$, $Ly6G^-$, $B220^+$. *P<0,05

Knowing the heart to be a well perfused organ and considering a defined population of leukocytes in blood, a two-stage staining was performed to distinguish the fraction of leukocytes that may be in contact with the coronary circulation and those, which are truly located in the myocardial parenchyma. First, an anti-CD45-antibody (labeled with fluorochrome eF450) was applied to stain intravascular leukocytes by perfusion of an isolated heart. Second, hearts were digested according to our protocol and stained with an anti-CD45-antibody marked to a different fluorochrome (FITC) to allow a precise discrimination of leukocyte localization. Flow cytometry analysis

revealed only about 13% of all cardiac leukocytes to be in direct contact with the circulation (Fig. 7B).

To further determine the leukocyte distribution within the myocardium, immunofluorescence microscopy was performed. Leukocytes turned out to be widely spread in the entire myocardium. Supporting previous findings, macrophages turned out to be the major represented group, but also smaller numbers of B-cells and T-cells were detectable. Visually, there was no general accumulation of leukocytes at any localization although monocytic cells were suggestive of being increased close to mitral valves (Fig. 7C).

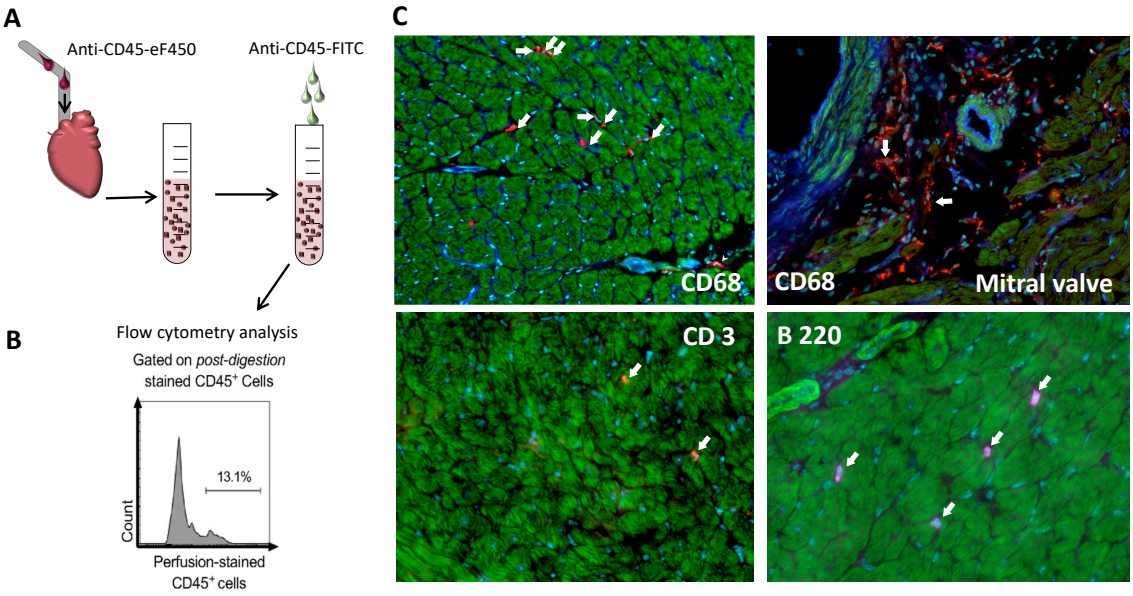

Fig. 7: Distribution of cardiac leukocytes
A: Murine hearts were stained in two steps utilizing differently labeled anti-CD45$^+$-antibodies to achieve discrimination between circulating and resident leukocytes. Intravascular leukocytes were defined as CD45-eF450$^+$ CD45-FITC$^-$ cells, whereas parenchymal leukocytes were CD45-eF450$^-$ CD45-FITC$^+$ cells. **B**: Flow cytometric measurement revealed about 13,1% of all leukocytes having intravascular origin.
C: Representative images of immunofluorescence microscopy studies of murine hearts. Cardiomyocytes were stained with Phalloidin-Atto 488 (green), nuclei using DAPI (blue) and leukocyte subsets appear red/magenta. The white arrows highlight leukocytes. Macrophages were defined as CD68$^+$, T-cells as CD3ε$^+$, B-cells were CD45/B220$^+$. Magnification: CD68 and CD3ε, 200 x; CD45/B220, 400×.

Standard histological methods only allow to examine a small section of myocardial tissue. Moreover, cell loss was expected to happen during cardiac tissue preparation and the staining process previous to flow cytometric measurements. To obtain a more accurate impression of absolute cell numbers, to achieve a more extensive view of the leukocyte distribution in the whole heart, and to investigate if leukocytes accumulate at specific areas, light sheet fluorescence microscopy (LSFM) was implemented. Unsliced entire hearts of non-manipulated, healthy mice were scanned, and 3D reconstructions were generated. Indeed, 3D reconstructions clearly depicted a wide, constant leukocyte distribution in the whole heart (Fig. 8). No myocardial areas with an outstanding accumulation of leukocytes were observed. In fact, one advantage of the LSFM approach was a reduction of cell loss during the preparation process. An absolute cell number of more than 3000 $CD45^+$ cells per mm^3 intact myocardium was measured, exceeding the recruitment in flow cytometry analysis where about 800 cells/mg tissue were counted.

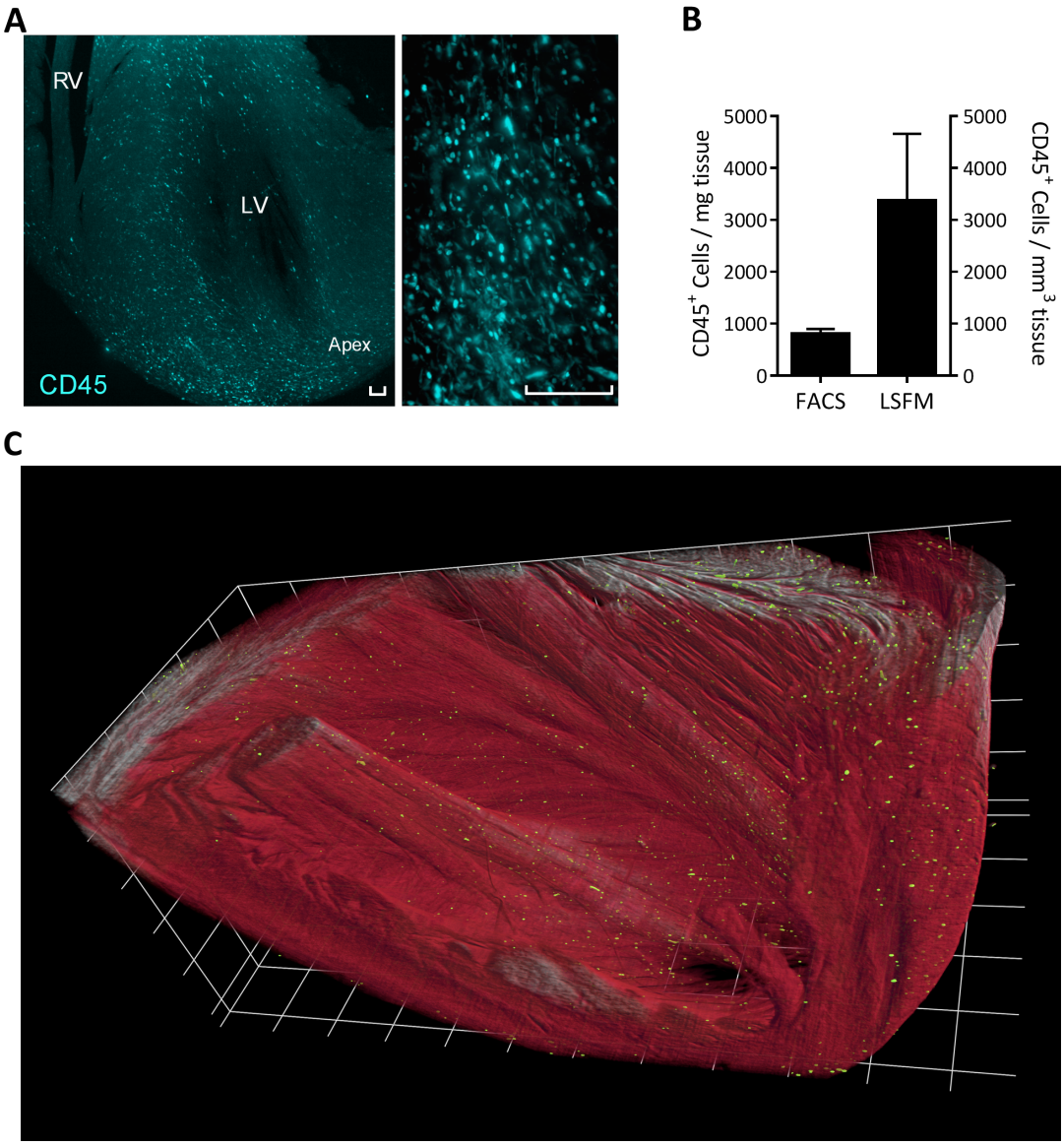

Fig. 8: Detection of cardiac leukocytes using light sheet fluorescence microscopy (LSFM)
A: Representative LSFM pictures of whole murine hearts stained with anti-CD45 antibodies. A Z-stack reconstruction spanning large myocardial areas in the longitudinal axis shows abundant resident leukocyte populations (*Left*, 150-µm Z axis, 5× magnification; *Right*, 1.5-mm *z* axis, 26× magnification). Scale bars: 50µm. RV= right ventricle, LV= left ventricle. **B:** Cell numbers of cardiac-resident leukocytes ($CD45^+$) detected either using a tissue digestion–flow cytometry protocol or LSFM (n=4-12). **C:** 3D reconstruction of the heart based on a calculation using single pictures as shown under A. Lymphocytes are visualized in green color (5x magnification, grid size 500µm per mesh). The reconstruction was generated by the group of Prof. K. Heinze, Würzburg.

4.2 THE TISSUE RESIDENT LEUKOCYTE COMPOSITION SHIFTS DURING THE MYOCARDIAL AGING PROCESS

In order to investigate possible differences between the leukocyte compositions in young and aged hearts, myocardial tissue from 2-3 months old mice (young animals), 6-8 months old mice (adult animals) and 12-15 months old mice (aged animals) was analyzed. Flow cytometry experiments showed distinct changes in the myocardial leukocyte composition during aging. A significant decrement of the total macrophage population in aged mice was observed, whereas the frequency of F4/80$^+$/CD206$^+$ and F4/80$^+$/206$^-$ macrophage subsets remained unaltered (Fig. 9A-C). Besides, the CCR2 expression on cardiac macrophages within the 12-15 months old group was slightly increased compared to the young group, indicating a potential replenishment of tissue resident macrophages by monocyte derived cells (Fig. 9D+E). Contemporaneous, the number of granulocytes in the myocardial tissue increased significantly with aging (Fig. 9A).

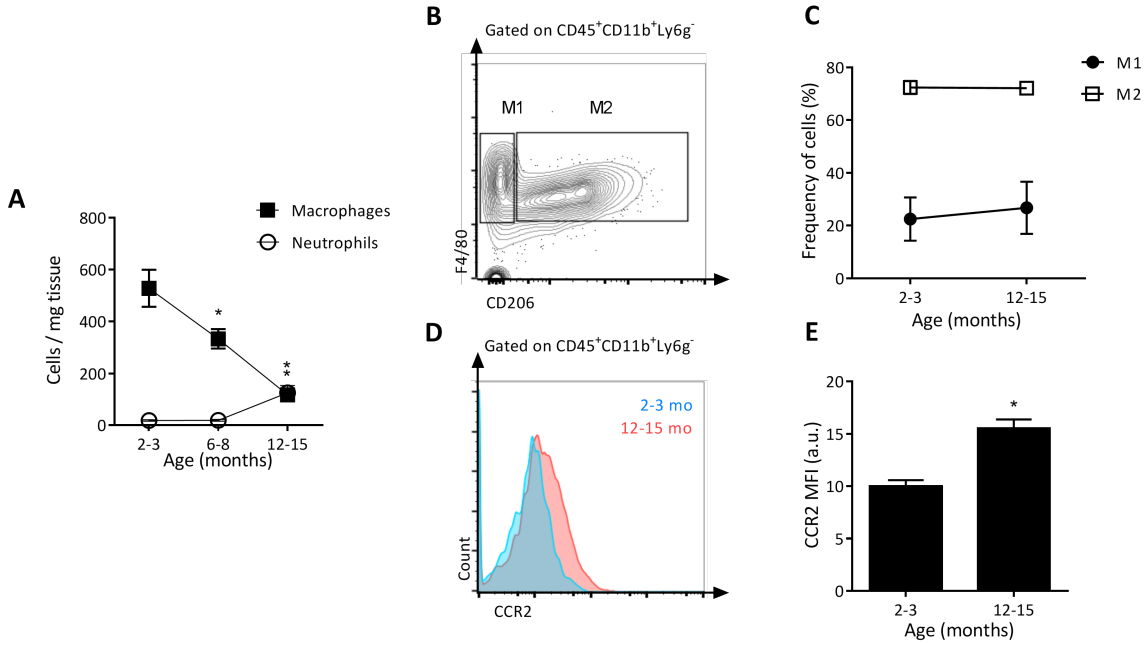

Fig. 9: Age related fluctuations in myocardial macrophage and granulocyte populations
Phenotypic characterization of cardiac resident leukocytes using flow cytometry. **A**: The total amount of macrophages and neutrophils shifts during aging. **B-E**: More detailed analysis of macrophage populations. **B**: Monocytic CD11b$^+$ Ly6g$^-$cells were further gated into F4/80$^+$ CD206$^-$ (M1) and F4/80$^+$ CD206$^+$ (M2) macrophages. **C**: Frequency of M1 and M2 macrophages among monocytic cells. **D** and **E**: Representative histogram and analysis depict the surface expression of CCR2 on cardiac macrophages at different times (n=5-8). *P<0,05, ** shows P<0,05 for overlapping lines.

Investigating the B-cell and T-cell populations, no important alterations regarding the absolute amount were found during the aging process. A more detailed characterization of the T-cell subsets revealed a higher frequency of $CD8^+$ cells, whereas the $CD4^+$ T-cell portion was reduced, resulting in an age-related decrease of CD4:CD8 ratio (Fig. 10D). For a more precise analysis of the B-cell compartment, IgM/IgD expression was used for phenotypic characterization and discrimination of the two major subtypes of mature follicular B-cells (defined as $IgD^{high}IgM^{low}$) and immature marginal zone B-cells (defined as $IgD^{ow}IgM^{high}$). Constant frequencies of the subtypes were measured in all ages (Fig. 10B).

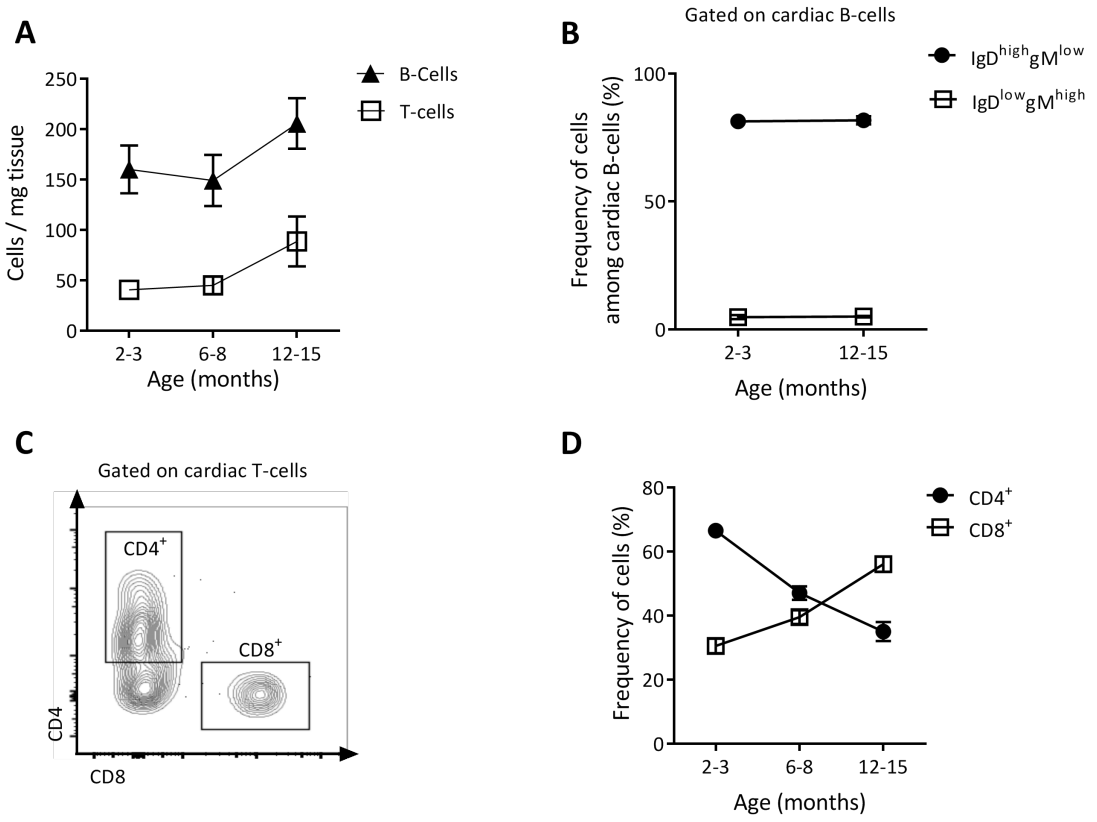

Fig. 10: Trends for cardiac T-cell and B-cell populations during aging
Characterization of T- and B-cells via flow cytometry. **A**: Time dependent fluctuations of absolute T-cell and B-cell numbers (n=5-8). **B:** B-cells were split into $IgD^{high}IgM^{low}$ (mainly follicular, mature B-cells) and $IgG^{low}IgM^{high}$ (mainly immature B-cells) subsets. Stable frequencies were observed (n=5). **C:** Representative plot showing differentiation of $CD4^+$ and $CD8^+$ T-cells. **D:** Frequencies of $CD4^+$ and $CD8^+$ cells among T-cells during aging (n=4-6).

4.3 SHIFTS IN MYOCARDIAL LEUKOCYTE COMPOSITION OCCUR SIMULTANEOUSLY WITH FUNCTIONAL AND STRUCTURAL CARDIAC ALTERATIONS

A number of tests investigating functional characteristics and structural features were performed to determine the cardiac development during aging. Echocardiographic examinations of functional parameters revealed an age related decrease of fraction shortening (FS) (young animals: 63.76 ± 1.35% vs. aged animals: 51.22 ± 3.51%, $P<0.05$), in combination with an increase of end-diastolic anterior wall thickness (young animals: 0.067± 0.003mm vs. aged animals: 0.084 ± 0.005mm, $P<0.05$) and end-diastolic area (young animals: 7.43 ± 0.41mm vs. aged animals 9.58 ± 0,35mm, $P<0.05$), pointing to a reduction of cardiac contractibility, augmented stiffness and higher volume stress in aged mice (Fig. 11A-E). 15,7% of the elderly mice presented with a FS<40% which is regarded as a clinically significant phenotype. These findings were strengthened when measuring end-diastolic volume (EDV) and ejection fraction (EF) by using a pressure-volume conductance catheter positioned in the left ventricle chamber. The results reported a lower EF (young animals: 58.57 ± 4.18% vs. aged animals: 39.27 ± 4.61%) and a higher EDV (young animals: 42.3 ± 2.01µl vs. aged animals: 64.92 ± 5.55µl) in aged animals (Fig. 11F-G).

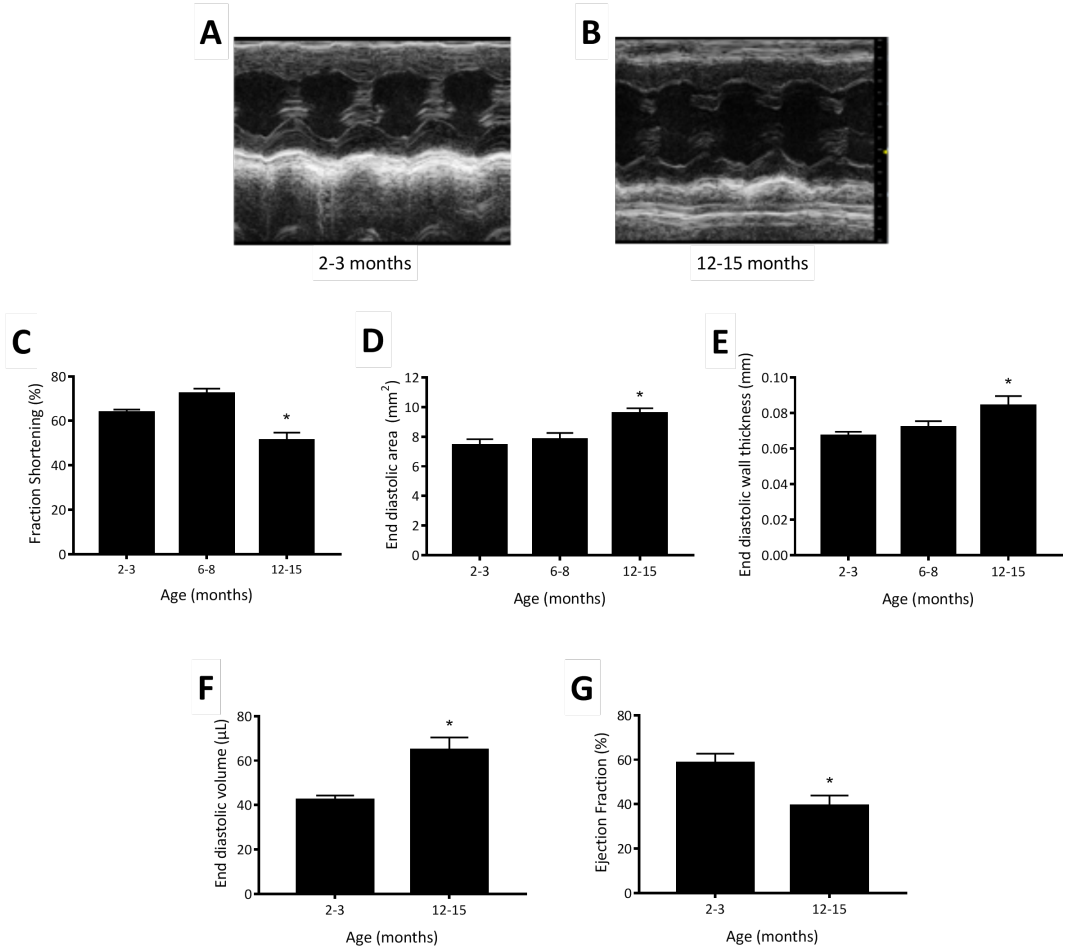

Fig. 11: Impact of myocardial aging on cardiac function (Myocardial function Folder)
A and **B**: Representative echocardiographic M-mode images of 2-3 month (A) and 12-15 month (B) old mice. **C-E**: Parameters of cardiac function investigated via echocardiography. Fraction shortening (C) was significantly reduced in elderly mice, whereas end diastolic area (D) and wall thickness (E) presented increased (n=6-19). **F-G**: Hemodynamic measurements revealed a higher end diastolic volume and lower ejection fraction in old compared to young mice (n=5-9). *P<0,05 in comparison to young animals.

As cardiac functional deterioration originates from structural changes, myocardial structure was assessed with histological approaches. An increase of interstitial collagen in the myocardium and the enlargement of cardiomyocyte cross sectional area in senescent hearts were observed (Fig. 12B-D). In accordance with this, a higher heart weight/ tibia length ratio indicating cardiac hypertrophy was measured in elderly mice (Fig. 12A).

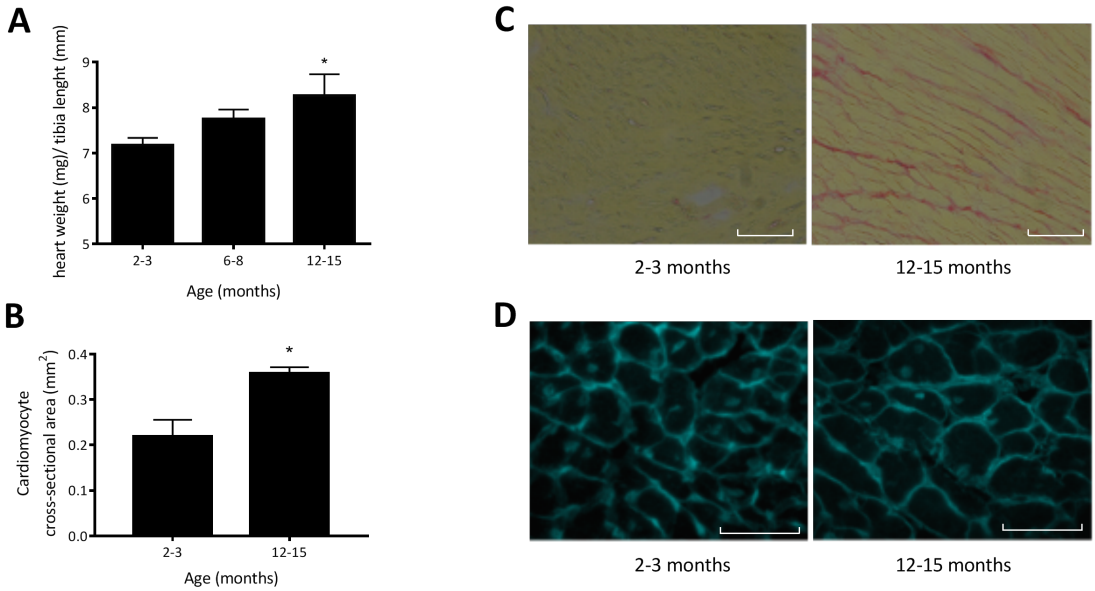

Fig. 12: Age-related structural alterations of the heart (Myocardial function Folder)
A: Heart weight/tibia length ratio was measured at three time points in a 15 months period, indicating alterations towards cardiac hypertrophy (n= 5-9). **B:** Results of cardiomyocyte cross-section area measurements (n=3-4). **C-D:** Representative pictures of sliced hearts stained with Picrosirius red to visualize collagen (C) and WGA staining to show cardiomyocyte surface (D). Scale bars 50µm. *P<0,05 in comparison with young controls.

The structural and histological changes prompted to investigate if the expression of related genes reflected similar changes. In accordance with the histological findings, gene expression levels of pro- hypertrophic and pro- fibrotic genes were upregulated significantly in aged mice (Fig. 13).

Concluding, structural remodeling and functional decline occur at the same time as leukocyte compositions shift in the myocardial tissue, indicating a possible correlation between both.

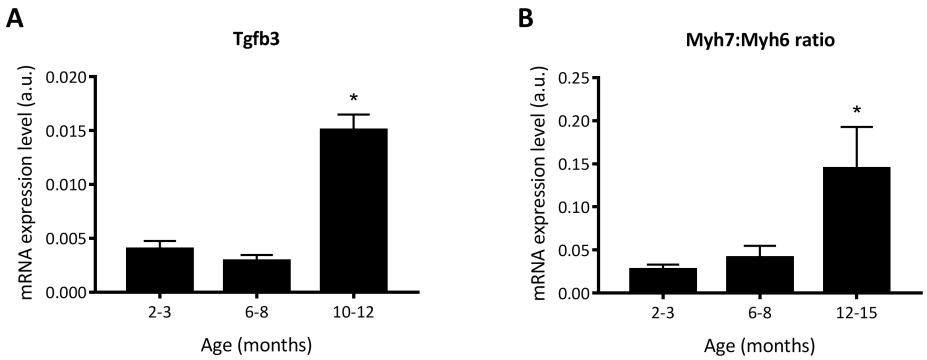

Fig. 13: Expression levels of structure associated genes measured with qPCR
A: Myocardial Transforming growth factor beta 3 (Tgfb 3) gene expression level increases during aging. **B:** Myosin heavy chain 7 (Myh7) to Myosin heavy chain 6 ratio is higher in elderly mice. (n=4-8). *P<0,05 compared to young controls.

4.4 GENE EXPRESSION ANALYSIS INDICATE INCREASED INFLAMMATORY STATUS IN ELDERLY MICE

Considering changes in function, structure, leukocyte composition and first evidence of gene expression alterations, further investigations were done to analyze the molecular myocardial environment with focus on gene expression. A custom quantitative PCR (qPCR) array was designed to measure the expression levels of 45 selected, potentially relevant genes. Representative genes were chosen for different sectors including cardiac physiology and cell stress, inflammation and immunity, angiogenesis, and fibrosis. Later on, standard qPCR approaches with additional replicates were done to confirm the results.

The expression level of TNF, reflecting a pro-inflammatory status, was significantly higher in myocardial tissue of 12-15 months old mice compared to young animals. Similarly, Ccl2 (C-C motif chemokine ligand 2) related to monocyte recruitment and Cxcl1 (C-X-C motif ligand 1), a chemokine with neutrophil attracting properties, were significantly increased in elderly. Moreover, the gene expression of lymphocyte chemo attractants Cxcl13 (C-X-C motif chemokine ligand 13) and Ccl5 (C-C motif chemokine ligand 5), as well as of INF-γ (Interferon gamma), a key player in adaptive immunity, were significantly upregulated, pointing to a possible involvement of lymphocytes in the

myocardial aging process. Summarized, an increased immune activity and a pro-inflammatory status were observed in elderly (Fig. 14).

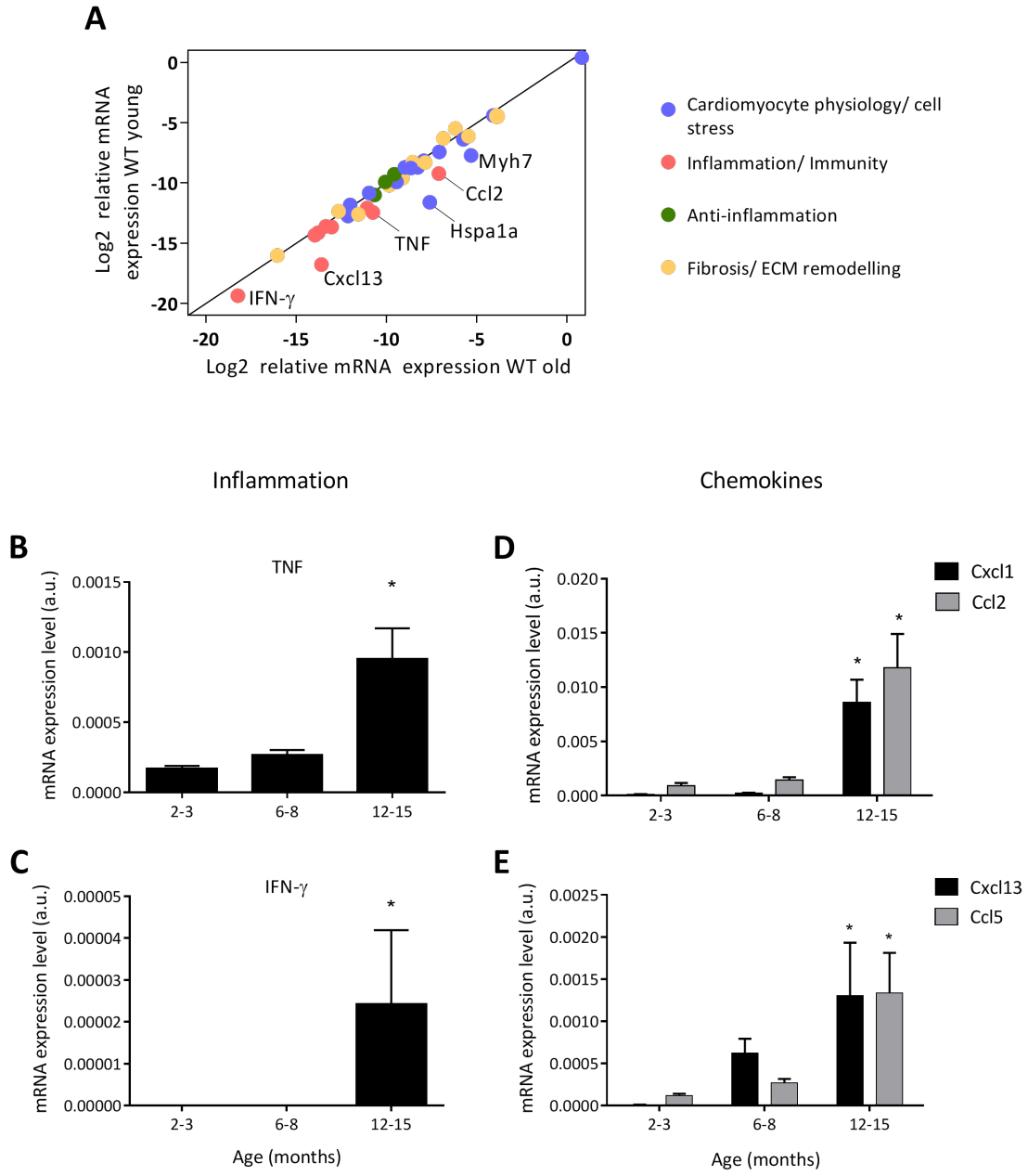

Fig. 14: Expression levels of genes linked to cell stress and inflammation in the myocardial environment
A: Scatter plot depicting normalized myocardial gene expression levels (Log2 relative gene expression) of naïve young (2-3 months) compared to old (12-15 months) mice. With a custom-made qPCR array 45 target and 3 housekeeping genes were examined. Pooled myocardial samples were testes in a single experiment (n=3). **B** and **C**: Representing inflammation associated genes mRNA expression levels of TNF and INF-γ were further tested with additional replicates. **D** and **E**: mRNA expression levels of chemokines related to adaptive immunity were further tested with additional replicates. **B-E**: qPCR was performed using samples from at least two independent experiments (n= 3-6). *P<0,05 in comparison with young controls

To assess which sort of environmental changes and cell stress situations might trigger or reinforce the process of myocardial aging and may contribute to senescence, cell stress genes were measured at different time points. The earliest alteration observed in 6 to 8 months old mice was a higher expression of GATA-binding protein 4 (Gata-4), which is upregulated under loading stress conditions [187]. Gene expression levels of Sirtuin 1 (Sirt1), responsive to redox stress, rose progressively during aging and Hspa1a (heat shock protein family a member 1a), associated with different cell stress conditions such as heat or tissue remodeling, were detected to be significantly higher in 12-15 months old mice compared to young animals. In contrast, no alteration of Hif1α (hypoxia inducible factor 1 alpha subunit) gene expression in myocardial tissue became apparent at any time suggesting that hypoxic stress might not be a mediator of myocardial senescence (Fig. 15). Altogether, age related cardiac functional impairment is associated with the gain of in situ inflammation and cell stress within the myocardium.

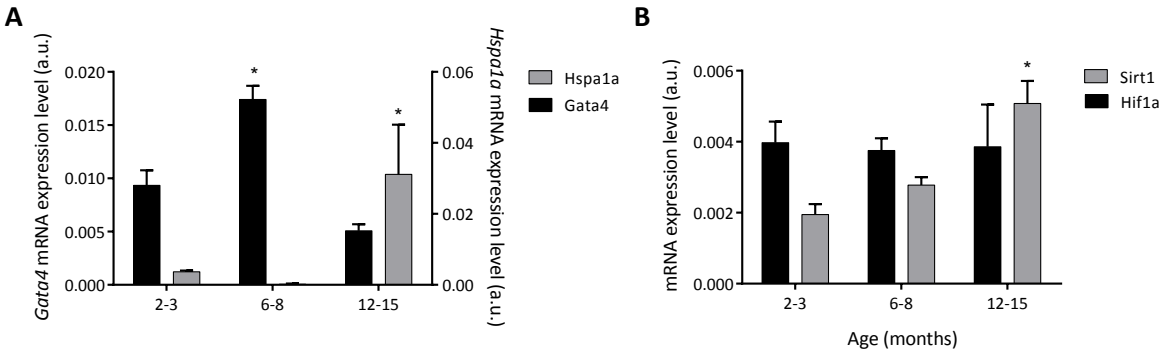

Fig. 15: Expression levels of cell stress related genes measured with qPCR
A and **B:** mRNA expression levels of heat shock protein family a member 1a (Hspa1-α), GATA-binding protein 4 (Gata4) (A), Sirtuin 1 (Sirt 1) and hypoxia inducible factor 1 alpha subunit (Hif 1a) (B) vary at different ages (n=4-8). *P<0,05 compared with young controls

4.5 SPONTANEOUS $CD4^+$ T-CELL ACTIVATION IN MEDIASTINAL LYMPH NODES OF AGED MICE

So far, a resident lymphocyte population under steady state conditions in the myocardium of healthy mice and rising levels of genes associated with inflammation and adaptive immunity had been observed during aging. Further experiments were arranged to further investigate the role of leukocytes in the context of myocardial senescence concrete. As lymph nodes are the major scene of lymphocyte activation, mediastinal heart draining lymph nodes were harvested from differently aged mice and lymphocyte populations were characterized carefully. As control, popliteal lymph nodes primarily draining hind limb skeletal muscle were examined.

At first sight, a macroscopic larger size of mediastinal lymph nodes compared to popliteal lymph nodes was conspicuous, most notably in aged mice. Measurements of the absolute cell numbers revealed distinctly higher values in mediastinal lymph nodes of aged mice compared to young ones, but also in comparison with cell numbers measured in popliteal lymph nodes. No increased cellularity was measured in popliteal lymphnodes. These findings suggest the immune activation occurring in elderly being a process with local focus on the heart (Fig. 16A). A more accurate characterization of the T-cell compartment showed a similar distribution of the overall T-cell population on $CD4^+$ and $CD8^+$ T-cells in both, mediastinal and popliteal lymph nodes of either age group (Fig. 16B+C). $CD4^+$ T-cells were beyond that divided into a subset of conventional T-cells (T_{conv}) and $FoxP3^+$ regulatory T-cells (T_{reg}). $CD4^+$ T-cells isolated from mediastinal lymph nodes were to a higher extent differentiated towards T_{conv}-cells in young and old mice respectively, implicating the T_{reg}-subset remaining rather small (Fig. 16D). In contrast, examinations of $CD4^+$ T-cells obtained from popliteal lymph nodes showed a significantly smaller portion of T_{conv} -cells with aging, whereas T_{reg}-frequencies were increased in 12-15 months old mice (Fig. 16E).

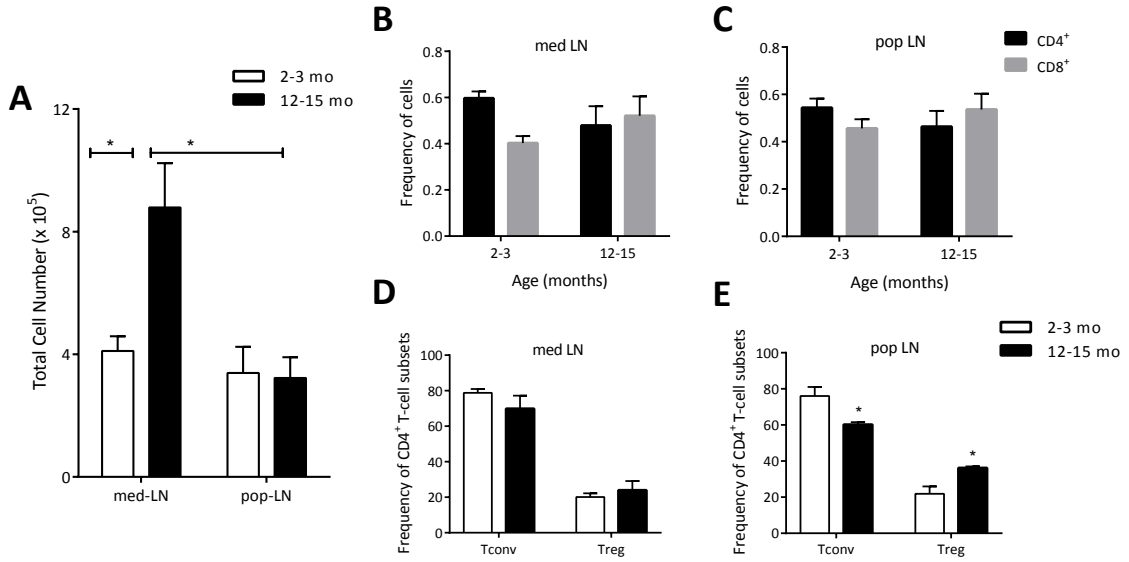

Fig. 16: Flow cytometry analyses of cell numbers and differentiation in mediastinal and popliteal lymph nodes

A: Total cell numbers isolated from mediastinal and popliteal lymph nodes of 2-3 months and 12-15 months old mice (n=8-9). **B** and **C:** Frequencies of $CD4^+$ T-cells and $CD8^+$ T-cells among the total T-cell population in mediastinal lymphnodes (B) and popliteal lymphnodes (C) of young and aged mice (n=3-5). **D** and **E**: Distribution of $CD4^+$ T-cells on conventional T-cells (T_{conv}) and regulatory T-cells (T_{reg}) regarding the mediastinal lymph node population (D) and popliteal lymph node population (E) at different times (n= 4-8). *P< 0,05 compared to young group or as indicated

Further flow cytometry analyses were performed to determine the activation status of above described T-cell populations. $CD4^+$ cells were differentiated by CD44 and CD62L surface expression, whereupon $CD44^{high}$ $CD62L^{low}$ $CD4^+$ T-cells were regarded as antigen experienced activated effector memory phenotype. In 12-15 months old mice, an obvious accumulation of $CD44^{high}$ $CD62L^{low}$ $CD4^+$ T-cells was observed in both lymph node stations that was more accentuated and significantly higher in mediastinal lymph nodes compared to popliteal lymph nodes (Fig. 17A+C). Among the antigen experienced T-cells, the frequency of $FoxP3^+$ T-cells was significantly reduced in mediastinal lymph nodes of aged mice, resulting in an altered T_{reg}:T_{conv} ratio shifted towards the T_{conv} subpopulation. A more precise examination revealed a significant increase of antigen experienced T_{conv}-cells being causative for this condition rather than a decrease of activated effector memory T_{reg}-cells (Fig. 17E+F).

Regarding popliteal lymphnodes, no changes in the portion of effector memory T_{conv}-cells became evident during time, whereas the ratio of activated effector memory T_{regs} was elevated in old mice. The majority of activated effector memory T-cells in both lymph node compartments were continuously Foxp3$^+$ regulatory T-cells suggesting an elevated necessity of regulatory, anti-inflammatory performance during the aging process in both localizations.

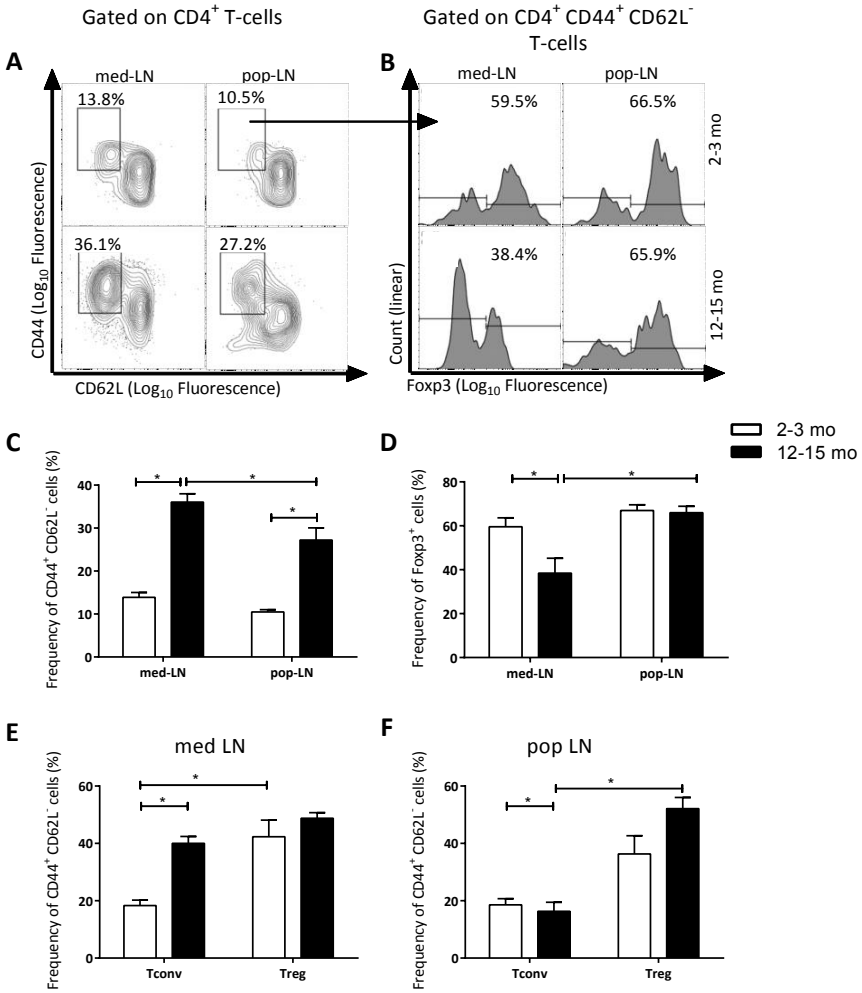

Fig. 17: CD4$^+$ T-cell populations and development during aging.
A: Representative flow cytometry plot reflecting the gating strategy to distinguish between CD44 and CD62L expression or absence on CD4$^+$ T-cells. B-F: Flow cytometry analysis of T-cell populations.
B: Quantitative analysis depicting the frequency of FoxP3$^+$ T-cells among CD4$^+$CD44$^+$CD62L$^-$ T-cells. **C:** Frequencies of CD44$^+$CD62L$^-$ T-cells (activated effector memory T-cells) among all T-cells in young and aged animals in both lymph node stations representing an accumulation of activated effector memory T-cells in elderly (n= 10-18). **D:** Analysis of FoxP3$^+$ regulatory T-cell frequencies among CD44$^+$CD62L$^-$ T-cells show a significant lower ratio of T_{regs} in mediastinal lymph nodes of 12-15 months old mice, whereas the ratio in popliteal lymph node remained stable (n= 4-8). **E** and **F**: Frequencies of CD44$^+$ T-cells among T_{conv} and T_{reg} were analyzed in mediastinal (med LN, E) and popliteal (pop LN, F) lymph nodes of young and old mice (n= 4-8). *P<0,05 compared to young controls or as indicated

In order to compare the findings observed in mediastinal lymph nodes with an additional lymph node side, the T-cell compartment of sub-iliac lymph nodes of young and aged mice was characterized. Similar to popliteal lymph nodes, aging was not accompanied by increased cellularity in sub-iliac lymph nodes. Moreover, age related alterations regarding the surface expression of CD44 and CD62L were closer to observations made for popliteal lymph nodes and divergent to findings made in mediastinal lymph nodes. In sub-iliac lymph nodes, the $CD44^{+}CD62L^{-}$ T-cell population was augmented in elderly and the ratio of $FoxP3^{+}$ T_{regs} among the effector memory compartment was not diminished but stable. Furthermore, the frequency of cells expressing the surface marker CXCR3, a chemokine receptor primarily detected on activated Th1-cells, was increased in old mice.

In summary, the results of sub-iliac lymph node analysis were more comparable to what was seen in popliteal lymph nodes than in mediastinal lymph nodes, reinforcing the consideration of shifts in mediastinal lymph node cell composition being site specific.

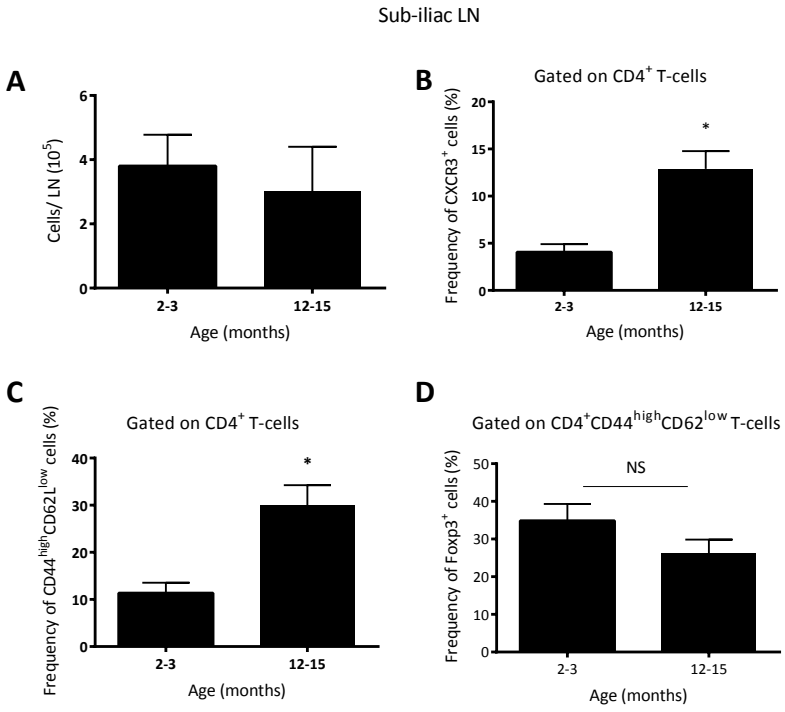

Fig. 18.: Characterization of the $CD4^{+}$ T-cell compartment in sub-iliacal lymph nodes
A: Total cell numbers isolated from sub iliac lymph nodes of young and old mice. **B**: Frequencies of $CXCR3^{+}$ expressing $CD4^{+}$ T-cells increase with aging. **C** and **D**: Analysis of the $CD44^{+}CD62L^{-}$ T-cell subset with aging (C) and Fox P^{+} T_{regs} among those (D) (n= 4-6). *P<0,05.

4.6 IN-VITRO STIMULATION REVEALS A PRO-INFLAMMATORY DIFFERENTIATION OF MEDIASTINAL T-CELLS

T-Cells were isolated from mediastinal and popliteal lymph nodes of young and aged mice and stimulated in vitro with phorbol 12-myristate 13 acetate (PMA) plus Ionomycin. $CD4^+$ T-cells harvested from mediastinal lymph nodes showed a significantly higher INF-γ production in aged animals compared to young animals and popliteal LN cells, where no increase was detected. Regarding the $CD8^+$ T-cell compartment, significantly higher numbers of INF-γ secreting cells were observed in both LN stations over time. Still, mediastinal lymph nodes contained significantly more INF-γ producing cells (Fig. 19 A+G).

In contrast, $CD4^+$ and $CD8^+$ T-cells from pop LN of aged mice showed most notable IL-10 response, whereas only a minor response in mediastinal LN and young animals has been measured. IL13 secretion after stimulation was hardly detectable regarding $CD4^+$ and $CD8^+$ T-cells in both LN stations.

The TNF production was slightly increased in T-cells of all LN stations in aged mice, indicating a slight generalized inflammation in old animals.

Furthermore, the surface expression of CXCR3 was upregulated in the elderly group in mediastinal lymph nodes and popliteal lymph nodes respectively. Still, the frequency of $CXCR3^+$ T-cells in mediastinal LN of old mice was nearly three times higher compared to popliteal lymph node populations of the same age, suggesting a polarization towards Th1-cell population.

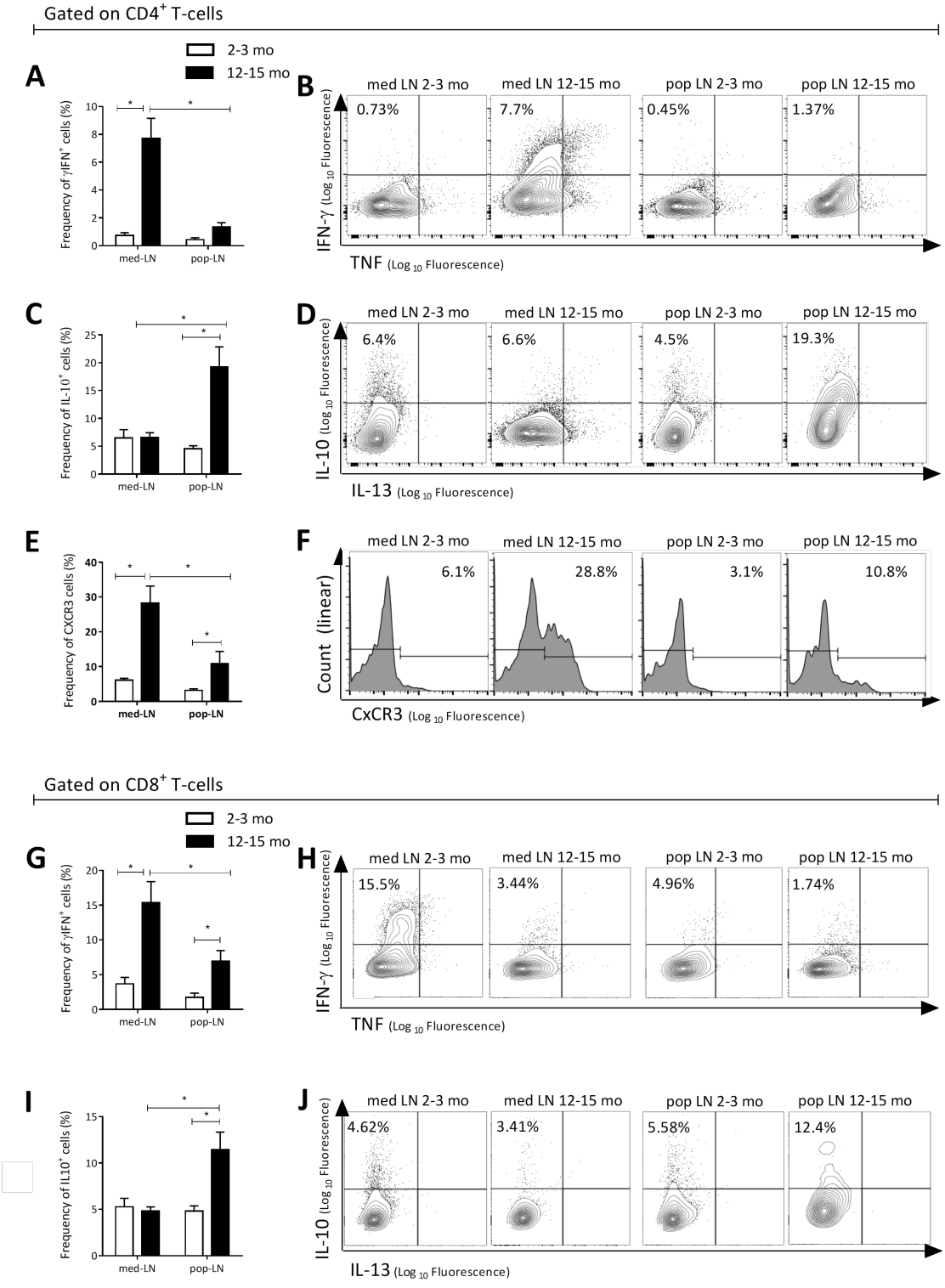

Fig. 19: Cytokine production of T-cells after stimulation with PMA plus ionomycin

T-cells were isolated from mediastinal and popliteal lymphnodes of young and aged mice and stimulated in vitro with PMA plus ionomycin. Frequencies of cytokine secreting cells were analyzed with flow cytometry. A-F show findings for $CD4^+$ T-cells, whereas G-J represent results for $CD8^+$ T-cells. **A**: $CD4^+$ T-cells harvested from mediastinal lymphnodes (med LN) of 12-15 months old mice produce distinctly higher levels of INF-γ compared with 2-3 months old mice and T-cells from popliteal lymph nodes (pop

LN). **B, D, H, J**: Representative flow cytometry plots showing INF-γ and TNF secretion (B and H) or IL10 and IL13 secretion (D and J). **C**: IL10 production was significantly increased in $CD4^+$ T-cells isolated from pop LN of aged mice. **E**: Frequencies of CXCR3 expressing $CD4^+$ T-cells was significantly upregulated in old mice. **F:** Representative flow cytometry plot for CXCR3 dependent cell count. **G:** $CD8^+$ T-cells isolated from 12-15 months old mice produce significantly higher levels compared with 2-3 months old mice. The production of med LN derived cells was additionally significantly higher than in T-cells from pop LN. **I**: IL10 production was significantly increased in $CD8^+$ T-cells isolated from pop LN of aged mice. (n= 5-8 per group). *P<0,05 compared as indicated.

4.7 HEART DIRECTED AUTOREACTIVITY ARISES WITH AGING

The observation that IFN-γ-producing $CD4^+$ effector T-cells accumulate in mediastinal lymph nodes raised the hypothesis of spontaneous heart directed autoimmunity being involved in myocardial aging. To detect heart specific IgM and IgG autoantibodies, plasma of young and old mice was incubated with heart slices from B-cell deficient and thereby antibody deficient mice. Autoantibodies binding to target antigens were visualized with green (IgG) and red (IgM) fluorochromes. Only minor autoreactivity was detected in young animals, whereas higher color intensity represented elevated levels of antibodies directed against cardiac antigens in plasma of aged mice. Images in high magnification indicate that most IgGs, which spontaneously arise with aging, target intracellular sarcomeric antigens, but do not bind to cardiomyocyte surface antigens.

Further investigations using indirect ELISA to quantify anti-myosin antibody titers confirmed previous findings and revealed significantly increased titers in 12-15 months old mice. As it is well understood that $CD4^+$-T-cells are involved in B-cell activation and required for class switch towards IgG antibody production, specific IgGs also reflect T-cell specificity for antigens. Therefore, these findings suggest that not only B-cell dependent, but also $CD4^+$-T-cell dependent heart directed autoimmune reactivity might arise in elderly mice.

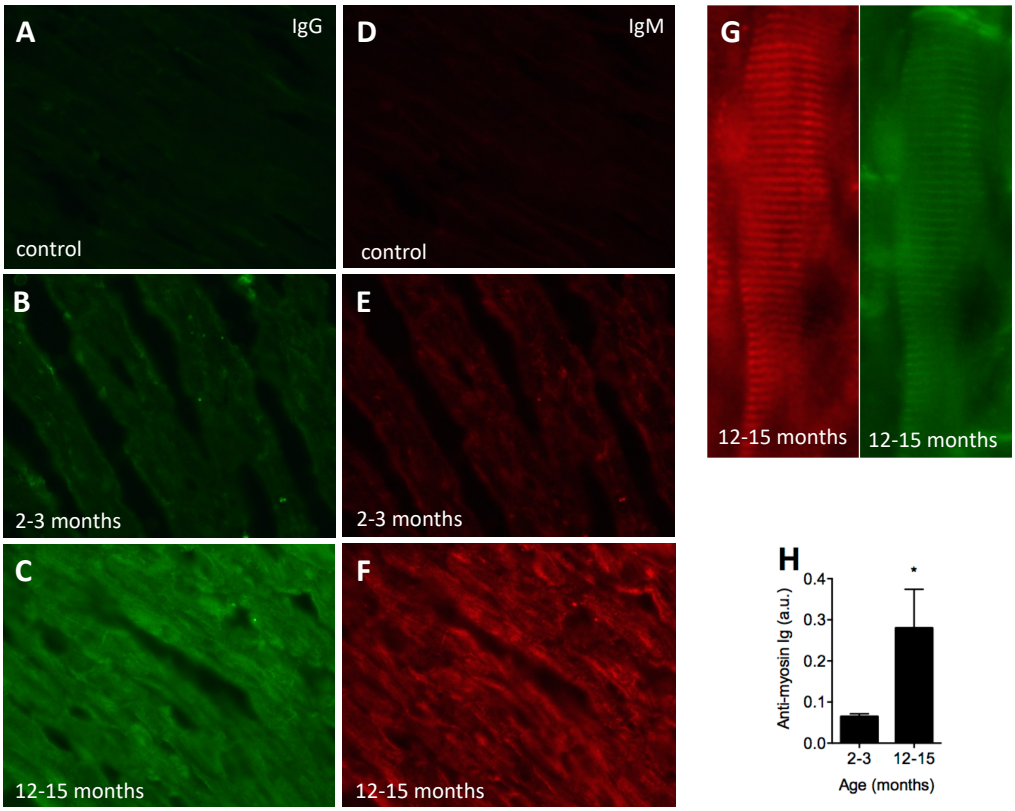

Fig. 20: Spontaneous autoreactivity arises with aging
A-F: Representative pictures of histological heart slices from B-cell deficient mice after incubation with plasma obtained from 2-3 months (B and E) and 12-15 months (C and F) old mice and visualization with secondary antibodies labeled to fluorochromes. IgGs targeting cardiac antigens appeared green while heart directed IgMs are depicted in red. As control, samples were solely incubated with secondary antibodies (A and D). Magnification 400x. **G**: IgGs emerging with age were found to target primarily intracellular sarcomeric antigens rather than reacting against surface antigens. Magnification 1000x. **H**: Myosin-specific antibodies quantified via indirect ELISA (n= 6-8). *P<0,05

4.8 ELDERLY $CD4^+$ DEFICIENT AND OVA-TCR TRANSGENIC MICE EXHIBITED ATTENUATED CARDIAC INFLAMMATION AND DYSFUNCTION AS COMPARED TO WILD TYPE MICE

To evaluate more precisely the impact of different immune cells on myocardial aging, a comprehensive cardiac phenotyping of genetic different mouse strains was performed. Following genotypes representing particular lymphocyte deficiencies were included and compared with wild type mice (WT):

First, $CD4^+$ T-cell deficiency was investigated on CD4 knockout mice (CD4KO) and MHCII receptor knockout mice (MHC-IIKO), the latter lacking functional $CD4^+$ T-cells as MHCII-receptors are indispensable for $CD4^+$ T-cell activation. Furthermore, cardiac parameters were examined in mice with $CD4^+$ T-cells expressing transgenic T-cell receptors (TCR) that recognize irrelevant $ovalbumin_{323-339}$ peptides presented in MHCII context (OT-II mice). Second, to assess the role of B-cells, mice lacking mature B-cells (µMT mice) were included in the analysis. All mouse strains descend from the same genetic background and were housed under identical conditions.

Initially, cardiac function of 2-3 months and 12-15 months old mice was examined using echocardiography. In contrast to WT mice, aged MHC-IIKOs exhibited preserved fraction shortening and end diastolic area with similar values observed in young counterparts. Additionally, no MCH-IIKO mice developed fraction shortening of less than 40%, as it was detected in WT mice. Old B-cell deficient µMT mice presented a slight reduction of fraction shortening and a distinct age-related increase of end diastolic area comparable to WT mice (Fig. 21). Given these findings, cardiac dysfunction in elderly might be predominantly T-cell, but to a smaller extent B-cell related.

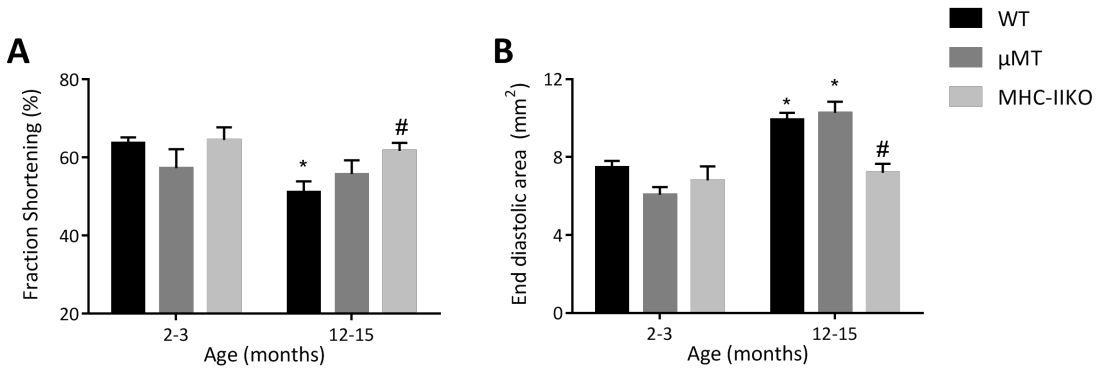

Fig. 21: Echocardiographic analysis of cardiac function in genetic different mouse strains

A: Age- related fraction shortening of wild type (WT), B-cell deficient (µMT), and $CD4^+$ deficient (MHCIIKO) mice. **B:** End diastolic area of 3 genotypes measures in young and old mice (n=5-19). # p< 0,05 compared with age matched WT mice. *p<0,05 compared with genotype matched young controls.

As the detailed mechanistic background of functional preservation specifically in $CD4^+$ T-cell deficient mice was unclear, gene expression of different mouse strains was analyzed to understand how T-cell deficiency is associated with cardiac function. Therefore, myocardial samples of 12-15 months old mice of all genotypes were probed for the expression of 45 target genes using the same custom-made PCR array mentioned in chapter 4.4 and immunodeficient mouse strains were matched to WT mice. Cardiac samples obtained from both, CD4KO and MCH-IIKO mice showed reduced gene expression levels of the pro-inflammatory cytokines TNF and IL1b compared to WT mice (Fig. 22). Although $CD4^+$ T-cells are missing in both mouse strains, these findings were even more pronounced in CD4KO in which, beyond that, the expression of INF-γ, IL6 and CCL2 was down regulated. Furthermore, the cell stress marker Hspa1a (heat shock protein family a member 1a) was lower in CD4KO mice in relation to the comparison group. Analysis of heart samples obtained from TCR deficient OT-II mice revealed similar gene expression levels as measured in CD4KO, indicating that autoantigen recognition by $CD4^+$ T-cells via TCR is important for their activation (Fig.22). In contrast, 12-15 months old B-cell deficient mice developed a gene expression profile nearly identical to WT mice, suggesting that the pro-inflammatory trend perceived in the myocardium is greatly associated with T-cell presence and less dependent on B-cells.

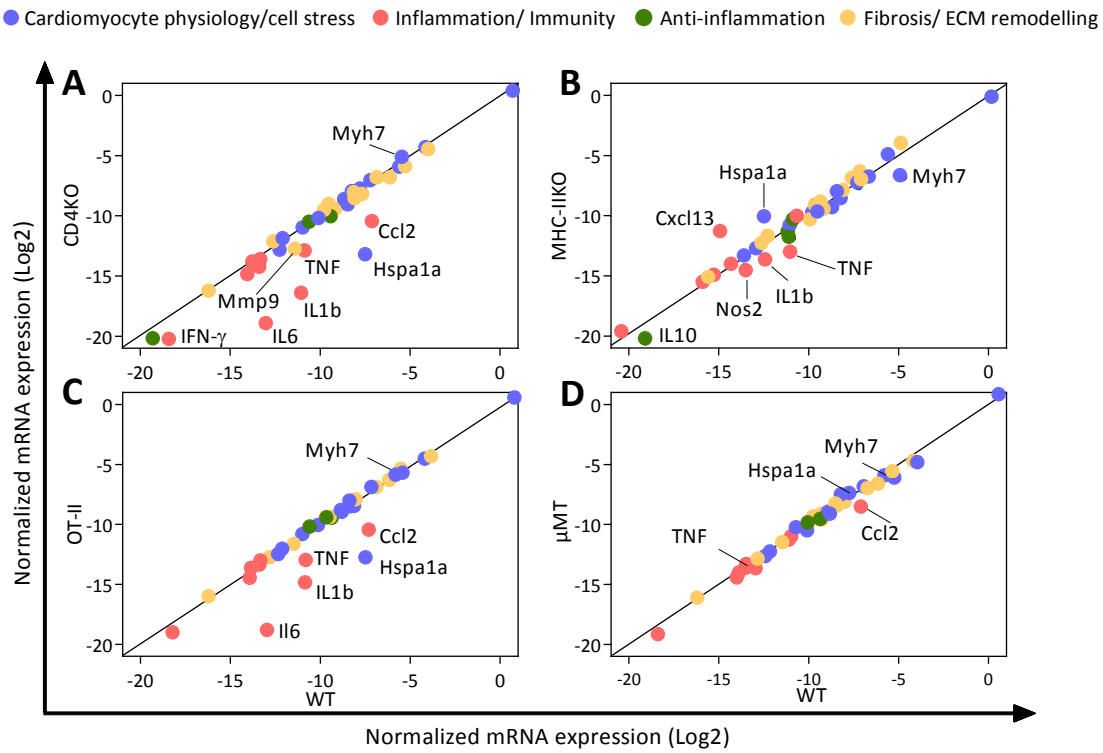

Fig. 22: Myocardial gene expression levels of different aged lymphocyte deficient mice compared to old wild type mice.

Representative scatter plots depicting normalized myocardial gene expression levels (Log2 relative gene expression) of 45 genes and 3 housekeeping genes in lymphocyte deficient mouse strains compared to age matched wild type (WT) animals. **A-C:** $CD4^+$ T-cell deficient mice express lower levels of pro-inflammatory genes compared to WT mice. These findings were more evident in CD4 T-cell knockouts (CD4KO) (A) and mice with T-cell receptors for irrelevant antigens (OT-II) (C) than in MHCII receptor knockout mice (MHC-IIKO) (B). **D:** No important differences were observed comparing gene expression of B-cell deficient mice (µMT) and WT mice. (n=3).

Based on the observations made during qPCR array analysis, some relevant target genes were analyzed with additional biological and technical replicates to validate the major findings and check for statistical significance. It was confirmed, that in CD4KO, MHC-IIKO and OT-II mice TNF expression levels in myocardial tissue are kept down and significantly lower compared to WT animals, whereas its expression in B-cell deficient mice was higher and closer to WT levels (Fig. 23A). The gene expression levels of Tgfb3 (Transforming growth factor beta 3) and Myh7 (myosin heavy chain 7), which were demonstrated to be upregulated during aging in hearts of WT mice, were identified to be nearly equal in old mice of all genotypes possibly being a hint that structural cardiac changes might be apparent in all genotypes (Fig. 23C). Moreover, the IL-6 gene

expression level was assessed as IL6 is associated with a more proinflammatory tone. Its general expression level presented on a low level, however, it was slightly less in aged CD4KO and OT-II mice compared to the WT and µMT group.

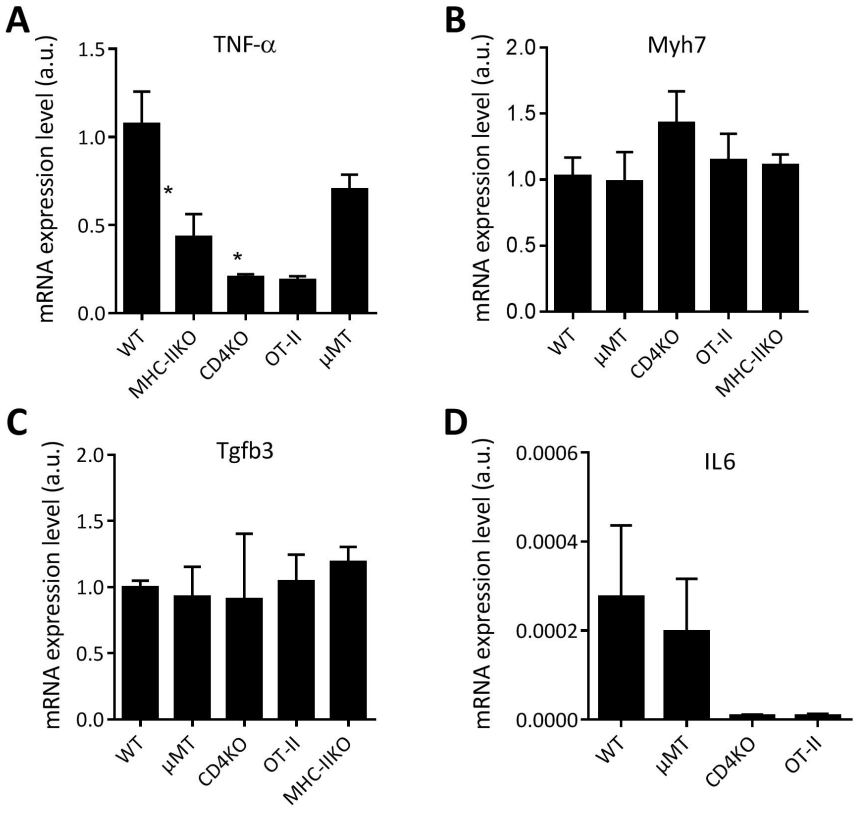

Fig. 23: Myocardial gene expression analysis of different aged mouse strains

A-C: Gene expression levels of tumor necrosis factor- alpha (TNF) (A), Myosin heavy chain 7 (Myh7) (B) and transforming growth factor 3 (tgfb3) (C) in WT, CD4 T-cell deficient (MHC-IIKO, CD4KO, OT-II) and B-cell deficient (µMT) mice. D: IL-6 expression in WT, µMT, CD4KO and OT-II mice. (n=3-6). *P<0,05 compared to WT.

5 DISCUSSION

5.1 LYMPHOCYTE POPULATIONS ARE CONSTANTLY PRESENT IN THE HEALTHY MYOCARDIUM

Leukocytes and their behavior are best characterized in blood, lymphatic tissue and lymphoid organs. In the last years, research turned to investigate the leukocyte distribution in non-lymphoid organs. Macrophages and their diverse appearances were the first to be described in various tissues, leading to progressive insight in their essential functions in tissue homeostasis and maintenance [188,189]. However, different tissue resident lymphocyte populations have been identified in recent years, modulating the molecular milieu and orchestrating further cell types [190-193]. Tissue resident memory T-cells have been described in several organs, not only after antigen contact, but also under steady state conditions, including barrier tissue like skin, female reproductive tract, intestines, lungs and even non-barrier organs like kidney, brain or liver [194-196]. Furthermore, T_{regs} regulate non-immunological processes like glucose metabolism in fat tissue or contribute to muscle regeneration by mediating satellite cells [197-199].

This work confirmed the assumption that all leukocyte types can be found in the uninjured heart and proved the presence of macrophages, granulocytes, B -cells and T-cells. Beyond that, the myocardial leukocyte population was directly compared to that one in skeletal muscle, examining both simultaneously using identical methods. A higher leukocyte number was detected in the myocardium, suggesting a higher immunological activity. As mentioned before, cardiac macrophages are no novelty, but have been studied before. They colonize the heart in the early neonatal period and later affect cardiac physiology in terms of electrical conduction, tissue homeostasis and remodeling [33,154,155,159]. Also, dendritic cells were detected in the heart and shown to present cardiac antigens in adjacent lymphnodes to T-cells, resulting in T-cell activation [163,164].

In contrast, the role of cardiac B- or T-cells has only been analyzed in detail under pathological conditions while their role under physiological conditions has been disregarded. So far, few comprehensive studies showed the presence of lymphocytes in

the healthy myocardium but did not provide a precise characterization [152,200]. This study supports the finding, that macrophages represent the major fraction of cardiac leukocytes and moreover illustrates that a small population of B- and T-cells can be consistently found in healthy hearts. The small numbers of detected cardiac lymphocytes might have been one reason to underestimate their importance in cardiac physiology in the past. However, the low recovery of tissue resident leukocytes due to methodological challenges is a well-known problem and should not be overlooked [201,202]. Here we used a refined 3D imaging approach that prevents cell loss during tissue digestion and preparation and therefore allows to obtain more accurate leukocyte numbers. About three-fold more leukocytes were detected, showing that the cardiac leukocyte population is larger than assumed. One further advance is the visualization of global cardiac tissue distribution of $CD45^+$ cells. Thereby, no myocardial area with an outstanding accumulation of leukocytes was observed. However, to find out if leukocyte subtypes are unequally distributed, further experiments must be performed.

Beyond that, this work includes a detailed characterization of cardiac leukocytes performed at different ages and in a number of mouse strains with lack of single lymphocyte subtypes that enables to draw new conclusions about immunological activity in the heart.

5.2 MYOCARDIAL AGING IN THE CONTEXT OF AN INCREASED INFLAMMATORY TONE

Myocardial aging is characterized by structural and functional changes including hypertrophy, fibrosis, ventricular stiffness and deterioration of diastolic function [8].
The mice studied here developed aforesaid characteristics and provided the basis for an investigation of the immune system´s impact regarding age-related alterations. Simultaneous changes of gene expression levels, immune cell composition and activation were observed, indicating myocardial und immunological aging being interrelated events.

Examining the myocardial tissue, a significant decline of macrophage numbers in advanced age is conspicuous. A more accurate investigation indicated a replacement of tissue resident macrophages by monocyte derived cells (defined as $CCR2^+$ cells). While for many tissues the local macrophage populations maintain themselves without replenishment by monocyte derived cells under steady state conditions, a replacement of cardiac embryo-derived macrophages by monocyte derived cells has been described, even without any tissue damage and injury [157,203]. Furthermore, monocyte derived cells have been detected to coordinate cardiac inflammation and have an increased inflammatory potential [155]. Under stressful conditions as for example hemodynamic pressure, their fraction increases, which is again associated with cardiac remodeling [204]. This work reinforces previous findings, as gene expression analysis reveal an increase of loading and cell stress parameters in the same temporal sequence as cellular alterations. Nevertheless, it did not focus on macrophages and does not provide further investigation allowing a more detailed picture of ongoing mechanisms.

By analyzing gene expression levels of proinflammatory cytokines and chemokines in the myocardium at different ages, it was possible to draw conclusions about the dynamics during aging. This is an advantage to having only one random sample at any time in the mice life on which conclusions have to be made. As a result, TNF and INF-γ increase during time and are significantly higher in elderly mice. Similar trends were observed for chemokines modulating the adaptive immune system. To date, several studies analyzed the molecular environment in aged individuals and detected elevated global IL6 and TNF levels [205]. Additionally, there is evidence that INF-γ induced inflammation occurs with aging [206]. One could argue, that inflamm-aging is an established concept and the aging heart is only part of the whole. Consequently, an increased inflammatory tone would be no surprise. This might be partly applicable. In fact, we detected TNF slightly increased at distributed measuring points within the body of aged mice. However, it was shown here that age dependent immunological activity arises with local focus on the heart. First, with age cellularity in mediastinal lymphnodes is increased, whereas cells numbers remain unaltered in further lymph node stations. Second, stimulation of isolated T-cells showed a significantly higher amount of secreted

pro-inflammatory cytokines in mediastinal and anti-inflammatory cytokines in popliteal lymphnodes. Third, cell markers indicated a significantly shifted polarization towards activated Th1 cells in mediastinal lymph nodes compared to popliteal and sub-iliac lymph nodes. Additionally, previous work has detected region specific variation in the antigen repertoire of different lymph node stations even under steady state conditions [207,208].

Lymph nodes are points of immunological response towards numerous antigens carried in the lymph. Lymph collected from one organ represents its individual proteome and degradome, mirroring the organs physiological and pathological conditions [209]. Considering aforesaid knowledge and our findings, it is likely that the myocardial output contains immune-stimulatory content. Gene expression analysis revealed genes connected to different cell stress conditions to be increased with aging. As cell stress conditions are characteristics of the inflamm-aging process, leading to cell death and release of antigens, the circuit could be completed.

However, although cell stress and leukocyte alterations were measured at different time points, the results do not allow to define a clear sequence. If myocardial cell stress triggered by different factors and antigen release stimulate inflammation, or if inflammation causes cell stress and antigen release remains vague. A combination of both is likely.

5.3 THE MEDIATING ROLE OF T-CELLS IN CARDIAC AGING

Primary examinations of cardiac lymph nodes indicated alterations in the T-cell differentiation and function with aging. Regarding the impact of aging, T-cells are the best analyzed lymphocyte compartment so far and senescence was shown to have tremendous effect on T-cell immunity [97,98]. That cardiac antigens are presented to T-cells under physiological conditions has been reported earlier [210]. Furthermore, cardiac T-cells modulate stressful and pathological conditions like ischemia or myocarditis and can contribute to the development of cardiac disease [179,211,212]. Consequently, T-cells are suspicious to be involved in the myocardial aging process.

To enable a more differentiated statement and to investigate the impact of individual leukocytes on cardiac aging, a comprehensive cardiac phenotyping of different aged lymphocyte- deficient mouse strains was performed.

Functional analysis revealed a preserved cardiac performance in mice lacking activated $CD4^+$ T-cells, whereas WT and B-cell deficient mice developed a comparable cardiac dysfunction. The expression of proinflammatory cytokines like TNF was reduced in mice lacking activated $CD4^+$ T-cells or total absence of $CD4^+$ T-cells whereupon differences were more pronounced in case of total $CD4^+$-T-cell deficiency. The same applies for cell stress gene expression. Comparable findings were observed in mice which do indeed generate $CD4^+$ T-cells that, however, do only carry a receptor recognizing irrelevant antigens. Latest finding indicates, that (auto-) antigen presentation might be important for an immune response with impact on cardiac aging. Again, the gene expression profile of B-cell deficient mice was comparable with WT mice. Conclusively, those findings underline the assumption of T-cells but not B-cells being required for a pro-inflammatory trend and functional decline during cardiac aging. It is worth mentioning that genes related to structural alterations and remodeling were similarly increased in old mice of all mouse strains. Therefore, a certain degree of remodeling and age-related alteration might occur independently of the presence or absence of cardiac immune cells.

Our group performed an extended adoptive cell transfer experiment to assess the pathogenic potential of lymphocytes harvested from mediastinal lymph nodes [213]. Cells harvested from mediastinal lymphnodes of young and old mice were transferred into young lymphocyte deficient mice. Analysis of the cardiac cell composition revealed significantly increased frequencies of myocardial B- and T-cells in recipients that received cells harvested from old donors. T-cells were the mayor infiltrating cell population, manly exhibiting an effector memory phenotype. Thereby, cardiotropism was demonstrated to develop with a clear dependency on age. Functional analysis detected no effect of the donors age on cardiac function of recipient mice [213]. These findings substantiate the hypothesis that T-cells are involved in the cardiac aging process

and required for the development of age dependent alterations, but are not able to cause senescence associated myocardial transformation.

What exactly changes in the T-cell compartment with aging? A more detailed analysis of the T-cell populations in different lymph node stations was performed in this work. As expected in the context of immunosenescence, an accumulation of antigen experienced activated effector memory T-cells was observed in different lymph node stations with aging. However, the ratio of antigen experienced activated effector memory T-cells was significantly higher in mediastinal lymph nodes compared to popliteal lymphnodes, indicating an augmented reactivation due to ongoing or repeated antigenic load. Among the memory T-cell compartment, the fraction of regulatory T- cells was reduced in mediastinal lymphnodes of aged mice due to a gain of conventional memory T-cells. Memory T_{regs}, just as effector T_{regs}, have high immunosuppressive potential and persist in absence of antigen or low-level antigen exposure [214]. A recent study found that the T-cell repertoire and differentiation can vary across different lymph node stations and suggested that activated memory T-cells recognize self-antigens and control autoimmune disease [215]. In case of an inflammatory response towards re-infection with a pathogen, memory T_{reg}-cells were shown to suppress pro-inflammatory effector memory T-cells and prevent collateral damage to affected tissue [216]. Considering this, memory T_{regs} could be helpful to suppress heart directed T-cell immunity during repeated stimulus. As the ratio shifts toward conventional T-cells with aging, the capacity of available T_{regs} might be insufficient to control pro-inflammatory T-cell response. If this problem finally relies on an inadequate total number of T_{regs} or their efficiency in antigen recognition cannot be specified here.

Regarding the effector regulatory T-cell compartment, the frequency of regulatory T-cells was much smaller than the frequency of conventional T-cells, in both young and old animals. The importance of T_{regs} for muscle homeostasis and repair during aging and under inflammatory conditions has been reported several times [217-220]. Other than in mediastinal lymph nodes, the frequency of T_{regs} was significantly increased in popliteal lymph nodes of elderly mice. As the inflammatory tone appeared lower in popliteal

lymph nodes, these findings might help to explain alterations in cardiac homeostasis with aging.

5.4 AUTOIMMUNITY IN CARDIAC AGING

When talking about cardiotropism of T-cells, reduced numbers of regulatory T-cells and a limited control of pro-inflammatory immune activity, the assumption that autoimmunity might be relevant in myocardial aging is obvious. T-cells with specificity to cardiac antigens are generated after myocardial infarction, but are also involved in the development of heart failure even without cardiac injury [164,180].

Regulatory T-cells can suppress autoreactive T-cells, are key players in maintaining peripheral tolerance towards self-structures and insufficient function has been demonstrated in several autoimmune disease [58,221] . For many years, the basic idea allocated tolerance against self-antigens as a task of tT_{regs}, whereas pT_{regs} should be responsible for limitations of immune responses against foreign antigens. However, in the last years there is new knowledge that tolerance against self is incomplete and deficient without pT_{regs} and that pT_{regs} allow the development T-cell repertoire adapted to evolving antigens encountered in the periphery [78,222]. Harbihai et al. discuss the expansion of TCR diversity by pT_{regs} as one mechanism [78]. With aging, the induction of peripheral T_{regs} was shown to be impaired and tT_{regs} accumulate while the pT_{reg} compartment shrinks [108,111]. Consequently, an age dependent decline of the TCR repertoire is expected with age causing a restriction of response to antigens. Myocardial aging is accompanied by remodeling and increased cell death causing an increased exposure of heart specific antigens. Considering that antigens may occur for the first time, it is supposable that a newly emerging autoreactive immune activity against cardiac antigens fails to be controlled.

Beside the cellular components of the immune system, antibodies play a well-established role in inducing autoimmune disease. Again, autoantibodies targeting cardiac antigens have been described in different heart failure conditions [223]. In this study the presence of heart specific antigens was proven. IgM and IgG antibodies were

detected. As class switch relies on T-cell help, this result reinforces for one more time the participation of T-cells in age dependent immune response. The antigens detected in mice´s plasma with increasing amounts during the aging process were found to bind to intracellular antigens, but do not target cardiomyocyte surface markers. Previous studies revealed autoantigens to be from clinical relevance when targeting surface receptors from functional importance [224,225]. Therefore, it is unlikely that the antibodies detected here induce or promote myocardial alterations or aging. This conclusion is strengthened by the finding that B-cell deficient and hence antibody deficient mice exhibit age related alterations comparable to WT-mice. It is more likely, that detected antibodies are result of life long antigenic exposure particularly to intracellular antigens released during cell stress and death.

However, it should not be disregarded that the medium which was analyzed for autoantibodies and the presence of myosin specific antibodies was plasma. The lymph was shown to carry an expanded self-antigen repertoire compared to plasma [226]. Therefore, analysis of the murine and human antigen compartment in the plasma might give first insights, but not provide an entire overview. Finally, the repertoire and significance of cardiac autoantibodies and their role in the aging process is far from being settled.

Autoreactivity might modulate the myocardial aging process, but in this study no evidence for autoimmunological processes being the basic cause for age related alterations could be detected.

5.5 FUTURE POTENTIAL FOR CONTINUATIVE RESEARCH

This study provides a first basic characterization of leukocytes in context of the myocardial aging process by doing baseline analysis in aged animals and by using different lymphocyte-deficient mouse models to study impact of singe cell types. It gives first evidence, that $CD4^+$ T-cells mediate cardiac aging, a condition of increased immune activity and sterile inflammation. While this work explains some underlying alteration

and contributes to the understanding of ongoing mechanisms, it is beyond that a link for future work and raises new questions.

The experiments were done in up to 15 months old mice. Experiments to investigate cardiac pathologies in other groups have been performed in even older rodents [227]. Although it requires higher methodological effort, it might be reasonable to conduct further research in older mice, assuming that age related changes will be more distinct. Moreover, experiments performed herein focused on age related alterations and their impact on the steady state condition. Still, it remains elusive how alterations in cardio-immune cross talk in elderly modulate age associated cardiovascular diseases as heart failure and myocardial infarction. Previous studies showed that basic cellular and molecular conditions change with aging and that these alterations have an effect on myocardial infarction and healing [228,229]. It was shown here that the immunological cardiac milieu changes significantly with aging and lymphocytes were shown to influence structural and functional alterations [170]. Therefore, myocardial infarction and healing in young and old individuals might be basically different. To date, research on myocardial infarction is primarily conducted in young mice. Considering afore mentioned aspects and the knowledge that myocardial infarction is a disease of the aging population, the use on older experimental models could provide more realistic fundament for future research.

One entire chapter of this work deals with autoimmunity. As mentioned before, autoantibodies have been identified under heart failure conditions and for example myosin, as one of the best studied cardiac antigens, has been detected in several heart diseases [230]. Furthermore, cardiac injury induces the generation of autoreactive T-cells [164]. Still, the targeted structures and released antigens are widely unknown. Identification of those could help to decode mechanisms and reveal potential targets for future therapies. Considering previous findings, research should not be restricted to plasma but also pay heed to lymphatic fluid [226].

Finally, the transferability of findings from bench to bedside is subject of permanent discussions. Although mice are the typical model for cardiac and immunological research, the immune systems is not 100% identical to the human one

and differences apply during aging [86,231]. In the end, hypotheses that developed from murine research have to be tested und verified for human beings.

6 SUMMARY

The prevalence of cardiovascular diseases (CVD) increases dramatically with age. Nevertheless, most of the basic research in cardiology has been conducted on young healthy animals which may not necessarily reflect the situation observed in the clinic. The heart undergoes profound changes in elderly, including molecular alterations, myocardial hypertrophy, interstitial fibrosis and functional decline. To date, numerous approaches exist to explain mechanisms of the cardiac aging process whereupon inflammation and immune activity are of increasing interest. Myocardial aging is temporally associated with chronic low-grade systemic inflammation and accumulation of memory T-cells. However, a possible causal relationship between these two phenomena has not yet been investigated. Thus, aim of the present study was to assess how immunological mechanisms contribute to the myocardial aging process.

Herein, the healthy murine heart was found to harbor all major resident leukocyte populations, including macrophages ($CD45^+CD11b^+Ly6G^-$), granulocytes ($CD45^+CD11b^+Ly6G^+$), T-cells ($CD45^+CD11b^-CD3e^+$), B-cells ($CD45^+CD11b^-B220^+$) at frequencies that largely surpass those found in skeletal muscles. Age-related structural alterations and functional impairment occur simultaneously with significant shifts of the tissue resident leukocyte composition. Gene expression analyses performed on bulk myocardial samples revealed higher expression levels of TNF and INF-γ suggesting that in situ inflammation plays a role in the myocardial aging process. Aging was furthermore accompanied by a significant increase in size and cellularity of mediastinal, heart draining lymph nodes (med LN). Moreover, the med LNs harvested from aged mice showed a strong accumulation of effector-memory T-cells ($CD44^+CD62L^-$), mainly exhibiting a pro-inflammatory phenotype ($Foxp3^-$, TNF^+, IFN- γ^+). None of these alterations were observed in popliteal lymph nodes of aged mice, indicating that they might be site-specific.

Next, to go beyond mere associative evidence and examine underlying mechanisms, the myocardial aging process was comprehensively characterized in mice lacking B- (μMT) or $CD4^+$ T-cells (CD4ko). Our analyses revealed that aged $CD4^+$ T-cell-deficient, but not B-cell-deficient mice, exhibit a lower in situ inflammatory tone and

preserved ventricular function, as compared to age-matched wild type controls. No differences in the expression levels of genes related to fibrosis were observed in the groups.

Taken together, the results of this study indicate that heart-directed immune responses may spontaneously arise in the elderly, even in the absence of a clear tissue damage or concomitant infection. The T-cell-mediated immunosenescence profile might be particularly associated with age-related myocardial inflammation and functional decline, but not with tissue remodeling. These observations might shed new light on the emerging role of T cells in myocardial diseases, which primarily affect the elderly population.

7 ZUSAMMENFASSUNG

Die Prävalenz kardiovaskulärer Erkrankungen nimmt mit dem Alter dramatisch zu. Dennoch wurde der größte Anteil der kardiologischen Grundlagenforschung bisher an jungen, gesunden Tieren durchgeführt. Dies spiegelt nicht zwangsläufig die in der Klinik beobachtete Situation wieder. Das Herz durchläuft während des Alterns einen tiefgreifenden Wandel, einschließlich molekularer Veränderungen, Hypertrophie des Myokards, interstitieller Fibrose und funktioneller Verschlechterung. Bis heute gibt es zahlreiche Ansätze, um die Mechanismen hinter dem kardialen Alterungsprozess zu erklären. Insbesondere Inflammation und Immunaktivität sind von zunehmendem Interesse. Das Altern des Myokards korreliert zeitlich mit geringer chronischer, systemischer Entzündungsaktivität und einer Akkumulation von Gedächtnis-T-Zellen. Trotzdem wurde ein kausaler Zusammenhang zwischen beiden Vorgängen bisher nicht tiefergehend untersucht. Ziel dieser Studie war es festzustellen, wie immunologische Mechanismen zum kardialen Alterungsprozess beitragen.

Im Rahmen dieser Arbeit konnte gezeigt werden, dass gesunde Maus Herzen alle bedeutenden, gewebeansässigen Leukozyten einschließlich Makrophagen ($CD45^+CD11b^+Ly6G^-$), Granulozyten ($CD45^+$ $CD11b^+Ly6G^+$), T-Zellen ($CD45^+CD11b^-CD3e^+$) und B-Zellen ($CD45^+CD11b^-B220^+$) beherbergen und dies in einer deutliche höherer Anzahl als die Skelettmuskulatur. Altersabhängige, strukturelle Veränderungen und funktionelle Verschlechterung treten zeitgleich mit signifikanten Veränderungen in der Zusammensetzung der ansässigen Leukozyten auf. Untersuchungen der Genexpression an Myokardproben ergaben ein erhöhtes Level der TNF und INF-γ Expression, was darauf hinweist, dass in-situ Inflammation eine Rolle im myokardialen Alterungsprozess spielt. Darüber hinaus zeigten mediastinale Lymphknoten im Alter eine deutliche Größenzunahme sowie einen signifikanten Anstieg der Zellzahl. In mediastinalen Lymphknoten von alten Mäusen konnte außerdem eine starke Akkumulation von Effektor-Gedächtnis-T-Zellen ($CD44^+CD62L^-$) nachgewiesen werden, welche vorwiegend einen pro-inflammatorischen Phänotyp ($Foxp3^-$, TNF^+, $IFN\text{-}\gamma^+$) aufwiesen. Keine dieser Veränderungen konnte in poplitealen Lymphknoten gezeigt werden, was darauf hindeutet, dass es sich um einen ortsspezifischen Prozess handeln könnte.

Um über eine rein assoziative Evidenz hinaus zu gehen und zugrundeliegende Vorgänge zu analysieren, wurde der myokardiale Alterungsprozess umfassend an Mäusen ohne B- Zellen (µMT) oder $CD4^+$ T-Zellen (CD4ko) charakterisiert. Die Untersuchungen ergaben, dass alte Mäuse ohne $CD4^+$ T-Zellen verglichen zu gleichalterigen Wildtyp Tieren einen geringeren inflammatorischen Tonus in-situ entwickeln. Diese Veränderung war für Mäuse ohne B-Zellen nicht zu beobachten. Keinen Unterschied gab es in den Versuchsgruppen hingegen bei der Expression von Genen, die mit Fibrose assoziiert sind.

Zusammenfassend weisen die Ergebnisse dieser Arbeit darauf hin, dass auf das Herz gerichtete Immunantworten im Alter spontan, auch ohne eindeutigen Gewebeschaden oder eine begleitende Infektion, auftreten können. Das T-Zell vermittelte Profil des alternden Immunsystems kann teilweise mit der altersabhängigen Entzündung des Myokards sowie funktionellen Einschränkung assoziiert sein, weniger jedoch mit dem Remodeling Prozess. Diese Beobachtungen geben neuen Aufschluss über die aufkommende Rolle von T-Zellen in Erkrankungen des Myokards, welche vor allem die ältere Bevölkerung betreffen.

8 REFERENCES

1 Organisation, W. H. *Cardiovascular diseases (CVDs) - Key facts*, 2017).

2 Iqbal, J., Francis, L., Reid, J., Murray, S. & Denvir, M. Quality of life in patients with chronic heart failure and their carers: a 3-year follow-up study assessing hospitalization and mortality. *Eur J Heart Fail* **12**, 1002-1008, doi:10.1093/eurjhf/hfq114 (2010).

3 Morys, J. M., Bellwon, J., Hofer, S., Rynkiewicz, A. & Gruchala, M. Quality of life in patients with coronary heart disease after myocardial infarction and with ischemic heart failure. *Arch Med Sci* **12**, 326-333, doi:10.5114/aoms.2014.47881 (2016).

4 Yusuf, S. *et al.* Effect of potentially modifiable risk factors associated with myocardial infarction in 52 countries (the INTERHEART study): case-control study. *Lancet* **364**, 937-952, doi:10.1016/S0140-6736(04)17018-9 (2004).

5 Chiao, Y. A. & Rabinovitch, P. S. The Aging Heart. *Cold Spring Harbor perspectives in medicine* **5**, doi:10.1101/cshperspect.a025148 (2015).

6 Benjamin, E. J. *et al.* Heart Disease and Stroke Statistics-2017 Update: A Report From the American Heart Association. *Circulation* **135**, e146-e603, doi:10.1161/CIR.0000000000000485 (2017).

7 Dai, D. F. & Rabinovitch, P. S. Cardiac aging in mice and humans: the role of mitochondrial oxidative stress. *Trends Cardiovasc Med* **19**, 213-220, doi:10.1016/j.tcm.2009.12.004 (2009).

8 Lakatta, E. G. & Levy, D. Arterial and cardiac aging: major shareholders in cardiovascular disease enterprises: Part II: the aging heart in health: links to heart disease. *Circulation* **107**, 346-354 (2003).

9 Redfield, M. M., Jacobsen, S. J., Borlaug, B. A., Rodeheffer, R. J. & Kass, D. A. Age- and gender-related ventricular-vascular stiffening: a community-based study. *Circulation* **112**, 2254-2262, doi:10.1161/CIRCULATIONAHA.105.541078 (2005).

10 Biernacka, A. & Frangogiannis, N. G. Aging and Cardiac Fibrosis. *Aging Dis* **2**, 158-173 (2011).

11 Zile, M. R., Baicu, C. F. & Gaasch, W. H. Diastolic heart failure--abnormalities in active relaxation and passive stiffness of the left ventricle. *N Engl J Med* **350**, 1953-1959, doi:10.1056/NEJMoa032566 (2004).

12 Zile, M. R. & Brutsaert, D. L. New concepts in diastolic dysfunction and diastolic heart failure: Part II: causal mechanisms and treatment. *Circulation* **105**, 1503-1508 (2002).

13 Benjamin, E. J. *et al.* Determinants of Doppler indexes of left ventricular diastolic function in normal subjects (the Framingham Heart Study). *Am J Cardiol* **70**, 508-515 (1992).

14 Schulman, S. P. *et al.* Age-related decline in left ventricular filling at rest and exercise. *Am J Physiol* **263**, H1932-1938, doi:10.1152/ajpheart.1992.263.6.H1932 (1992).

15 Khouri, S. J., Maly, G. T., Suh, D. D. & Walsh, T. E. A practical approach to the echocardiographic evaluation of diastolic function. *J Am Soc Echocardiogr* **17**, 290-297, doi:10.1016/j.echo.2003.08.012 (2004).

16 Swinne, C. J., Shapiro, E. P., Lima, S. D. & Fleg, J. L. Age-associated changes in left ventricular diastolic performance during isometric exercise in normal subjects. *Am J Cardiol* **69**, 823-826 (1992).
17 Nakou, E. S. *et al.* Healthy aging and myocardium: A complicated process with various effects in cardiac structure and physiology. *International journal of cardiology* **209**, 167-175, doi:10.1016/j.ijcard.2016.02.039 (2016).
18 Lakatta, E. G. Age-associated cardiovascular changes in health: impact on cardiovascular disease in older persons. *Heart failure reviews* **7**, 29-49 (2002).
19 Ouzounian, M., Lee, D. S. & Liu, P. P. Diastolic heart failure: mechanisms and controversies. *Nat Clin Pract Cardiovasc Med* **5**, 375-386, doi:10.1038/ncpcardio1245 (2008).
20 Domenighetti, A. A. *et al.* Angiotensin II-mediated phenotypic cardiomyocyte remodeling leads to age-dependent cardiac dysfunction and failure. *Hypertension* **46**, 426-432, doi:10.1161/01.HYP.0000173069.53699.d9 (2005).
21 Ferrara, N. *et al.* beta-adrenergic receptor responsiveness in aging heart and clinical implications. *Front Physiol* **4**, 396, doi:10.3389/fphys.2013.00396 (2014).
22 Dai, D. F., Chiao, Y. A., Marcinek, D. J., Szeto, H. H. & Rabinovitch, P. S. Mitochondrial oxidative stress in aging and healthspan. *Longev Healthspan* **3**, 6, doi:10.1186/2046-2395-3-6 (2014).
23 Bergmann, O. *et al.* Evidence for cardiomyocyte renewal in humans. *Science* **324**, 98-102, doi:10.1126/science.1164680 (2009).
24 Yan, L. *et al.* Type 5 adenylyl cyclase disruption increases longevity and protects against stress. *Cell* **130**, 247-258, doi:10.1016/j.cell.2007.05.038 (2007).
25 Fares, E. & Howlett, S. E. Effect of age on cardiac excitation-contraction coupling. *Clin Exp Pharmacol Physiol* **37**, 1-7, doi:10.1111/j.1440-1681.2009.05276.x (2010).
26 Marín-García, J. *Aging and the Heart - A Post-Genomic View*. 1st Edition edn, Vol. 1 (Springer, 2008).
27 Kulinsky, V. I. Biochemical aspects of inflammation. *Biochemistry (Mosc)* **72**, 595-607 (2007).
28 Fulop, T., Dupuis, G., Witkowski, J. M. & Larbi, A. The Role of Immunosenescence in the Development of Age-Related Diseases. *Rev Invest Clin* **68**, 84-91 (2016).
29 Chung, H. Y., Sung, B., Jung, K. J., Zou, Y. & Yu, B. P. The molecular inflammatory process in aging. *Antioxid Redox Signal* **8**, 572-581, doi:10.1089/ars.2006.8.572 (2006).
30 Franceschi, C. *et al.* Inflamm-aging. An evolutionary perspective on immunosenescence. *Ann N Y Acad Sci* **908**, 244-254 (2000).
31 Murphy, K. M. *Janeway's Immunobiology*. 8th edition edn, (Garland Science, 2012).
32 Sattler, S. The Role of the Immune System Beyond the Fight Against Infection. *Adv Exp Med Biol* **1003**, 3-14, doi:10.1007/978-3-319-57613-8_1 (2017).
33 Hulsmans, M. *et al.* Macrophages Facilitate Electrical Conduction in the Heart. *Cell* **169**, 510-+, doi:10.1016/j.cell.2017.03.050 (2017).

34 Krysko, D. V. *et al.* Emerging role of damage-associated molecular patterns derived from mitochondria in inflammation. *Trends Immunol* **32**, 157-164, doi:10.1016/j.it.2011.01.005 (2011).
35 Varol, C., Mildner, A. & Jung, S. Macrophages: development and tissue specialization. *Annual review of immunology* **33**, 643-675, doi:10.1146/annurev-immunol-032414-112220 (2015).
36 Borregaard, N. Neutrophils, from marrow to microbes. *Immunity* **33**, 657-670, doi:10.1016/j.immuni.2010.11.011 (2010).
37 Wang, J. Neutrophils in tissue injury and repair. *Cell Tissue Res* **371**, 531-539, doi:10.1007/s00441-017-2785-7 (2018).
38 Bardoel, B. W., Kenny, E. F., Sollberger, G. & Zychlinsky, A. The balancing act of neutrophils. *Cell Host Microbe* **15**, 526-536, doi:10.1016/j.chom.2014.04.011 (2014).
39 Park, J. E. & Barbul, A. Understanding the role of immune regulation in wound healing. *Am J Surg* **187**, 11S-16S, doi:10.1016/S0002-9610(03)00296-4 (2004).
40 Davies, L. C., Jenkins, S. J., Allen, J. E. & Taylor, P. R. Tissue-resident macrophages. *Nature immunology* **14**, 986-995, doi:10.1038/ni.2705 (2013).
41 Wynn, T. A. & Vannella, K. M. Macrophages in Tissue Repair, Regeneration, and Fibrosis. *Immunity* **44**, 450-462, doi:10.1016/j.immuni.2016.02.015 (2016).
42 Abul K. Abbas, A. H. H. L., Shiv Pillai. *Cellular and molecular immunology* Vol. 8th Edition (Saunders, 2014).
43 Bonilla, F. A. & Oettgen, H. C. Adaptive immunity. *J Allergy Clin Immunol* **125**, S33-40, doi:10.1016/j.jaci.2009.09.017 (2010).
44 Pieper, K., Grimbacher, B. & Eibel, H. B-cell biology and development. *J Allergy Clin Immunol* **131**, 959-971, doi:10.1016/j.jaci.2013.01.046 (2013).
45 Goodnow, C. C., Adelstein, S. & Basten, A. The need for central and peripheral tolerance in the B cell repertoire. *Science* **248**, 1373-1379 (1990).
46 LeBien, T. W. & Tedder, T. F. B lymphocytes: how they develop and function. *Blood* **112**, 1570-1580, doi:10.1182/blood-2008-02-078071 (2008).
47 Chung, J. B., Silverman, M. & Monroe, J. G. Transitional B cells: step by step towards immune competence. *Trends Immunol* **24**, 343-349 (2003).
48 Forthal, D. N. Functions of Antibodies. *Microbiol Spectr* **2**, AID-0019-2014, doi:10.1128/microbiolspec.AID-0019-2014 (2014).
49 Keppner, L. *et al.* Antibodies aggravate the development of ischemic heart failure. *Am J Physiol Heart Circ Physiol*, doi:10.1152/ajpheart.00144.2018 (2018).
50 Chan, O. & Shlomchik, M. J. A new role for B cells in systemic autoimmunity: B cells promote spontaneous T cell activation in MRL-lpr/lpr mice. *Journal of immunology* **160**, 51-59 (1998).
51 Harris, D. P. *et al.* Reciprocal regulation of polarized cytokine production by effector B and T cells. *Nature immunology* **1**, 475-482, doi:10.1038/82717 (2000).
52 Goodnow, C. C., Sprent, J., Fazekas de St Groth, B. & Vinuesa, C. G. Cellular and genetic mechanisms of self tolerance and autoimmunity. *Nature* **435**, 590-597, doi:10.1038/nature03724 (2005).

53 Rawlings, D. J., Metzler, G., Wray-Dutra, M. & Jackson, S. W. Altered B cell signalling in autoimmunity. *Nature reviews. Immunology* **17**, 421-436, doi:10.1038/nri.2017.24 (2017).
54 Schwarz, B. A. & Bhandoola, A. Trafficking from the bone marrow to the thymus: a prerequisite for thymopoiesis. *Immunol Rev* **209**, 47-57, doi:10.1111/j.0105-2896.2006.00350.x (2006).
55 Petrie, H. T. Role of thymic organ structure and stromal composition in steady-state postnatal T-cell production. *Immunol Rev* **189**, 8-19 (2002).
56 Koch, U. & Radtke, F. Mechanisms of T cell development and transformation. *Annu Rev Cell Dev Biol* **27**, 539-562, doi:10.1146/annurev-cellbio-092910-154008 (2011).
57 Starr, T. K., Jameson, S. C. & Hogquist, K. A. Positive and negative selection of T cells. *Annual review of immunology* **21**, 139-176, doi:10.1146/annurev.immunol.21.120601.141107 (2003).
58 Josefowicz, S. Z., Lu, L. F. & Rudensky, A. Y. Regulatory T cells: mechanisms of differentiation and function. *Annual review of immunology* **30**, 531-564, doi:10.1146/annurev.immunol.25.022106.141623 (2012).
59 Krueger, A., Zietara, N. & Lyszkiewicz, M. T Cell Development by the Numbers. *Trends Immunol* **38**, 128-139, doi:10.1016/j.it.2016.10.007 (2017).
60 van den Broek, T., Borghans, J. A. M. & van Wijk, F. The full spectrum of human naive T cells. *Nature reviews. Immunology* **18**, 363-373, doi:10.1038/s41577-018-0001-y (2018).
61 Hunter, M. C., Teijeira, A. & Halin, C. T Cell Trafficking through Lymphatic Vessels. *Frontiers in immunology* **7**, 613, doi:10.3389/fimmu.2016.00613 (2016).
62 von Andrian, U. H. & Mackay, C. R. T-cell function and migration. Two sides of the same coin. *N Engl J Med* **343**, 1020-1034, doi:10.1056/NEJM200010053431407 (2000).
63 Guermonprez, P., Valladeau, J., Zitvogel, L., Thery, C. & Amigorena, S. Antigen presentation and T cell stimulation by dendritic cells. *Annual review of immunology* **20**, 621-667, doi:10.1146/annurev.immunol.20.100301.064828 (2002).
64 Reis e Sousa, C. Activation of dendritic cells: translating innate into adaptive immunity. *Curr Opin Immunol* **16**, 21-25 (2004).
65 Sprent, J. & Surh, C. D. T cell memory. *Annual review of immunology* **20**, 551-579, doi:10.1146/annurev.immunol.20.100101.151926 (2002).
66 Zhou, L., Chong, M. M. & Littman, D. R. Plasticity of CD4+ T cell lineage differentiation. *Immunity* **30**, 646-655, doi:10.1016/j.immuni.2009.05.001 (2009).
67 Boyton, R. J. & Altmann, D. M. Is selection for TCR affinity a factor in cytokine polarization? *Trends Immunol* **23**, 526-529 (2002).
68 Pennock, N. D. *et al.* T cell responses: naive to memory and everything in between. *Adv Physiol Educ* **37**, 273-283, doi:10.1152/advan.00066.2013 (2013).

69 Hori, S., Nomura, T. & Sakaguchi, S. Control of regulatory T cell development by the transcription factor Foxp3. *Science* **299**, 1057-1061, doi:10.1126/science.1079490 (2003).
70 Fontenot, J. D., Gavin, M. A. & Rudensky, A. Y. Foxp3 programs the development and function of CD4+CD25+ regulatory T cells. *Nature immunology* **4**, 330-336, doi:10.1038/ni904 (2003).
71 Coombes, J. L., Robinson, N. J., Maloy, K. J., Uhlig, H. H. & Powrie, F. Regulatory T cells and intestinal homeostasis. *Immunol Rev* **204**, 184-194, doi:10.1111/j.0105-2896.2005.00250.x (2005).
72 Vignali, D. A., Collison, L. W. & Workman, C. J. How regulatory T cells work. *Nature reviews. Immunology* **8**, 523-532, doi:10.1038/nri2343 (2008).
73 Kretschmer, K., Apostolou, I., Jaeckel, E., Khazaie, K. & von Boehmer, H. Making regulatory T cells with defined antigen specificity: role in autoimmunity and cancer. *Immunol Rev* **212**, 163-169, doi:10.1111/j.0105-2896.2006.00411.x (2006).
74 Ohkura, N., Kitagawa, Y. & Sakaguchi, S. Development and maintenance of regulatory T cells. *Immunity* **38**, 414-423, doi:10.1016/j.immuni.2013.03.002 (2013).
75 Kanamori, M., Nakatsukasa, H., Okada, M., Lu, Q. & Yoshimura, A. Induced Regulatory T Cells: Their Development, Stability, and Applications. *Trends Immunol* **37**, 803-811, doi:10.1016/j.it.2016.08.012 (2016).
76 Chen, W. *et al.* Conversion of peripheral CD4+CD25- naive T cells to CD4+CD25+ regulatory T cells by TGF-beta induction of transcription factor Foxp3. *The Journal of experimental medicine* **198**, 1875-1886, doi:10.1084/jem.20030152 (2003).
77 Josefowicz, S. Z. *et al.* Extrathymically generated regulatory T cells control mucosal TH2 inflammation. *Nature* **482**, 395-399, doi:10.1038/nature10772 (2012).
78 Haribhai, D. *et al.* A requisite role for induced regulatory T cells in tolerance based on expanding antigen receptor diversity. *Immunity* **35**, 109-122, doi:10.1016/j.immuni.2011.03.029 (2011).
79 Collison, L. W. *et al.* The inhibitory cytokine IL-35 contributes to regulatory T-cell function. *Nature* **450**, 566-569, doi:10.1038/nature06306 (2007).
80 Sakaguchi, S., Wing, K., Onishi, Y., Prieto-Martin, P. & Yamaguchi, T. Regulatory T cells: how do they suppress immune responses? *Int Immunol* **21**, 1105-1111, doi:10.1093/intimm/dxp095 (2009).
81 Barnes, M. J. *et al.* CTLA-4 promotes Foxp3 induction and regulatory T cell accumulation in the intestinal lamina propria. *Mucosal Immunol* **6**, 324-334, doi:10.1038/mi.2012.75 (2013).
82 Pandiyan, P., Zheng, L., Ishihara, S., Reed, J. & Lenardo, M. J. CD4+CD25+Foxp3+ regulatory T cells induce cytokine deprivation-mediated apoptosis of effector CD4+ T cells. *Nature immunology* **8**, 1353-1362, doi:10.1038/ni1536 (2007).
83 Sallusto, F., Geginat, J. & Lanzavecchia, A. Central memory and effector memory T cell subsets: function, generation, and maintenance. *Annual review*

of immunology **22**, 745-763, doi:10.1146/annurev.immunol.22.012703.104702 (2004).
84 Sallusto, F., Lenig, D., Forster, R., Lipp, M. & Lanzavecchia, A. Two subsets of memory T lymphocytes with distinct homing potentials and effector functions. *Nature* **401**, 708-712, doi:10.1038/44385 (1999).
85 Schenkel, J. M. & Masopust, D. Tissue-resident memory T cells. *Immunity* **41**, 886-897, doi:10.1016/j.immuni.2014.12.007 (2014).
86 Goronzy, J. J. & Weyand, C. M. Understanding immunosenescence to improve responses to vaccines. *Nature immunology* **14**, 428-436, doi:10.1038/ni.2588 (2013).
87 Jaiswal, S. *et al.* Age-related clonal hematopoiesis associated with adverse outcomes. *N Engl J Med* **371**, 2488-2498, doi:10.1056/NEJMoa1408617 (2014).
88 Fulop, T. *et al.* Potential role of immunosenescence in cancer development. *Ann N Y Acad Sci* **1197**, 158-165, doi:10.1111/j.1749-6632.2009.05370.x (2010).
89 Goronzy, J. J., Fang, F., Cavanagh, M. M., Qi, Q. & Weyand, C. M. Naive T cell maintenance and function in human aging. *Journal of immunology* **194**, 4073-4080, doi:10.4049/jimmunol.1500046 (2015).
90 Gosain, A. & DiPietro, L. A. Aging and wound healing. *World J Surg* **28**, 321-326, doi:10.1007/s00268-003-7397-6 (2004).
91 Spyridopoulos, I. *et al.* CMV seropositivity and T-cell senescence predict increased cardiovascular mortality in octogenarians: results from the Newcastle 85+ study. *Aging Cell* **15**, 389-392, doi:10.1111/acel.12430 (2016).
92 Moro-Garcia, M. A. *et al.* Immunosenescence and inflammation characterize chronic heart failure patients with more advanced disease. *International journal of cardiology* **174**, 590-599, doi:10.1016/j.ijcard.2014.04.128 (2014).
93 Linton, P. J. & Dorshkind, K. Age-related changes in lymphocyte development and function. *Nature immunology* **5**, 133-139, doi:10.1038/ni1033 (2004).
94 den Braber, I. *et al.* Maintenance of peripheral naive T cells is sustained by thymus output in mice but not humans. *Immunity* **36**, 288-297, doi:10.1016/j.immuni.2012.02.006 (2012).
95 Nikolich-Zugich, J., Li, G., Uhrlaub, J. L., Renkema, K. R. & Smithey, M. J. Age-related changes in CD8 T cell homeostasis and immunity to infection. *Semin Immunol* **24**, 356-364, doi:10.1016/j.smim.2012.04.009 (2012).
96 Czesnikiewicz-Guzik, M. *et al.* T cell subset-specific susceptibility to aging. *Clin Immunol* **127**, 107-118, doi:10.1016/j.clim.2007.12.002 (2008).
97 Goronzy, J. J. & Weyand, C. M. Successful and Maladaptive T Cell Aging. *Immunity* **46**, 364-378, doi:10.1016/j.immuni.2017.03.010 (2017).
98 Naylor, K. *et al.* The influence of age on T cell generation and TCR diversity. *Journal of immunology* **174**, 7446-7452 (2005).
99 Goronzy, J. J. & Weyand, C. M. T cell development and receptor diversity during aging. *Curr Opin Immunol* **17**, 468-475, doi:10.1016/j.coi.2005.07.020 (2005).
100 Johnson, P. L., Yates, A. J., Goronzy, J. J. & Antia, R. Peripheral selection rather than thymic involution explains sudden contraction in naive CD4 T-cell diversity with age. *Proceedings of the National Academy of Sciences of the United States of America* **109**, 21432-21437, doi:10.1073/pnas.1209283110 (2012).

101 Yanes, R. E., Gustafson, C. E., Weyand, C. M. & Goronzy, J. J. Lymphocyte generation and population homeostasis throughout life. *Semin Hematol* **54**, 33-38, doi:10.1053/j.seminhematol.2016.10.003 (2017).
102 Goronzy, J. J., Li, G., Yang, Z. & Weyand, C. M. The janus head of T cell aging - autoimmunity and immunodeficiency. *Frontiers in immunology* **4**, 131, doi:10.3389/fimmu.2013.00131 (2013).
103 Kieper, W. C., Burghardt, J. T. & Surh, C. D. A role for TCR affinity in regulating naive T cell homeostasis. *Journal of immunology* **172**, 40-44 (2004).
104 Rudd, B. D. *et al.* Nonrandom attrition of the naive CD8+ T-cell pool with aging governed by T-cell receptor:pMHC interactions. *Proceedings of the National Academy of Sciences of the United States of America* **108**, 13694-13699, doi:10.1073/pnas.1107594108 (2011).
105 Goronzy, J. J., Li, G., Yu, M. & Weyand, C. M. Signaling pathways in aged T cells - a reflection of T cell differentiation, cell senescence and host environment. *Semin Immunol* **24**, 365-372, doi:10.1016/j.smim.2012.04.003 (2012).
106 Goronzy, J. J. & Weyand, C. M. Immune aging and autoimmunity. *Cell Mol Life Sci* **69**, 1615-1623, doi:10.1007/s00018-012-0970-0 (2012).
107 Jefferson, T. *et al.* Efficacy and effectiveness of influenza vaccines in elderly people: a systematic review. *Lancet* **366**, 1165-1174, doi:10.1016/S0140-6736(05)67339-4 (2005).
108 Jagger, A., Shimojima, Y., Goronzy, J. J. & Weyand, C. M. Regulatory T cells and the immune aging process: a mini-review. *Gerontology* **60**, 130-137, doi:10.1159/000355303 (2014).
109 Lages, C. S. *et al.* Functional regulatory T cells accumulate in aged hosts and promote chronic infectious disease reactivation. *Journal of immunology* **181**, 1835-1848 (2008).
110 Simone, R., Zicca, A. & Saverino, D. The frequency of regulatory CD3+CD8+CD28- CD25+ T lymphocytes in human peripheral blood increases with age. *J Leukoc Biol* **84**, 1454-1461, doi:10.1189/jlb.0907627 (2008).
111 Carpentier, M. *et al.* Extrathymic induction of Foxp3(+) regulatory T cells declines with age in a T-cell intrinsic manner. *European journal of immunology* **43**, 2598-2604, doi:10.1002/eji.201343532 (2013).
112 van der Geest, K. S. *et al.* Aging disturbs the balance between effector and regulatory CD4+ T cells. *Exp Gerontol* **60**, 190-196, doi:10.1016/j.exger.2014.11.005 (2014).
113 Gregg, R. *et al.* The number of human peripheral blood CD4+ CD25high regulatory T cells increases with age. *Clin Exp Immunol* **140**, 540-546, doi:10.1111/j.1365-2249.2005.02798.x (2005).
114 Nishioka, T., Shimizu, J., Iida, R., Yamazaki, S. & Sakaguchi, S. CD4+CD25+Foxp3+ T cells and CD4+CD25-Foxp3+ T cells in aged mice. *Journal of immunology* **176**, 6586-6593 (2006).
115 Sun, L. *et al.* Aged regulatory T cells protect from autoimmune inflammation despite reduced STAT3 activation and decreased constraint of IL-17 producing T cells. *Aging Cell* **11**, 509-519, doi:10.1111/j.1474-9726.2012.00812.x (2012).

116 Suzuki, M. *et al.* CD8+CD45RA+CCR7+FOXP3+ T cells with immunosuppressive properties: a novel subset of inducible human regulatory T cells. *Journal of immunology* **189**, 2118-2130, doi:10.4049/jimmunol.1200122 (2012).
117 Min, H., Montecino-Rodriguez, E. & Dorshkind, K. Effects of aging on the common lymphoid progenitor to pro-B cell transition. *Journal of immunology* **176**, 1007-1012 (2006).
118 Cancro, M. P. *et al.* B cells and aging: molecules and mechanisms. *Trends Immunol* **30**, 313-318, doi:10.1016/j.it.2009.04.005 (2009).
119 Scholz, J. L., Diaz, A., Riley, R. L., Cancro, M. P. & Frasca, D. A comparative review of aging and B cell function in mice and humans. *Curr Opin Immunol* **25**, 504-510, doi:10.1016/j.coi.2013.07.006 (2013).
120 Gibson, K. L. *et al.* B-cell diversity decreases in old age and is correlated with poor health status. *Aging Cell* **8**, 18-25, doi:10.1111/j.1474-9726.2008.00443.x (2009).
121 Frasca, D. & Blomberg, B. B. Effects of aging on B cell function. *Curr Opin Immunol* **21**, 425-430, doi:10.1016/j.coi.2009.06.001 (2009).
122 Ademokun, A., Wu, Y. C. & Dunn-Walters, D. The ageing B cell population: composition and function. *Biogerontology* **11**, 125-137, doi:10.1007/s10522-009-9256-9 (2010).
123 Shaw, A. C., Goldstein, D. R. & Montgomery, R. R. Age-dependent dysregulation of innate immunity. *Nature reviews. Immunology* **13**, 875-887, doi:10.1038/nri3547 (2013).
124 Ray, D. & Yung, R. Immune senescence, epigenetics and autoimmunity. *Clin Immunol*, doi:10.1016/j.clim.2018.04.002 (2018).
125 Solana, R. *et al.* Innate immunosenescence: effect of aging on cells and receptors of the innate immune system in humans. *Semin Immunol* **24**, 331-341, doi:10.1016/j.smim.2012.04.008 (2012).
126 Butcher, S. K. *et al.* Senescence in innate immune responses: reduced neutrophil phagocytic capacity and CD16 expression in elderly humans. *J Leukoc Biol* **70**, 881-886 (2001).
127 Sapey, E. *et al.* Phosphoinositide 3-kinase inhibition restores neutrophil accuracy in the elderly: toward targeted treatments for immunosenescence. *Blood* **123**, 239-248, doi:10.1182/blood-2013-08-519520 (2014).
128 Tseng, C. W. & Liu, G. Y. Expanding roles of neutrophils in aging hosts. *Curr Opin Immunol* **29**, 43-48, doi:10.1016/j.coi.2014.03.009 (2014).
129 Hazeldine, J. *et al.* Impaired neutrophil extracellular trap formation: a novel defect in the innate immune system of aged individuals. *Aging Cell* **13**, 690-698, doi:10.1111/acel.12222 (2014).
130 Wessels, I., Jansen, J., Rink, L. & Uciechowski, P. Immunosenescence of polymorphonuclear neutrophils. *ScientificWorldJournal* **10**, 145-160, doi:10.1100/tsw.2010.14 (2010).
131 Aprahamian, T., Takemura, Y., Goukassian, D. & Walsh, K. Ageing is associated with diminished apoptotic cell clearance in vivo. *Clin Exp Immunol* **152**, 448-455, doi:10.1111/j.1365-2249.2008.03658.x (2008).

132 Villanueva, J. L., Solana, R., Alonso, M. C. & Pena, J. Changes in the expression of HLA-class II antigens on peripheral blood monocytes from aged humans. *Dis Markers* **8**, 85-91 (1990).
133 Herrero, C., Marques, L., Lloberas, J. & Celada, A. IFN-gamma-dependent transcription of MHC class II IA is impaired in macrophages from aged mice. *The Journal of clinical investigation* **107**, 485-493, doi:10.1172/JCI11696 (2001).
134 van Duin, D. *et al.* Prevaccine determination of the expression of costimulatory B7 molecules in activated monocytes predicts influenza vaccine responses in young and older adults. *J Infect Dis* **195**, 1590-1597, doi:10.1086/516788 (2007).
135 Montgomery, R. R. & Shaw, A. C. Paradoxical changes in innate immunity in aging: recent progress and new directions. *J Leukoc Biol* **98**, 937-943, doi:10.1189/jlb.5MR0315-104R (2015).
136 Agrawal, A. *et al.* Altered innate immune functioning of dendritic cells in elderly humans: a role of phosphoinositide 3-kinase-signaling pathway. *Journal of immunology* **178**, 6912-6922 (2007).
137 Panda, A. *et al.* Age-associated decrease in TLR function in primary human dendritic cells predicts influenza vaccine response. *Journal of immunology* **184**, 2518-2527, doi:10.4049/jimmunol.0901022 (2010).
138 Agrawal, A. & Gupta, S. Impact of aging on dendritic cell functions in humans. *Ageing Res Rev* **10**, 336-345, doi:10.1016/j.arr.2010.06.004 (2011).
139 Della Bella, S. *et al.* Peripheral blood dendritic cells and monocytes are differently regulated in the elderly. *Clin Immunol* **122**, 220-228, doi:10.1016/j.clim.2006.09.012 (2007).
140 Agrawal, A., Agrawal, S. & Gupta, S. Role of Dendritic Cells in Inflammation and Loss of Tolerance in the Elderly. *Frontiers in immunology* **8**, 896, doi:10.3389/fimmu.2017.00896 (2017).
141 Ferrucci, L. *et al.* The origins of age-related proinflammatory state. *Blood* **105**, 2294-2299, doi:10.1182/blood-2004-07-2599 (2005).
142 Singh, T. & Newman, A. B. Inflammatory markers in population studies of aging. *Ageing Res Rev* **10**, 319-329, doi:10.1016/j.arr.2010.11.002 (2011).
143 Morrisette-Thomas, V. *et al.* Inflamm-aging does not simply reflect increases in pro-inflammatory markers. *Mech Ageing Dev* **139**, 49-57, doi:10.1016/j.mad.2014.06.005 (2014).
144 Franceschi, C., Garagnani, P., Vitale, G., Capri, M. & Salvioli, S. Inflammaging and 'Garb-aging'. *Trends Endocrinol Metab* **28**, 199-212, doi:10.1016/j.tem.2016.09.005 (2017).
145 Bartlett, D. B. *et al.* The age-related increase in low-grade systemic inflammation (Inflammaging) is not driven by cytomegalovirus infection. *Aging Cell* **11**, 912-915, doi:10.1111/j.1474-9726.2012.00849.x (2012).
146 Campisi, J. & d'Adda di Fagagna, F. Cellular senescence: when bad things happen to good cells. *Nat Rev Mol Cell Biol* **8**, 729-740, doi:10.1038/nrm2233 (2007).

147 Franceschi, C. & Campisi, J. Chronic inflammation (inflammaging) and its potential contribution to age-associated diseases. *J Gerontol A Biol Sci Med Sci* **69 Suppl 1**, S4-9, doi:10.1093/gerona/glu057 (2014).
148 Medina, C. B. & Ravichandran, K. S. Do not let death do us part: 'find-me' signals in communication between dying cells and the phagocytes. *Cell Death Differ* **23**, 979-989, doi:10.1038/cdd.2016.13 (2016).
149 Fadok, V. A. *et al.* Macrophages that have ingested apoptotic cells in vitro inhibit proinflammatory cytokine production through autocrine/paracrine mechanisms involving TGF-beta, PGE2, and PAF. *The Journal of clinical investigation* **101**, 890-898, doi:10.1172/JCI1112 (1998).
150 Zitvogel, L., Kepp, O. & Kroemer, G. Decoding cell death signals in inflammation and immunity. *Cell* **140**, 798-804, doi:10.1016/j.cell.2010.02.015 (2010).
151 Frasca, D. & Blomberg, B. B. Inflammaging decreases adaptive and innate immune responses in mice and humans. *Biogerontology* **17**, 7-19, doi:10.1007/s10522-015-9578-8 (2016).
152 Pinto, A. R. *et al.* Revisiting Cardiac Cellular Composition. *Circulation research* **118**, 400-409, doi:10.1161/CIRCRESAHA.115.307778 (2016).
153 Pinto, A. R. *et al.* An abundant tissue macrophage population in the adult murine heart with a distinct alternatively-activated macrophage profile. *PloS one* **7**, e36814, doi:10.1371/journal.pone.0036814 (2012).
154 Swirski, F. K., Robbins, C. S. & Nahrendorf, M. Development and Function of Arterial and Cardiac Macrophages. *Trends Immunol* **37**, 32-40, doi:10.1016/j.it.2015.11.004 (2016).
155 Epelman, S. *et al.* Embryonic and adult-derived resident cardiac macrophages are maintained through distinct mechanisms at steady state and during inflammation. *Immunity* **40**, 91-104, doi:10.1016/j.immuni.2013.11.019 (2014).
156 Epelman, S., Liu, P. P. & Mann, D. L. Role of innate and adaptive immune mechanisms in cardiac injury and repair. *Nature reviews. Immunology* **15**, 117-129, doi:10.1038/nri3800 (2015).
157 Molawi, K. *et al.* Progressive replacement of embryo-derived cardiac macrophages with age. *The Journal of experimental medicine* **211**, 2151-2158, doi:10.1084/jem.20140639 (2014).
158 Lavine, K. J. *et al.* Distinct macrophage lineages contribute to disparate patterns of cardiac recovery and remodeling in the neonatal and adult heart. *Proceedings of the National Academy of Sciences of the United States of America* **111**, 16029-16034, doi:10.1073/pnas.1406508111 (2014).
159 Aurora, A. B. *et al.* Macrophages are required for neonatal heart regeneration. *The Journal of clinical investigation* **124**, 1382-1392, doi:10.1172/JCI72181 (2014).
160 Frantz, S. & Nahrendorf, M. Cardiac macrophages and their role in ischaemic heart disease. *Cardiovascular research* **102**, 240-248, doi:10.1093/cvr/cvu025 (2014).
161 Leor, J., Palevski, D., Amit, U. & Konfino, T. Macrophages and regeneration: Lessons from the heart. *Semin Cell Dev Biol* **58**, 26-33, doi:10.1016/j.semcdb.2016.04.012 (2016).

162 van Amerongen, M. J., Harmsen, M. C., van Rooijen, N., Petersen, A. H. & van Luyn, M. J. Macrophage depletion impairs wound healing and increases left ventricular remodeling after myocardial injury in mice. *Am J Pathol* **170**, 818-829, doi:10.2353/ajpath.2007.060547 (2007).
163 Choi, J. H. *et al.* Identification of antigen-presenting dendritic cells in mouse aorta and cardiac valves. *The Journal of experimental medicine* **206**, 497-505, doi:10.1084/jem.20082129 (2009).
164 Van der Borght, K. *et al.* Myocardial Infarction Primes Autoreactive T Cells through Activation of Dendritic Cells. *Cell Rep* **18**, 3005-3017, doi:10.1016/j.celrep.2017.02.079 (2017).
165 Frangogiannis, N. G. The immune system and cardiac repair. *Pharmacol Res* **58**, 88-111, doi:10.1016/j.phrs.2008.06.007 (2008).
166 Nah, D. Y. & Rhee, M. Y. The inflammatory response and cardiac repair after myocardial infarction. *Korean Circ J* **39**, 393-398, doi:10.4070/kcj.2009.39.10.393 (2009).
167 Lichtman, A. H. The heart of the matter: protection of the myocardium from T cells. *J Autoimmun* **45**, 90-96, doi:10.1016/j.jaut.2013.05.004 (2013).
168 Neu, N. *et al.* Cardiac myosin induces myocarditis in genetically predisposed mice. *Journal of immunology* **139**, 3630-3636 (1987).
169 Smith, S. C. & Allen, P. M. Myosin-induced acute myocarditis is a T cell-mediated disease. *Journal of immunology* **147**, 2141-2147 (1991).
170 Hofmann, U. & Frantz, S. Role of T-cells in myocardial infarction. *Eur Heart J* **37**, 873-879, doi:10.1093/eurheartj/ehv639 (2016).
171 Curato, C. *et al.* Identification of noncytotoxic and IL-10-producing CD8+AT2R+ T cell population in response to ischemic heart injury. *Journal of immunology* **185**, 6286-6293, doi:10.4049/jimmunol.0903681 (2010).
172 Hofmann, U. *et al.* Activation of CD4+ T lymphocytes improves wound healing and survival after experimental myocardial infarction in mice. *Circulation* **125**, 1652-1663, doi:10.1161/CIRCULATIONAHA.111.044164 (2012).
173 Ramos, G., Hofmann, U. & Frantz, S. Myocardial fibrosis seen through the lenses of T-cell biology. *J Mol Cell Cardiol* **92**, 41-45, doi:10.1016/j.yjmcc.2016.01.018 (2016).
174 Weirather, J. *et al.* Foxp3+ CD4+ T cells improve healing after myocardial infarction by modulating monocyte/macrophage differentiation. *Circulation research* **115**, 55-67, doi:10.1161/CIRCRESAHA.115.303895 (2014).
175 Saxena, A. *et al.* Regulatory T cells are recruited in the infarcted mouse myocardium and may modulate fibroblast phenotype and function. *Am J Physiol Heart Circ Physiol* **307**, H1233-1242, doi:10.1152/ajpheart.00328.2014 (2014).
176 Matsumoto, K. *et al.* Regulatory T lymphocytes attenuate myocardial infarction-induced ventricular remodeling in mice. *Int Heart J* **52**, 382-387 (2011).
177 Boag, S. E. *et al.* T lymphocytes and fractalkine contribute to myocardial ischemia/reperfusion injury in patients. *The Journal of clinical investigation* **125**, 3063-3076, doi:10.1172/JCI80055 (2015).

178 Laroumanie, F. *et al.* CD4+ T cells promote the transition from hypertrophy to heart failure during chronic pressure overload. *Circulation* **129**, 2111-2124, doi:10.1161/CIRCULATIONAHA.113.007101 (2014).
179 Nevers, T. *et al.* Left Ventricular T-Cell Recruitment Contributes to the Pathogenesis of Heart Failure. *Circ Heart Fail* **8**, 776-787, doi:10.1161/CIRCHEARTFAILURE.115.002225 (2015).
180 Groschel, C. *et al.* T helper cells with specificity for an antigen in cardiomyocytes promote pressure overload-induced progression from hypertrophy to heart failure. *Sci Rep* **7**, 15998, doi:10.1038/s41598-017-16147-1 (2017).
181 Brede, C. *et al.* Mapping immune processes in intact tissues at cellular resolution. *The Journal of clinical investigation* **122**, 4439-4446, doi:10.1172/JCI65100 (2012).
182 Frantz, S. *et al.* Peroxisome proliferator activated-receptor agonism and left ventricular remodeling in mice with chronic myocardial infarction. *Br J Pharmacol* **141**, 9-14, doi:10.1038/sj.bjp.0705585 (2004).
183 Pacher, P., Nagayama, T., Mukhopadhyay, P., Batkai, S. & Kass, D. A. Measurement of cardiac function using pressure-volume conductance catheter technique in mice and rats. *Nature protocols* **3**, 1422-1434, doi:10.1038/nprot.2008.138 (2008).
184 Picot, J., Guerin, C. L., Le Van Kim, C. & Boulanger, C. M. Flow cytometry: retrospective, fundamentals and recent instrumentation. *Cytotechnology* **64**, 109-130, doi:10.1007/s10616-011-9415-0 (2012).
185 Gallagher, S. R. Quantitation of DNA and RNA with Absorption and Fluorescence Spectroscopy. *Curr Protoc Immunol* **116**, A 3L 1-A 3L 14, doi:10.1002/cpim.20 (2017).
186 Bustin, S. A. Absolute quantification of mRNA using real-time reverse transcription polymerase chain reaction assays. *J Mol Endocrinol* **25**, 169-193 (2000).
187 Hautala, N., Tenhunen, O., Szokodi, I. & Ruskoaho, H. Direct left ventricular wall stretch activates GATA4 binding in perfused rat heart: involvement of autocrine/paracrine pathways. *Pflugers Arch* **443**, 362-369, doi:10.1007/s004240100699 (2002).
188 Epelman, S., Lavine, K. J. & Randolph, G. J. Origin and functions of tissue macrophages. *Immunity* **41**, 21-35, doi:10.1016/j.immuni.2014.06.013 (2014).
189 Gordon, S., Pluddemann, A. & Martinez Estrada, F. Macrophage heterogeneity in tissues: phenotypic diversity and functions. *Immunol Rev* **262**, 36-55, doi:10.1111/imr.12223 (2014).
190 Burzyn, D., Benoist, C. & Mathis, D. Regulatory T cells in nonlymphoid tissues. *Nature immunology* **14**, 1007-1013, doi:10.1038/ni.2683 (2013).
191 Heath, W. R. & Carbone, F. R. The skin-resident and migratory immune system in steady state and memory: innate lymphocytes, dendritic cells and T cells. *Nature immunology* **14**, 978-985, doi:10.1038/ni.2680 (2013).

192 Ziv, Y. *et al.* Immune cells contribute to the maintenance of neurogenesis and spatial learning abilities in adulthood. *Nature neuroscience* **9**, 268-275, doi:10.1038/nn1629 (2006).
193 DiSpirito, J. R. *et al.* Molecular diversification of regulatory T cells in nonlymphoid tissues. *Sci Immunol* **3**, doi:10.1126/sciimmunol.aat5861 (2018).
194 Takamura, S. Niches for the Long-Term Maintenance of Tissue-Resident Memory T Cells. *Frontiers in immunology* **9**, 1214, doi:10.3389/fimmu.2018.01214 (2018).
195 Park, C. O. & Kupper, T. S. The emerging role of resident memory T cells in protective immunity and inflammatory disease. *Nature medicine* **21**, 688-697, doi:10.1038/nm.3883 (2015).
196 Schreiner, D. & King, C. G. CD4+ Memory T Cells at Home in the Tissue: Mechanisms for Health and Disease. *Frontiers in immunology* **9**, 2394, doi:10.3389/fimmu.2018.02394 (2018).
197 Ilan, Y. *et al.* Induction of regulatory T cells decreases adipose inflammation and alleviates insulin resistance in ob/ob mice. *Proceedings of the National Academy of Sciences of the United States of America* **107**, 9765-9770, doi:10.1073/pnas.0908771107 (2010).
198 Burzyn, D. *et al.* A special population of regulatory T cells potentiates muscle repair. *Cell* **155**, 1282-1295, doi:10.1016/j.cell.2013.10.054 (2013).
199 Eller, K. *et al.* Potential role of regulatory T cells in reversing obesity-linked insulin resistance and diabetic nephropathy. *Diabetes* **60**, 2954-2962, doi:10.2337/db11-0358 (2011).
200 Bonner, F., Borg, N., Burghoff, S. & Schrader, J. Resident cardiac immune cells and expression of the ectonucleotidase enzymes CD39 and CD73 after ischemic injury. *PloS one* **7**, e34730, doi:10.1371/journal.pone.0034730 (2012).
201 Steinert, E. M. *et al.* Quantifying Memory CD8 T Cells Reveals Regionalization of Immunosurveillance. *Cell* **161**, 737-749, doi:10.1016/j.cell.2015.03.031 (2015).
202 Aronoff, L., Epelman, S. & Clemente-Casares, X. Isolation and Identification of Extravascular Immune Cells of the Heart. *J Vis Exp*, doi:10.3791/58114 (2018).
203 Ginhoux, F. & Guilliams, M. Tissue-Resident Macrophage Ontogeny and Homeostasis. *Immunity* **44**, 439-449, doi:10.1016/j.immuni.2016.02.024 (2016).
204 Hulsmans, M., Sam, F. & Nahrendorf, M. Monocyte and macrophage contributions to cardiac remodeling. *J Mol Cell Cardiol* **93**, 149-155, doi:10.1016/j.yjmcc.2015.11.015 (2016).
205 Costa, E. *et al.* Aging is Associated with Impaired Renal Function, INF-gamma Induced Inflammation and with Alterations in Iron Regulatory Proteins Gene Expression. *Aging Dis* **5**, 356-365, doi:10.14366/AD.2014.0500356 (2014).
206 Minciullo, P. L. *et al.* Inflammaging and Anti-Inflammaging: The Role of Cytokines in Extreme Longevity. *Arch Immunol Ther Exp (Warsz)* **64**, 111-126, doi:10.1007/s00005-015-0377-3 (2016).
207 Clement, C. C., Rotzschke, O. & Santambrogio, L. The lymph as a pool of self-antigens. *Trends Immunol* **32**, 6-11, doi:10.1016/j.it.2010.10.004 (2011).
208 Leak, L. V. *et al.* Proteomic analysis of lymph. *Proteomics* **4**, 753-765, doi:10.1002/pmic.200300573 (2004).

209 Clement, C. C. & Santambrogio, L. The lymph self-antigen repertoire. *Frontiers in immunology* **4**, 424, doi:10.3389/fimmu.2013.00424 (2013).
210 Smith, S. C. & Allen, P. M. Expression of myosin-class II major histocompatibility complexes in the normal myocardium occurs before induction of autoimmune myocarditis. *Proceedings of the National Academy of Sciences of the United States of America* **89**, 9131-9135 (1992).
211 Vdovenko, D. & Eriksson, U. Regulatory Role of CD4(+) T Cells in Myocarditis. *J Immunol Res* **2018**, 4396351, doi:10.1155/2018/4396351 (2018).
212 Bansal, S. S. *et al.* Activated T Lymphocytes are Essential Drivers of Pathological Remodeling in Ischemic Heart Failure. *Circ Heart Fail* **10**, e003688, doi:10.1161/CIRCHEARTFAILURE.116.003688 (2017).
213 Ramos, G. C. *et al.* Myocardial aging as a T-cell-mediated phenomenon. *Proceedings of the National Academy of Sciences of the United States of America* **114**, E2420-E2429, doi:10.1073/pnas.1621047114 (2017).
214 Rosenblum, M. D., Way, S. S. & Abbas, A. K. Regulatory T cell memory. *Nature reviews. Immunology* **16**, 90-101, doi:10.1038/nri.2015.1 (2016).
215 Bergot, A. S. *et al.* TCR sequences and tissue distribution discriminate the subsets of naive and activated/memory Treg cells in mice. *European journal of immunology* **45**, 1524-1534, doi:10.1002/eji.201445269 (2015).
216 Brincks, E. L. *et al.* Antigen-specific memory regulatory CD4+Foxp3+ T cells control memory responses to influenza virus infection. *Journal of immunology* **190**, 3438-3446, doi:10.4049/jimmunol.1203140 (2013).
217 Kuswanto, W. *et al.* Poor Repair of Skeletal Muscle in Aging Mice Reflects a Defect in Local, Interleukin-33-Dependent Accumulation of Regulatory T Cells. *Immunity* **44**, 355-367, doi:10.1016/j.immuni.2016.01.009 (2016).
218 Villalta, S. A. *et al.* Regulatory T cells suppress muscle inflammation and injury in muscular dystrophy. *Sci Transl Med* **6**, 258ra142, doi:10.1126/scitranslmed.3009925 (2014).
219 Antiga, E. *et al.* Characterization of regulatory T cells in patients with dermatomyositis. *J Autoimmun* **35**, 342-350, doi:10.1016/j.jaut.2010.07.006 (2010).
220 Vercoulen, Y. *et al.* Increased presence of FOXP3+ regulatory T cells in inflamed muscle of patients with active juvenile dermatomyositis compared to peripheral blood. *PloS one* **9**, e105353, doi:10.1371/journal.pone.0105353 (2014).
221 Dominguez-Villar, M. & Hafler, D. A. Regulatory T cells in autoimmune disease. *Nature immunology* **19**, 665-673, doi:10.1038/s41590-018-0120-4 (2018).
222 Nguyen, T. L., Sullivan, N. L., Ebel, M., Teague, R. M. & DiPaolo, R. J. Antigen-specific TGF-beta-induced regulatory T cells secrete chemokines, regulate T cell trafficking, and suppress ongoing autoimmunity. *Journal of immunology* **187**, 1745-1753, doi:10.4049/jimmunol.1004112 (2011).
223 Kaya, Z., Leib, C. & Katus, H. A. Autoantibodies in heart failure and cardiac dysfunction. *Circulation research* **110**, 145-158, doi:10.1161/CIRCRESAHA.111.243360 (2012).

224 Boivin-Jahns, V., Jahns, R. & Boege, F. Relevant effects of beta1-adrenoceptor autoantibodies in chronic heart failure. *Front Biosci (Landmark Ed)* **23**, 2146-2156 (2018).
225 Matsui, S. *et al.* Dilated cardiomyopathy defines serum autoantibodies against G-protein-coupled cardiovascular receptors. *Autoimmunity* **21**, 85-88 (1995).
226 Clement, C. C. *et al.* An expanded self-antigen peptidome is carried by the human lymph as compared to the plasma. *PloS one* **5**, e9863, doi:10.1371/journal.pone.0009863 (2010).
227 Hulsmans, M. *et al.* Cardiac macrophages promote diastolic dysfunction. *The Journal of experimental medicine* **215**, 423-440, doi:10.1084/jem.20171274 (2018).
228 Yabluchanskiy, A. *et al.* Myocardial Infarction Superimposed on Aging: MMP-9 Deletion Promotes M2 Macrophage Polarization. *J Gerontol A Biol Sci Med Sci* **71**, 475-483, doi:10.1093/gerona/glv034 (2016).
229 Martinod, K. *et al.* Peptidylarginine deiminase 4 promotes age-related organ fibrosis. *The Journal of experimental medicine* **214**, 439-458, doi:10.1084/jem.20160530 (2017).
230 Nussinovitch, U. & Shoenfeld, Y. The clinical and diagnostic significance of anti-myosin autoantibodies in cardiac disease. *Clin Rev Allergy Immunol* **44**, 98-108, doi:10.1007/s12016-010-8229-8 (2013).
231 Mestas, J. & Hughes, C. C. Of mice and not men: differences between mouse and human immunology. *Journal of immunology* **172**, 2731-2738 (2004).

9 APPENDIX

9.1 ABBREVIATIONS

°C	Degrees Celsius
3D	Three dimensional
a.u.	Arbitrary unit
Ab	Antibody
Ag	Antigen
AICD	Activation induced cell death
ANOVA	Analysis of variance
APC	Antigen presenting cell
BABB	Benzyl alcohol + Benzyl benzoate
BSA	Bovine Serum albumin
BSS	Balanced salt solution
Ccl	C-C motif ligand
CCR	Chemokine receptor type
CD	Cluster of differentiation
cDNA	Complementary deoxyribonucleic acid
CMV	Cytomegalovirus
Ct	Threshold cycle
Cxcl	C-X-C motif Ligand
DAMP	Damage associated molecular pattern
DAPI	4´6-diamino-2-phenylindole
DC	Dendritic Cell
DNA	Deoxyribonucleic acid
EDD	End-diastolic diameter
EDV	End-diastolic volume
EF	Ejection fraction
EF	Ejection fraction
ELISA	Enzyme-linked immunosorbent assay
ESD	End-systolic diameter
et al.	et alteri
FACS	Fluorescence activated cell sorting
FC	Fragment crystallizable
FCS	Fetal Calf Serum
Fig.	Figure
FITC	Fluorescein isothiocyanate

FoxP3	Forkhead Box Protein 3
FS	Fraction shortening
GAPDH	Glycerinaldehyd-3-phosphate-Dehydrogenase
Gata-4	GATA 4 binding protein
h	Hour
HE	Hematoxylin and Eosin
Hif	Hypoxia inducible factor
HRP	Horseradish peroxidase streptavidin
HSC	Hematopoietic stem cell
Hsp	Heat shock protein
Ig	Immunoglobulin
IL	Interleukin
INF- γ	Interferon Gamma
IU	International units
KO	Knock-out
L	ligand
LN	Lymph node
Log	Logarithm
LSFM	Light sheet fluorescence microscopy
LV	Left ventricle
Ly6C	Lymphocyte antigen 6 complex, locus C
Ly6G	Lymphocyte antigen 6 complex, locus G
M.	Muscle
med	Mediastinal
mg	Milligram
MHC	Major histocompatibility complex
MhZ	Megahertz
min	Minute
ml	Milliliter
mM	Milli Mol
mm3	Cubic millimeter
Mmp	Matrix-Metalloprotease
mo	Months
MPVS	Micro-Tip®Pressure Volume System
mRNA	Messenger ribonucleic acid
Myh	Myosin heavy chain
NAHNES	National Health and Nutrition Examination Survey
nm	Nano meter
NS	Not significant
OVA	Ovalbumin

PAMP	Pathogen associated molecular pattern
PBS	Phosphate buffered saline
PMA	12-myristate 13 acetate
PNAS	Proceedings of the National Academy of Science
pop	Popliteal
PRR	Pattern recognition particle
pT_{reg}	Peripheral, induced regulatory T-cells
qPCR	Quantitative polymerase chain reaction
RNA	Ribonucleic acid
rpm	Rounds per minute
RT-PCR	Real time polymerase chain reaction
RV	Right ventricle
sec	Seconds
SEM	Standard Error of mean
Sirt	Sirtuin
SPF	Specific pathogen free
T_{CM}	Central memory T-cells
T_{conv}	Conventional T-cells
TCR	T-cell receptor
T_{EM}	Effector memory T-cells
TGF - ß	Transforming growth factor beta
Tgfb	Transforming growth factor beta
Th	T-helper cell
TNF	Tumor necrosis factor
T_{reg}	Regulatory T-cell
T_{RM}	Tissue resident memory T-cells
tT_{reg}	Thymus derived, naturally occurring, regulatory T-cells
TVA	Tierversuchsantrag
U.S.	United states
vs.	Versus
VZV	Varicella zoster virus
WGA	Wheat Germ Agglutinin
WT	Wild type
µg	Microgram
µl	Microliter

9.2 ACKNOWLEDGEMENTS

Die Anfertigung dieser Doktorarbeit wäre ohne vielseitige Unterstützung nicht möglich gewesen. An dieser Stelle möchte ich mich herzlich bei allen bedanken, die mir geholfen und mich begleitet haben.

An erster Stelle gilt Dank meinem Doktorvater Herrn Prof. Dr. med. Stefan Frantz, für die Möglichkeit diese Doktorarbeit in seiner Arbeitsgruppe anzufertigen, für die hervorragende Betreuung zu jedem Zeitpunkt im Anfertigungsprozess dieser Dissertation, sowie für die Anregungen zu eigenständigem, wissenschaftlichem Denken.

Ganz besonderer Dank gilt Dr. Gustavo Ramos, der mich seit dem Beginn dieser Arbeit begleitet hat. Er war es, der mir neben zahlreichen Methoden auch die Begeisterung an der Wissenschaft vermittelt hat. Im Rahmen des Projektes zu dieser Arbeit konnte ich mir seiner Unterstützung zu jedem Zeitpunkt sicher sein. Ich habe nicht nur einen fabelhaften Betreuer, sondern auch einen guten Freund hinzugewonnen.

Für die Entstehung dieser Arbeit und das Voranbringen wichtiger Experimente war außerdem die Unterstützung der Kolleginnen und Kollegen unserer Arbeitsgruppe unverzichtbar. PD Dr. Ulrich Hofmann, Dr. Johannes Weirather, Dr. Laura Peters, Dr. Margarete Heinrichs, Dr. Edit Tanai, Dr. Matthias Burkhard und Dr. Benjamin Vogel möchte ich danken für die kompetente fachliche Mithilfe, die stets offenen Diskussionen und die wunderbare Arbeitsatmosphäre im Labor.

Dank gilt Helga Wagner, Andrea Leopold, Elisabeth Bauer, Sandra Umbenhauer und Charlotte Dienesch für die hervorragende technische Assistenz bei den Experimenten, sowie die wertvollen Hilfestellungen durch ihre jahrelange methodologische Expertise im Bereich der Grundlagenforschung.

Dank aussprechen möchte ich auch der Deutschen Gesellschaft für Kardiologie, für die Förderung durch das „Otto-Hess-Promotionsstipendium“.

Von ganzem Herzen danken möchte ich letztlich meiner Familie, insbesondere meinen Eltern Elisabeth und Stephan van den Berg, meiner Schwester Sophie und meinem Bruder Martin, sowie meinen Großeltern. Sie haben mich in meinem gesamten bisherigen Werdegang stets unterstützt, ermutigt, mitgefiebert und mir die Möglichkeit gegeben, meine Ziele zu erreichen. Mit fürsorglichen und auch mahnenden Worten standen sie mit stets zur Seite.
Ein außerordentlicher Dank gilt auch meinem Freund Maarten für sein liebevolles Verständnis, große Geduld und Unterstützung, wann immer diese notwendig war.

Zuletzt möchte ich mich bei meinen Freundinnen und Freunden bedanken. Danke für die unzählbaren, wertvollen Gespräche, das Korrekturlesen dieser Arbeit, die vielen unvergesslichen Momente der letzten Jahre und für die Augenblicke, in denen wir uns nicht zu ernst genommen haben.

Danke!

9.4 PUBLICATIONS AND PRESENTATIONS

9.4.1 Publication

‘Myocardial Aging as a T-cell-mediated phenomenen’

G. Ramos, A. van den Berg, V. Nunes-Silva, J. Weirather, L. Peters, M. Burkard, M. Friedrich, J. Pinnecker, M. Abeßer, K. Heinze, K. Schuh, N. Beyersdorf, T.Kerkau, J. Dememgeot, S. Frantz, U. Hofmann. Proceedings of the National Academy of Sciences (PNAS, IF 9,4) 2016-21047

9.4.2 Poster presentations

‘Myocardial aging as a T-cell mediated phenomenon’
Fall-conference of the German Cardiac Society, October 2015

‘Cardiac resident Leukocyte Populations in Steady State and Aging’
American Heart Association, Scientific Session, Chicago USA, November 2014

‘Cardiac resident Leukocyte Populations in Steady State and Aging’
International Symposium Cardiology, September 2014, Charité Berlin

9.5 AFFIDAVIT

I hereby confirm that my thesis entitled 'Age-related alterations of the immune system aggravate the myocardial aging process' is the result of my own work. I did not receive any help or support from commercial consultants. All sources and/ or materials applied are listed and specified in the thesis.

Furthermore, I confirm that this thesis has not yet been submitted as part of another examination process neither in identical nor in similar form.

Würzburg, _____

Date, Signature

Eidesstattliche Erklärung

Hiermit erkläre ich an Eides statt, die Dissertation „Altersabhängige Veränderungen des Immunsystems verstärken den Alterungsprozess des Myokards" eigenständig, d.h. insbesondere selbständig und ohne Hilfe eines kommerziellen Promotionsberaters, angefertigt und keine anderen als die von mir angegebenen Quellen und Hilfsmittel verwendet zu haben.

Ich erkläre außerdem, dass die Dissertation weder in gleicher noch in ähnlicher Form bereits in einem anderen Prüfungsverfahren vorgelegen hat.

Würzburg, den _____

Datum, Unterschrift